nagra National Cooperative for the Disposal of Radioactive Waste

TECHNICAL REPORT 97-04

Experimental and Theoretical Studies on Alkaline Degradation of Cellulose and its Impact on the Sorption of Radionuclides

May 1998

L.R. Van Loon
M.A. Glaus

PSI, Würenlingen and Villigen

Hardstrasse 73, CH-5430 Wettingen/Switzerland, Telephone +41-56-437 11 11

nagra National Cooperative for the Disposal of Radioactive Waste

TECHNICAL REPORT 97-04

Experimental and Theoretical Studies on Alkaline Degradation of Cellulose and its Impact on the Sorption of Radionuclides

May 1998

L.R. Van Loon
M.A. Glaus

PSI, Würenlingen and Villigen

Hardstrasse 73, CH-5430 Wettingen/Switzerland, Telephone +41-56-437 11 11

This report was prepared on behalf of Nagra. The viewpoints presented and conclusions reached are those of the author(s) and do not necessarily represent those of Nagra.

PREFACE

The Laboratory for Waste Management at the Paul Scherrer Institut is performing work to develop and test models as well as to acquire specific data relevant to performance assessments of planned Swiss nuclear waste repositories. These investigations are undertaken in close co-operation with, and with the financial support of, the National Co-operative for the Disposal of Radioactive Waste (Nagra). The present report is issued simultaneously as a PSI-Bericht and a Nagra Technical Report.

ISSN 1015-2636

CONTENT

ABSTRACT

For more than ten years, cellulose degradation has been regarded as an important process which can adversely effect the sorption of radionuclides on cement in a radioactive waste repository. However, so far, it was not possible to quantify this effect. This study reports new experimental data on alkaline degradation of cellulose, together with a re-evaluation of old literature data. For the first time now, it becomes possible to quantitatively estimate the potential rôle of cellulose degradation in performance assessment studies.

In the first part of this study (chapters 1-4), a literature overview of other studies on alkaline degradation of cellulose is given, together with a general discussion on the effect of organic ligands on the sorption of radionuclides. Further, an overview of the important mechanisms of alkaline degradation of cellulose and some kinetic aspects of the main reactions taking place is presented. The relevance of the processes for performance assessment is explained in detail. The discussion forms the starting-point for a detailed experimental program for evaluating the rôle of alkaline degradation of cellulose in performance assessment.

In the second part (chapters 5-8), experimental studies on alkaline degradation are presented. Different cellulosic materials were degraded in an artificial cement pore water, representing the first stage of cement degradation. The most important degradation products (α- and β-isosaccharinic acid) were characterised and the results compared with other studies. Kinetic parameters for the main reactions were measured and discussed. A good agreement was found between the measured values and values extrapolated from the literature. The solubility of the sparingly soluble Ca-salt of α-isosaccharinic acid (ISA) was studied as well as the interaction of ISA with cement. Sorption of ISA on cement can keep the ISA concentration in the pore water of a repository at a low level. The effect of pure ISA and degradation products on the sorption of radionuclides on feldspar at pH 13.3 was investigated. It was shown that both α-isosaccharinic acid and cellulose degradation products have an adverse effect on the sorption of Eu-152, Th-234 and Ni-63. The effect observed for degradation products could be satisfactorily explained by the presence of α-ISA. For Eu(III) and Th(IV), the concentration of α-ISA must be larger than 10^{-4}-10^{-3} M in order to significantly reduce sorption. For Ni(II), the concentration has to be larger than 10^{-2} M. β-ISA was shown to affect the sorption of Eu at concentrations $>10^{-2}$ M only.

The last part of the report (chapter 9) deals with the application of the theoretical and experimental studies in performance assessment. It shows how a combination of the different parameters and processes discussed (cellulose loading, kinetics of degradation, sorption of ISA, sorption of metals, etc.) can be used in performance assessment studies to quantitatively evaluate the rôle of alkaline cellulose degradation on radionuclide mobility.

RESUME

Il est depuis longtemps connu, que la dégradation de la cellulose en milieu alcalin peut diminuer significativement la sorption des radionucléides sur le ciment dans un site de stockage définitif de déchets radioactifs. Jusqu'alors, il n'était malheureusement pas possible de décrire quantitativement l'ampleur de cet effet. Ce travail présente de nouvelles données expérimentales ainsi qu'une synthèse critique de la littérature qui permettent de décrire de manière quantitative le rôle de la dégradation de la cellulose en milieu alcalin dans l'analyse de sûreté.

La dégradation de différents matériaux contenant de la cellulose a été étudiée dans des conditions chimiques proches de celles régnant dans une eau interstitielle d'un site de stockage définitif pour les déchets à faible et moyenne activité. L'influence des produits de dégradation sur la sorption du Ni-63, de l'Eu-152 et du Th-234 a été mesurée.

Dans une première partie (chapitres 1 à 4) sont présentées d'une part une synthèse des travaux effectués dans le domaine de la dégradation de la cellulose trouvés dans la littérature, et d'autre part une discussion générale sur l'effet qu'exercent les ligands organiques sur la sorption des radionucléides. Les principaux chemins réactionnels intervenant dans la dégradation de la cellulose en milieu alcalin ainsi que la cinétique correspondante sont expliqués. L'importance des processus dans l'analyse de sûreté est expliquée de manière détaillée. De cette discussion débute un programme détaillé évaluant le rôle de la dégradation de la cellulose en milieu alcalin dans l'analyse de sûreté.

La seconde partie (chapitres 5 à 8) présente les travaux expérimentaux menés sur la dégradation de la cellulose en milieu alcalin. Différents matériaux à base de cellulose ont été dégradés dans une eau interstitielle de ciment synthétique présentant la même composition qu'une eau de ciment dans la première phase de dégradation de ciment. Les principaux produits de dégradation de la cellulose (acides α- et β-isosacchariniques) ont été caractérisés et les résultats comparés avec ceux d'autres travaux. Les paramètres cinétiques ont été mesurés et discutés pour les réactions principales. Les résultats sont comparables à ceux extrapolés dans la littérature. La solubilité du sel Ca-acide α-isosaccharinique (peu soluble) ainsi que les réactions entre l'acide isosaccharinique et le ciment ont été étudiées.

La concentration maximale d'acide isosaccharinique dans une eau interstitielle de ciment est limitée par sa sorption sur le ciment. L'effet exercé par l'acide isosaccharinique et par les produits de dégradation de la cellulose sur la sorption des radionucléides sur le feldspath à pH 13.3 a été mesuré. L'acide isosaccharinique et les produits de dégradation limitent la sorption du Ni-63, de l'Eu-152 et du Th-234. Les effets observés par les produits de dégradation ont pu être entièrement expliqués à l'aide de la concentration connue en acide isosaccharinique. Une concentration en acide α-isosaccharinique comprise entre 10^{-4} et 10^{-3} M sont nécessaires pour réduire la sorption de l'Eu(III) et du Th(IV) de manière significative; Pour réduire la sorption du Ni(II), la concentration minimale requise est d'environ 10^{-2} M. L'acide β-isosaccharinique n'exerce une influence sur la sorption de l'Eu(III) qu'au-delà de 10^{-2} M.

La dernière partie du rapport (chapitre 9) est consacrée à l'application des découvertes théoriques et expérimentales dans l'analyse de sûreté. Il est démontré que les différentes valeurs prédéfinies et les réactions chimiques discutées (fraction en cellulose dans le ciment, cinétique de dégradation, sorption de l'acide isosaccharinique, sorption des radionucléides, etc...) peuvent être combinées pour évaluer quantitativement l'effet de la dégradation de la cellulose en milieu alcalin dans l'analyse de sûreté.

ZUSAMMENFASSUNG

Seit Jahren ist bekannt, dass der alkalische Celluloseabbau die Sorption von Radionukliden am Zement eines Endlagers für radioaktive Abfälle negativ beeinflussen kann. Allerdings liess sich das Ausmass dieses Effekts nicht quantitativ beschreiben. In der vorliegenden Untersuchung werden neue experimentelle Daten zusammen mit einer Neubeurteilung von Literaturergebnissen vorgelegt. Als Folge davon lässt sich nun die vermutliche Rolle des alkalischen Celluloseabbaus in der Sicherheitsanalyse erstmals quantitativ beschreiben.

Der Abbau von verschiedenen Cellulosematerialien wurde unter chemischen Bedingungen, welche denjenigen im Porenwasser eines Endlagers für schwach- und mittelaktive Abfälle nahekommen, untersucht. Ferner wurde der Einfluss der dabei entstehenden Abbauprodukte auf das Sorptionsverhalten von Ni-63, Eu-152 und Th-234 gemessen.

Im ersten Teil der Arbeit (Kapitel 1-4) wird eine Literaturübersicht über andere Studien auf dem Gebiet des Celluloseabbaus gegeben und eine allgemeine Diskussion über den Effekt von organischen Liganden auf die Sorption von Radionukliden präsentiert. Eine Übersicht über die wichtigsten Reaktionspfade, welche beim alkalischen Abbau von Cellulose möglich sind, und die zugehörige Kinetik werden beleuchtet. Die Bedeutung der Prozesse für die Sicherheitsanalyse wird detailliert erklärt. Diese Diskussion bildet den Startpunkt für ein detailliertes Programm zur Beurteilung der Rolle des alkalischen Abbaus von Cellulose in der Sicherheitsanalyse.

Im zweiten Teil (Kapitel 5-8) werden experimentelle Studien zum alkalischen Abbau von Cellulose präsentiert. Verschiedene Cellulose-materialien wurden in einem für die erste Stufe der Zementdegradation relevanten künstlichen Zementporenwasser abgebaut. Die wichtigsten Abbauprodukte (α- und β-Isosaccharinsäure) wurden charakterisiert und die Resultate mit anderen Studien verglichen. Kinetische Parameter für die Hauptreaktionen wurden gemessen und diskutiert. Diese Messwerte und aus Literaturdaten extrapolierte Werte weisen eine gute Übereinstimmung auf. Die Löslichkeit des schwerlöslichen Salzes von Ca mit α-Isosaccharinsäure, wie auch die Wechselwirkung von Isosaccharinsäure mit Zement wurden untersucht. Die Sorption von Isosaccharinsäure an Zement kann deren maximal mögliche

Konzentration in Zementporenwasser niedrig halten. Der Effekt von reiner Isosaccharinsäure und der Celluloseabbauprodukte auf die Sorption von Radionukliden an Feldspat bei pH 13.3 wurde gemessen. Sowohl Isosaccharinsäure wie auch die Abbauprodukte haben einen negativen Effekt auf die Sorption von Eu-152, Th-234 und Ni-63. Diese beobachteten Auswirkungen der Abbauprodukte konnten vollumfänglich mit der vorliegenden Konzentration an Isosaccharinsäure erklärt werden. Um die Sorption von Eu(III) und von Th(IV) signifikant zu reduzieren, sind Konzentrationen von α-Isosaccharinsäure zwischen 10^{-4} und 10^{-3} M nötig; im Falle von Ni(II) liegt der Schwellenwert bei ca. 10^{-2} M. β-Isosaccharinsäure beeinflusst die Sorption von Eu(III) erst ab Konzentrationen > 10^{-2} M.

Der letzte Teil des Berichts (Kapitel 9) befasst sich mit der Anwendung der theoretischen und experimentellen Befunde in der Sicherheitsanalyse. Es wird gezeigt, wie die verschiedenen diskutierten Vorgabewerte und Prozesse (Cellulosebeladung, Abbaukinetik, Sorption von Isosaccharinsäure, Sorption von Radionukliden, etc.) zu einem kompletten Bild kombiniert werden können, welches eine quantitative Beurteilung des alkalischen Abbaus von Cellulose in der Sicherheitsanalyse ermöglicht.

LIST OF FIGURES

LIST OF TABLES

1 INTRODUCTION

1.1 General

In Switzerland, low- and intermediate level radioactive waste will be disposed of in an underground repository (NAGRA 1992). The use of large amounts of cement for constructing such a repository and the presence of cementitious wastes and engineered barrier materials produce alkaline environments in which the pH of the cement pore water remains above 12.5 for periods of the order of 10^5 years (BERNER 1990). This ensures a slow release of most of the radionuclides, because of their strong sorption on the cement phases under such conditions (NAGRA 1994). Low- and intermediate level radioactive waste may contain substantial amounts of cellulosic materials. In Switzerland, about 50 % of the organic waste planned to be emplaced in the repository for low- and intermediate radioactive waste (L/ILW-repository) is cellulosic (NAGRA 1994). It is well known in the literature that cellulose is unstable under alkaline conditions (WHISTLER & BeMILLER 1958) and will degrade in such a chemical environment to water-soluble, low molecular weight compounds. The type of degradation products formed depends strongly on the composition of the solution in contact with the cellulose. In the presence of Ca^{2+}, as is the case for cement pore water, isosaccharinic acid (denoted hereafter as ISA) is expected to be the main degradation product (BLEARS et al. 1957, MACHELL & RICHARDS 1958, MACHELL & RICHARDS 1960). ISA is assumed to form, in analogy with gluconic acid (Figure 1), stable complexes with tri- and tetravalent radionuclides such as Am(III), Pu(IV) (SAWYER 1964, MORETON 1993) which adversely influences their sorption on the cement phases (BRADBURY & SAROTT 1995) and/or increases their solubility (MORETON 1993, GREENFIELD et al. 1993, GREENFIELD et al. 1995, BOURBON 1994, BOURBON & TOULHOAT 1996). This could lead to an enhanced release of such radionuclides to the geo- and biosphere.

Although there are still some uncertainties on the effect of cellulose degradation products on the mobilisation of radionuclides, it becomes increasingly clear that the most important degradation products with respect to their complexing properties are α- and β-ISA (Figure 1). GREENFIELD et al. (1993, 1995) degraded cellulose in a cement/water mixture at elevated temperature (80 °C) for different timescales and found that ISA was the main

degradation product. The effect of the degradation products on the solubility of Pu(IV) was explained by a strong complexation of Pu(IV) by ISA. BOURBON (1994) studied the degradation of cellulose in artificial cement pore waters (containing hydroxides of Na, K and Ca) at pH 13.0 and 13.5 at 60 °C and 20 °C. He came to the same conclusion, that ISA was the main degradation product. This is in agreement with the knowledge on the alkaline degradation of cellulose in presence of Ca^{2+} (BLEARS et al. 1957, MACHELL & RICHARDS 1960).

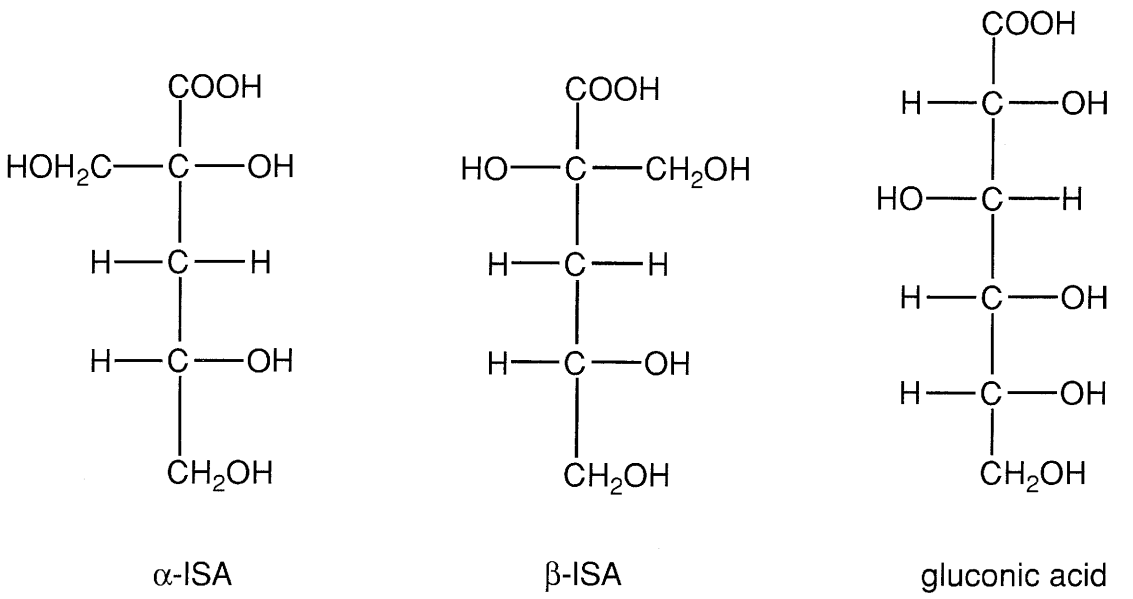

Figure 1: Chemical structure of α-ISA, β-ISA and gluconic acid

1.2 Effect of ligands on the sorption of radionuclides

1.2.1 Reversible sorption

The coordination of a sorbing metal, M, by a ligand, L, in solution, competes with the metal binding (sorption) on a solid phase, S. The main parameters determining the distribution of M between the liquid and the solid phase in a ternary system of M, L and S, are the stability of the aqueous complexes formed, the sorption mechanisms (reversible/irreversible sorption of M, surface precipitation of M, sorption of ligands, sorption of complexes) and the sorption strength (interaction coefficient).

The most simple situation is the case where only the metal (radionuclide) sorbs in a reversible way on the solid phase and the ligand and complexes formed do not sorb. Assume that a metal M sorbs on a site S of any solid phase as given by the following reaction:

$$M + S \Leftrightarrow MS \qquad (1)$$

The extent of sorption is usually expressed as a distribution ratio (R_d).
In absence of an organic ligand L, the distribution coefficient (R_d^o) is defined as:

$$R_d^o = \frac{\text{amount of metal sorbed on the solid phase}}{\text{amount of metal in solution}} = \frac{\{MS\}}{[M] + [MI_m^k]} \qquad (2)$$

where {MS} is the amount of metal sorbed on the solid in $mol \cdot kg^{-1}$, [M] is the concentration of free, uncomplexed metal in the equilibrium solution in $mol \cdot l^{-1}$, and $[MI_m^k]$ represents the concentration of complexes of M with any ligand I^k in solution. Note that these MI_m^k complexes are mainly complexes with inorganic ligands (OH^-, carbonate,...). Equation (2) can also be written as:

$$R_d^o = \frac{\{MS\}}{[M] \cdot \left(1 + \sum_k \sum_m \beta_m^k \cdot [I^k]^m\right)} \qquad (3)$$

where β_m^k are the overall stability constants of the MI_m^k species and $[I^k]$ are the concentrations of the free, uncomplexed ligands I^k.
In presence of an organic ligand L, forming mononuclear 1:n complexes with M according to:

$$M + nL \Leftrightarrow ML_n \qquad (4)$$

the distribution ratio (R_d) can be expressed as:

$$R_d = \frac{\{MS\}}{[M] + [MI_m^k] + [ML_n]} \qquad (5)$$

or

$$R_d = \frac{\{MS\}}{[M] + \sum_k \sum_m [M] \cdot \beta_m^k \cdot [I^k]^m + \sum_n [M] \cdot \beta_n \cdot [L]^n} \quad (6)$$

$$R_d = \frac{\{MS\}}{[M] \cdot A \cdot \left(1 + \frac{\sum_n \beta_n \cdot [L]^n}{A}\right)} \quad (7)$$

where:

$$A = 1 + \sum_k \sum_m \beta_m^k \cdot [I^k]^m \quad (8)$$

β_n are the stability constants of the ML_n complexes and [L] is the concentration of the free, i.e. uncomplexed, organic ligand L. For situations where the sorbed metal covers only a small fraction of the total amount of available sorption sites (this is mostly the case at low metal concentration), sorption can be assumed to be linear (BROUWER et al. 1983, BRADBURY & BAEYENS 1995), i.e.:

$$\{MS\} << \{S\} \quad \Rightarrow \frac{\{MS\}}{\{M\}} = \text{constant} \quad (9)$$

where {MS} is the amount of sorbed metal M ($mol \cdot kg^{-1}$) and {S} is the amount of sorption sites S ($mol \cdot kg^{-1}$). Combining equation (7) and (3) gives:

$$R_d = \frac{R_d^o}{\left(1 + \frac{\sum_n \beta_n \cdot [L]^n}{A}\right)} \quad (10)$$

The sorption reduction caused by the presence of a ligand L in solution can be expressed as a sorption reduction factor (F_{red}) and is defined as:

$$F_{red} = \frac{R_d^o}{R_d} = 1 + \frac{\sum_n \beta_n \cdot [L]^n}{A} \quad (11)$$

Expression (11) shows that the sorption reduction caused by a given organic ligand L, depends on the stability constants of the ML_n complexes and on the

concentration of the free ligand L. Only when the ML_n complexes dominate the speciation in solution, i.e. when:

$$\sum_n \beta_n \cdot [L]^n \quad >> \quad A \qquad (12)$$

ligand L has a significant effect on the sorption of M. The solid line in Figure 2 illustrates F_{red} as a function of the free ligand concentration L for the case where only a 1:1 complex is formed with a stability constant logK = 6 and where A = 1 (no other ligands present).

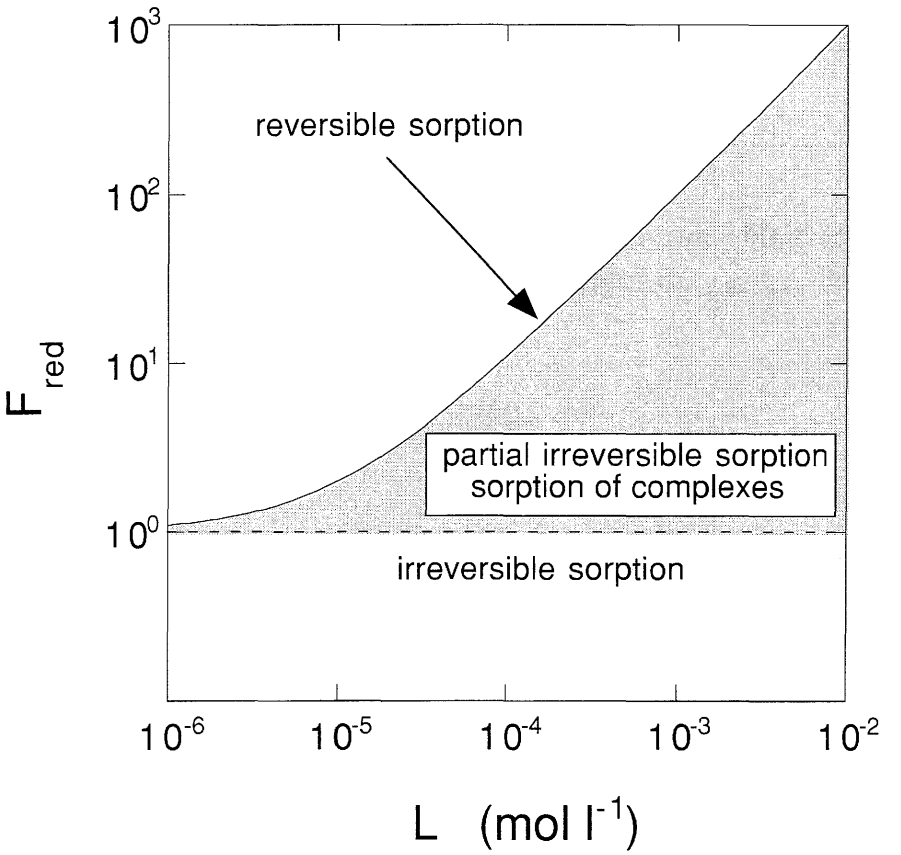

Figure 2: Dependence of the sorption reduction factor (F_{red}) on the ligand concentration L. The solid line represents the maximal effect that can be expected for a ligand forming a 1:1 complex.

1.2.2 Irreversible sorption (incorporation) and partial irreversible sorption

The assumptions that metals sorb reversibly on the solid phase and that metal complexes do not sorb at all might not be realistic. It is possible that a sorbed metal is incorporated in a solid phase. This process can be regarded as a kind of non-reversible sorption. Non-reversible sorption results in a smaller (or even no) effect of a ligand than can be expected from calculations based on equation (11). Assume that a fraction of the reversibly sorbed metal (MS_{rev}) is incorporated in the solid phase and transformed in an irreversibly bound species MS_{irr}:

$$M + S \Leftrightarrow MS_{rev} \tag{13}$$

$$MS_{rev} \rightarrow MS_{irr} \tag{14}$$

where MS_{rev} represents the metal reversibly sorbed and MS_{irr} represents the metal irreversibly sorbed. For the reversibly sorbed metal, one can write a R_d expression as:

$$R_{d,rev} = \frac{\{MS_{rev}\}}{[M_{sol}]} \tag{15}$$

where $\{MS_{rev}\}$ is the reversibly sorbed part of the metal ($mol \cdot kg^{-1}$) and $[M_{sol}]$ is the concentration of the metal in solution. For the irreversibly sorbed metal, the R_d concept cannot be applied since we are not dealing with equilibrium processes from a thermodynamic point of view. The further use of the R_d concept in such a case requires the introduction of a constant term C – representing the irreversibly sorbed metal – in the R_d expression of the reversibly sorbed metal:

$$R_{d,mix} = R_{d,rev} + C \tag{16}$$

When a ligand L, forming a complex with the metal M according to reaction (4), is now added to such a system, only the metal that is sorbed reversibly on the surface (MS_{rev}) can be affected by the complexation reaction. Assuming that

the sorption behaviour of the reversibly sorbed metal is a linear one, $R_{d,rev}$ in equation (16) equals R_d in equation (10). Combining equation (10) and (16) gives:

$$R_{d,mix} = \frac{R^o_{d,rev}}{\left(1+\frac{\sum_n \beta_n \cdot [L]^n}{A}\right)} + C \qquad (17)$$

where $R^o_{d,rev}$ represents the R_d of the reversibly sorbed metal in absence of a ligand L. In case where the metal is completely incorporated in the solid phase, $R^o_{d,rev}$ in equation (17) equals zero and a ligand L will have no effect on the sorption. This situation is represented by the dashed line in Figure 2. In case where the metal is only reversibly sorbed, the constant C in equation (17) equals zero and a ligand L will have its maximal effect on sorption. In such a case equation (17) equals equation (10). As already discussed earlier, the solid line in Figure 2 represents this case. In case of a partially irreversible sorption, the sorption reduction lies between the two boundaries represented by the solid and the dashed lines, depending on the fraction of irreversibly sorbed metal.

1.2.3 Sorption of metal complexes

For situations where metal complexes sorb, i.e.:

$$ML_n + S \Leftrightarrow ML_nS \qquad (18)$$

the distribution coefficient (R_d^{ter}) can be written as:

$$R_d^{ter} = \frac{\{MS\} + \{ML_nS\}}{[M] + [M_mL_n^k] + [ML_n]} \qquad (19)$$

Comparison of equation (5) and (19) shows that:

$$R_d^{ter} \geq R_d \qquad (20)$$

In case of metal-complex sorption, the sorption reduction factor will be lower than given in equation (11). How much lower depends on the sorption mechanism of ML_n and the interaction strength (SCHINDLER 1990). The shaded area in Figure 2 represents, beside partially irreversible sorption, the situation where metal-complexes sorb themselves on the solid phase.

It is clear that the solid line in Figure 2 represents the maximum sorption reduction that can be expected for a given ligand L. Therefore, assuming reversible sorption simplifies the problem and is a good first approximation for evaluating the effect of a ligand on sorption. The effect of the ligand depends only on its concentration in solution and on its interaction strength with the radionuclides. Hence, the concentration of a ligand together with the stability constant of the complexes formed, are key parameters for safety assessment, enabling one to calculate the most adverse effect of a ligand on sorption of radionuclides.

1.3 Experimental studies needed

As already mentioned, ISA is suspected to be the main ligand formed during alkaline degradation of cellulose. Its concentration in a cement pore solution is a key parameter in the assessment of cellulose degradation. Its concentration depends on several factors such as:

- the amount and type of cellulose emplaced in the cement (cellulose loading)
- the type of degradation reactions and the kinetics involved
- the extent of cellulose degradation
- the stability of ISA formed
- the sorption of ISA on cement phases
- the formation of sparingly soluble salts with e.g. Ca^{2+}

These factors have been little studied, or not studied at all and motivated us to initiate a study on the degradation of cellulose. A long term degradation experiment (4 years) was started in February 1995. The degradation conditions chosen were very similar to those of the near field of a cementitious repository in the first stage of cement degradation (BERNER 1990). The main goal of the long term study is to get information on:

- the most important degradation products formed under the near field conditions of the first stage of cement degradation
- the degradation kinetics and extent of cellulose degradation
- the effect of the type of cellulose on the degradation products formed
- the stability of the degradation products under alkaline conditions
- the sorption of the degradation products on cement
- the influence of the degradation products and pure ISA on the sorption of Ni(II), Eu(III) and Th(IV). The rational behind the use of these metals is to have a representative for three classes of important metals. Ni(II) represents the bivalent metals (transition metals), Eu(III) the trivalent and Th(IV) the tetravalent metals. The effect on the sorption of Cs(I) and Sr(II) was not studied because no or only very weak complexation for these elements is expected (see VERCAMMEN et al. 1997).

The information coming out of the study will be used to estimate the most likely concentration of ISA in a cement pore water for a given cellulose loading and to evaluate (quantify) the overall effect of cellulose degradation on the sorption of radionuclides on cement. The results will be integrated in a sorption data base to estimate sorption reduction factors for different radionuclides in those parts of the repository where cellulose is present (BRADBURY & VAN LOON 1998).

The intention of the present study is surely not to get a complete and detailed mechanistic view on alkaline degradation of cellulose, but to understand the processes so far, that an estimation of maximum effects that can be expected on the release of radionuclides, can be made.

2 THE CHEMISTRY OF CEMENT PORE WATER

The chemistry of cement pore water in a repository has been discussed in detail by BERNER (1990) and NEALL (1994). They assumed a homogeneous repository and used a mixing tank model to study the evolution of the pore water as a function of pore water exchange cycles. The composition of the pore water is, to a large extent, determined by the composition of the cement and the water flow through the repository. The evolution of the pore water chemistry can be grossly divided into three stages. In a first stage, the dissolution of NaOH and KOH – present in cement as "impurities" – causes a (Na,K)OH cement pore water saturated with respect to $Ca(OH)_2$. The pH of this initial pore water lies around 13.4 (concentration of OH^- is 0.3 M) and the Ca concentration is about 2 mM. In a second stage, after all NaOH and KOH has been leached out, the composition of the pore water is determined by the dissolution of $Ca(OH)_2$. The pH of the pore water falls to 12.5 and the Ca concentration increases up to 20 mM. In a third stage - when all the $Ca(OH)_2$ has dissolved - the pH falls further and hydrated Ca-Si phases (CSH-gels) start dissolving.

Based on assumptions made for the waterflow and the permeability and porosity of the cement, the pH of the cement pore water was calculated to remain above 12.5 for periods of the order of 10^5 years (BERNER 1990).

3 COMPOSITION AND STRUCTURE OF CELLULOSE AND HEMICELLULOSE

3.1 Cellulose

Cellulose is the most abundant organic material in the biosphere. It is the main component of plant sources, serving as the structural material by which plants, trees, as well as grasses sustain the strength to stay upright. It occurs in almost pure form in cotton fibers (90 %) and to a less extent in flax (80%), jute (60-70 %) and wood (40-50 %). Cellulose is a linear macromolecule composed of up to 10,000 (1,4)-β-D-glucopyranose units (Figure 3), and only the configuration of the C_1 position is different from that of amylose that is made of (1,4)-α-D-glucopyranose (OKAMURA 1991). The number of glucose units in cellulose represents its degree of polymerisation (DP).

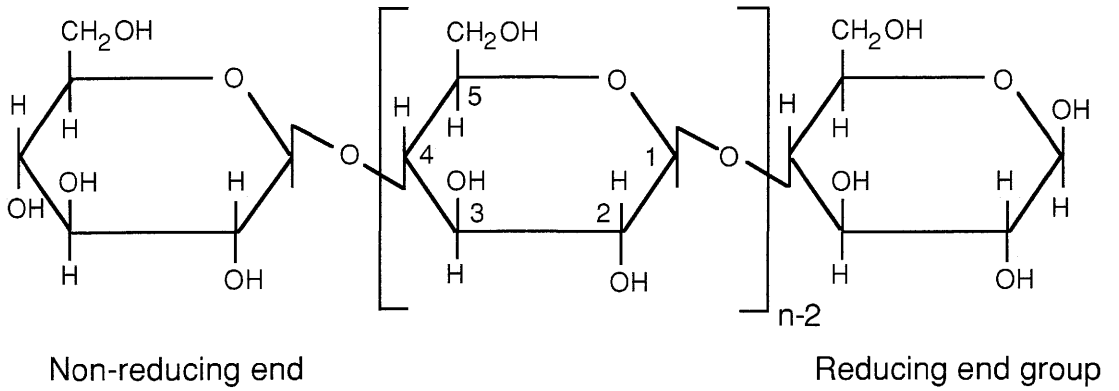

Figure 3: Chemical structure of cellulose (DP = n).

The cellulose molecule has a non-reducing end and a reducing one. The reducing end is a latent aldehyde and, like an aldehydo function, responds to both reduction and oxidation processes. As will be seen later, the reducing end group plays a key rôle in the alkaline degradation of cellulose.

The cellulose molecular chains are ordered into strands as cellulose microfibrils through inter- and intra-molecular hydrogen bonding (KRÄSSIG 1985). These microfibrils contain approximately 40 cellulose chains and have a diameter of 35 Å. They also have crystalline and amorphous regions as depicted in Figure 4. The alkaline degradation takes place in the amorphous regions of cellulose (HAAS et al. 1967, LEWIN 1985).

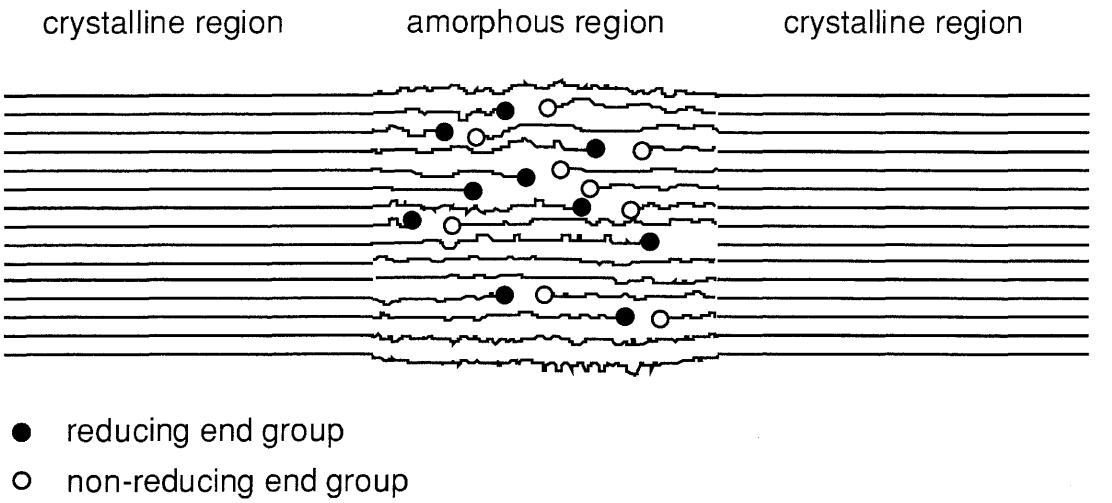

Figure 4: Microfibrillar structure of hydrocellulose (HAAS et al. 1967).

3.2 Hemicelluloses

Hemicelluloses are polysaccharides that occur in plant tissues together with cellulose, and are, next to cellulose, the most abundant organic materials in the biosphere. Structurally, the hemicelluloses differ from cellulose in that they are branched and have much lower molecular weights. Hemicelluloses are primarily modified xylans, galactoglucomannans, glucomannans and arabinogalactans. All of these polysaccharides are built up from a relatively limited number of sugar residues; the principal ones are: D-xylose, D-mannose, D-glucose, D-galactose, L-arabinose and 4-O-methyl-D-glucuronic acid.

3.2.1 Hemicelluloses in hardwoods (Angiosperms)

In hardwoods, 4-O-methylglucuronoxylan is the most important hemicellulose (20-35 %). Xylan is, compared to cellulose, a small molecule. Its backbone is composed of up to 150-200 (1,4)-β-D-xylopyranose units (Figure 5). Every tenth xylose residue, on the average, is substituted at C-2 by a 4-O-methylglucuronic acid residue. Hence, the xylose content in xylan is approximately 80 % and the 4-O-methylglucuronic acid content is 20 %.
Minor amounts of glucomannan are present in hardwoods (3-5%). They are composed of randomly β-(1,4)-linked D-glucopyranose and D-mannopyra-

nose residues in a ratio 1:2. The number-average degree of polymerisation is about 70 (McGINNIS & SHAFIZADEH 1980).

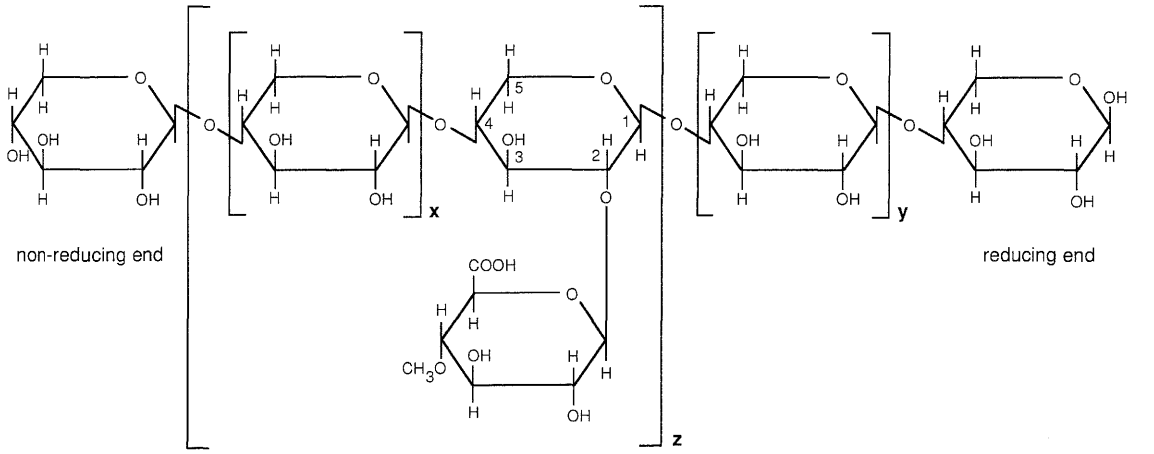

Figure 5: Chemical structure of xylan (from SAARNIO et al. 1954) with x = y = 9, $z = \frac{DP - y - 2}{x + 2}$ (DP = degree of polymerisation).

3.2.2 Hemicelluloses in softwoods (Gymnosperms)

In softwoods such as pines, glucomannan is the main hemicellulose. Glucomannans of softwoods are essentially linear polysaccharides composed of β-(1,4)-linked D-mannose and β-(1,4)-linked D-glucose residues, to which are attached various amounts of α-linked D-galactose end groups. The mannose and glucose residues are present in the ratio 3:1 and are randomly distributed in the chain. These glucomannans are classified as galacto-glucomannan or glucomannan, according to the content of the D-galactose residue. The polysaccharide that has higher proportions of D-galactose residues (D-Gal:D-Gluc:D-Man = 1:1:3) is called galactoglucomannan and the one that has less proportions of D-galactose residues (D-Gal:D-Gluc:D-Man = 0.1:1:3) is called glucomannan (SHIMIDZU 1991). The former is soluble in water, the latter in alkali. In softwoods, galactoglucomannan is the main glucomannan present (12-18 %).

Besides galactoglucomannan, substantial amounts of arabino-(4-O-methylglucurono)-xylan are present (7-15%). Arabino-(4-O-methylglucurono)-xylan contains generally one 4-O-methyl-D-glucuronic acid residue per 5-6

and one L-arabinose per 5-12 D-xylose residues, attached to C-2 and C-3, respecively, of β-(1,4)-linked D-xylose residues (McGINNIS & SHAFIZADEH 1980, SHIMIDZU 1991).

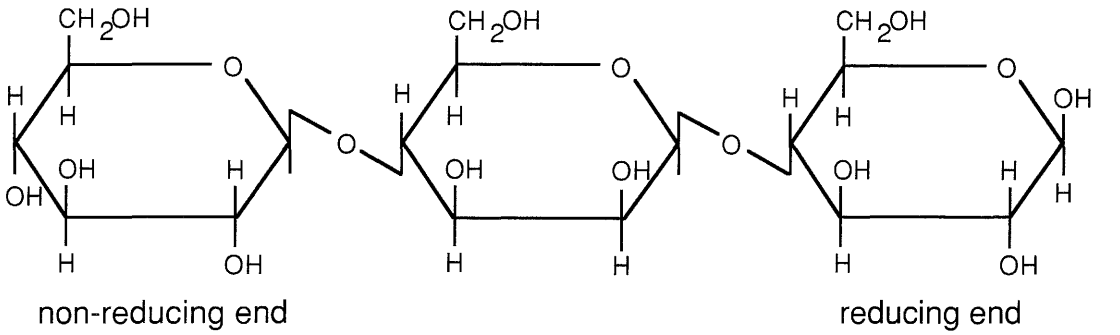

Figure 6: Partial chemical structure of glucomannan (backbone).

3.2.3 Conclusions

Based on the previous discussion of the presence of hemicellulose in wood, one can expect that hemicelluloses will be present in paper. The amount of hemicelluloses present in paper, however, is variable and depends strongly on the type of raw material used for paper production (hardwoods or softwoods) and from the pulping process used. Quantification of the fraction of hemicellulose is difficult, but a value of several percents up to 10% seems to be a reasonable estimation.

Hemicelluloses are, in contrast to cellulose, soluble in alkali. Aqueous KOH selectively extracts xylan and leaves glucomannan in the wood. Glucomannan is soluble in aqueous NaOH. Both xylan and glucomannan are expected to be soluble in cement pore water, containing both Na- and KOH.

4 THEORETICAL ASPECTS OF ALKALINE DEGRADATION OF CELLULOSE

This chapter represents a literature study on alkaline degradation of cellulose. It gives an overview of the most important degradation mechanisms involved and shows how alkaline degradation of cellulose can be quantified and which parameters are necessary for doing such calculations. It further shows how these parameters can be extrapolated from literature data.

4.1 Peeling off reaction

4.1.1 General reaction mechanism

The peeling off reaction is an endwise degradation process by which a reducing end group is split off from the cellulose chain resulting in soluble degradation products such as isosaccharinic acid. The peeling off reaction is controlled by two competing reactions: a progressive shortening of the cellulose molecule in which glucose units are progressively eliminated from the cellulose molecule (starting at the reducing end group) and a stopping reaction in which the reducing end group is converted to an alkalistable end group while it is still attached to the cellulose chain. The degradation reaction starts with and aldose-ketose isomerisation which proceeds via a Lobry de Bruyn-Alberda van Ekenstein transformation (LAI 1991, WHISTLER & BeMILLER 1958, SPECK 1958). After this transformation, the end unit is liberated from the chain by an elimination of the rest of the cellulose chain as a glycoxy anion. This elimination takes place when the chain is in the position β to a carbonyl group. The liberated end unit forms a 2,3-diketone intermediate and undergoes a benzilic acid type of rearrangement to isosaccharinic acid (LAI 1991, WHISTLER & BeMILLER 1958, BLEARS et al. 1957, MACHELL & RICHARDS 1960) or can undergo fragmentation by a reversed aldol condensation to give smaller molecules such as glyceraldehyde, which is then converted via methylglyoxal to lactic acid (SJÖSTRÖM 1977). In another reaction, the formation of 2,5-dihydroxyvaleric acid proceeds by elimination of formic acid, followed by a benzilic acid rearrangement (SJÖSTRÖM 1977). The rest of the chain is free to continue degradation. A detailed reaction scheme is given in Figure 7.

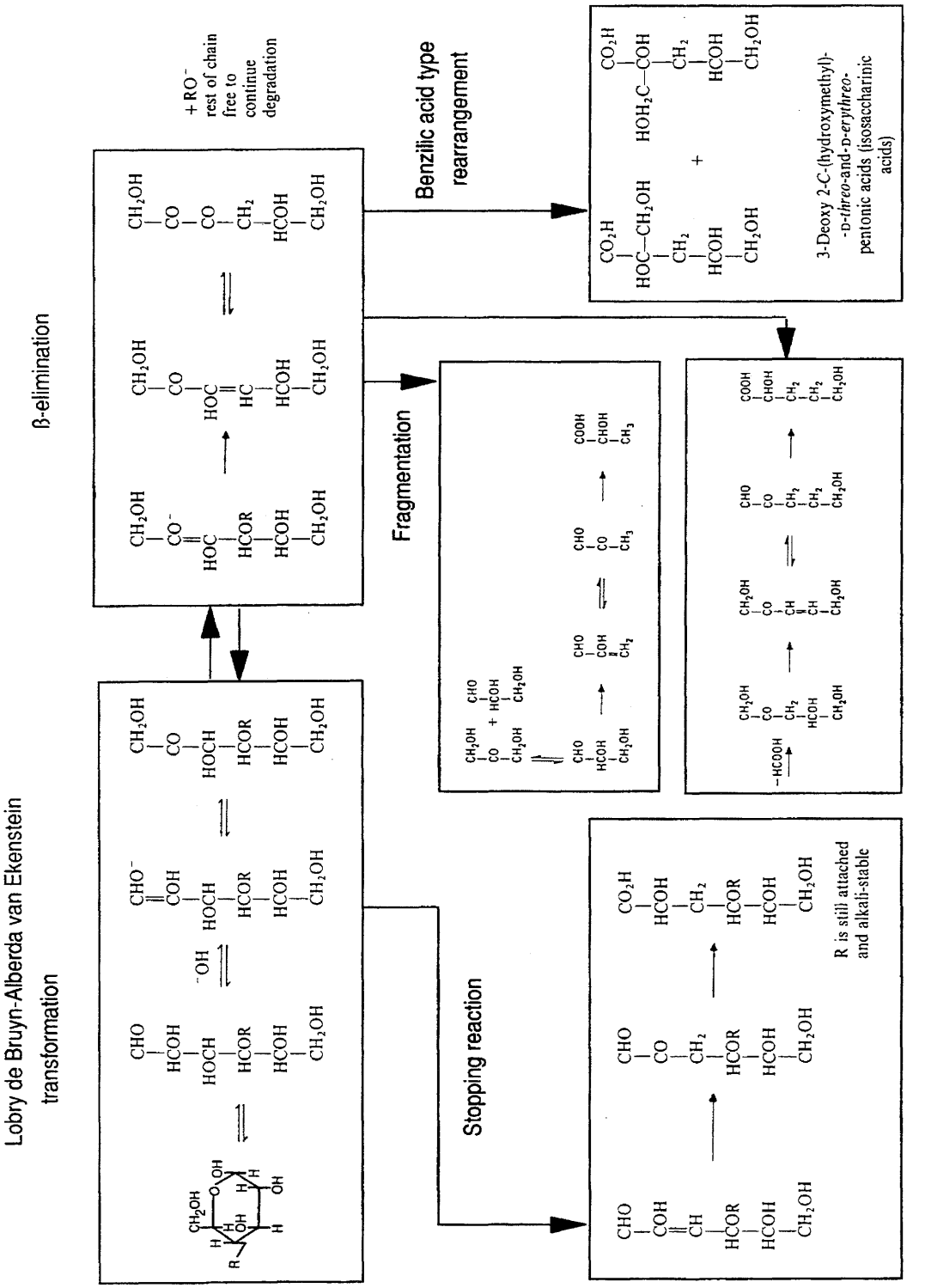

Figure 7: Alkaline degradation of 4-O substituted residues in polysaccharides.

The stopping reaction can be sub-divided in a *chemical* and a *physical stopping reaction*. The former is the transformation of a reducing end group into a stable metasaccharinic acid end group (Figure 7). The latter implies that a reducing end group reaches the crystalline region of the cellulose and is no longer accessible to alkali (HAAS et al. 1967). The physical stopping reaction is not an abrupt process since there is a gradual transition from the amorphous to the crystalline region rather than a distinct interface. A more schematic presentation of the peeling off process is given in Figure 8.

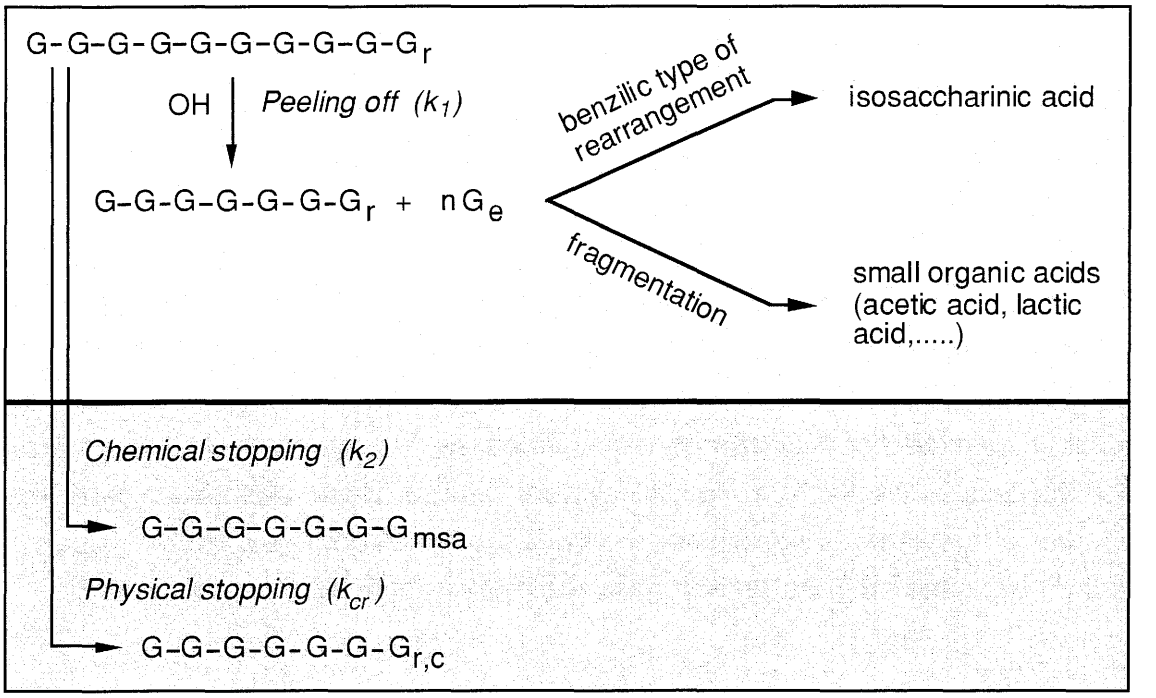

Figure 8: Schematic presentation of the peeling off reaction. G is a glucose monomeric unit (glucopyranose), G_{msa} is a stable metasaccharinic acid end group, G_e is a glucose unit eliminated and n are the number of glucose units eliminated (n = 50 - 60). G_r is a reducing end group in the amorphous region of the cellulose fibre and $G_{r,c}$ is a reducing end group in the crystalline region of the cellulose fibre.

4.1.2 Kinetic aspects of the peeling off reaction

4.1.2.1 General reaction kinetics

The kinetics of the peeling off reaction of cellulose have been studied in detail by HAAS et al. (1967). They performed kinetic studies on hydrocellulose (prepared from cotton) with a degree of polymerisation (DP) of 166 at different temperatures (ranging from 65 °C to 132 °C) in 1.25 M NaOH solutions. The liquid/solid ratio in their studies was so high (100/1) that the NaOH concentration remained practically constant during the whole reaction time.
For the progressive chain degradation, at a constant concentration of OH^-, the following equation can be written:

$$\frac{d(G_e)}{dt} = k_1 \cdot (G_r) \qquad (21)$$

(G_e) is the mole fraction of glucose units eliminated, (G_r) the mole fraction of reducing end groups available for the reaction and k_1 the pseudo first order reaction rate constant. The mole fraction of a component is defined as the number of moles of that component divided by the number of moles of all components in the system. For the system with cellulose described here, the number of moles of all components equals the initial degree of polymerisation of the cellulose (DP_o). As an example, the mole fraction of G_e is defined as:

$$(G_e) = \frac{G_e}{DP_o} \qquad (22)$$

For the chemical stopping reaction, the following rate equation can be written:

$$\frac{d(MSA)}{dt} = k_2 \cdot (G_r) \qquad (23)$$

where (MSA) is the mole fraction of stable metasaccharinic acid end groups formed and k_2 the pseudo first order reaction rate constant for the chemical stopping reaction. Although no chemical reaction is involved in the physical stopping process, a similar rate equation can be written for this physical stopping reaction:

$$\frac{d(G_{r,c})}{dt} = k_{cr} \cdot (G_r) \tag{24}$$

where $(G_{r,c})$ is the mole fraction of reducing end groups not available for reaction and k_{cr} is the formal reaction rate constant of termination caused by inaccessibility. The decrease in reactive reducing end groups is caused by the two stopping reactions and can be combined as:

$$-\frac{d(G_r)}{dt} = k_2 \cdot (G_r) + k_{cr} \cdot (G_r) = k_t \cdot (G_r) \tag{25}$$

where k_t ($k_t = k_2 + k_{cr}$) is the total reaction rate constant for chain termination. At t=0, $(G_r) = (G_r)_o$, the initial reducing end group content. Integration of equation (25) gives:

$$(G_r) = (G_r)_o \cdot e^{-k_t \cdot t} \tag{26}$$

Substitution of equation (26) in equation (21) gives:

$$\frac{d(G_e)}{dt} = k_1 \cdot (G_r)_o \cdot e^{-k_t \cdot t} \tag{27}$$

At t=0, $(G_e) = 0$ and equation (27), after integration, give:

$$(G_e) = \frac{k_1}{k_t} \cdot (G_r)_o \cdot (1 - e^{-k_t \cdot t}) \tag{28}$$

Substitution of equation (26) in equation (23) and (24) gives:

$$\frac{d(MSA)}{dt} = k_2 \cdot (G_r)_o \cdot e^{-k_t \cdot t} \tag{29}$$

and

$$\frac{d(G_{r,c})}{dt} = k_{cr} \cdot (G_r)_o \cdot e^{-k_t \cdot t} \tag{30}$$

At t=0, (MSA) and $(G_{r,c}) = 0$ and integration of equations (29) and (30) gives:

$$(MSA) = \frac{k_2}{k_t} \cdot (G_r)_o \cdot (1 - e^{-k_t \cdot t}) \quad (31)$$

and

$$(G_{r,c}) = \frac{k_{cr}}{k_t} \cdot (G_r)_o \cdot (1 - e^{-k_t \cdot t}) \quad (32)$$

The maximum amount of (G_e) at $t = \infty$ can be calculated from equation (28):

$$(G_e)_{max} = \frac{k_1}{k_t} (G_r)_o \quad (33)$$

The maximum amount of cellulose degraded, $(celdeg)_{max}$, equals the maximum amount of glucose units peeled off, $(G_e)_{max}$, and can be written as:

$$(cel\,deg)_{max} = (G_e)_{max} = \frac{k_1}{k_t} (G_r)_o \quad (34)$$

Equation (34) shows that $(celdeg)_{max}$ depends on the initial mole fraction of reducing end groups in the cellulose, $(G_r)_o$, and on the ratio of the reaction rate constants of the propagation reaction (k_1) and the stopping reactions (k_t).
The initial mole fraction of reducing end groups is defined as:

$$(G_r)_o = \frac{\text{moles of reducing end groups}}{\text{moles of glucose units in the chain}} \quad (35)$$

The mole fraction of reducing end groups depends on the average amount of reducing end groups in a cellulose molecule and on the degree of polymerisation (DP). Both these parameters have an effect on the amount of cellulose that will be degraded. In theory, a cellulose molecule has one reducing end group. In reality, not all cellulose molecules have reducing end groups because the reducing end groups may have been transformed to non-reducing end groups during the pulping process (PROCTER & WIEKENKAMP 1969, PROCTER & APELT 1969, BRYCE 1980, CHIANG & SARKANEN 1984). The average number of reducing end groups lies between 0 and 1. Consequently, the mole fraction of reducing end groups in cellulose with a degree of polymerisation DP is:

$$0 \leq (G_r)_o \leq \frac{1}{DP} \tag{36}$$

The presence of one reducing end group per cellulose molecule results in the maximum value of the concentration of reducing end groups $(G_r)_o$ for a cellulose molecule with a given degree of polymerisation, DP, and consequently results in the upper limit of the maximum amount of degradable cellulose. The amount of cellulose degraded by the peeling off reaction depends also strongly on the degree of polymerisation of cellulose. The larger the cellulose molecule, the lower the mole fraction of reducing end groups (as can be seen from equation 35) and the lower the extent of degradation (Figure 9).

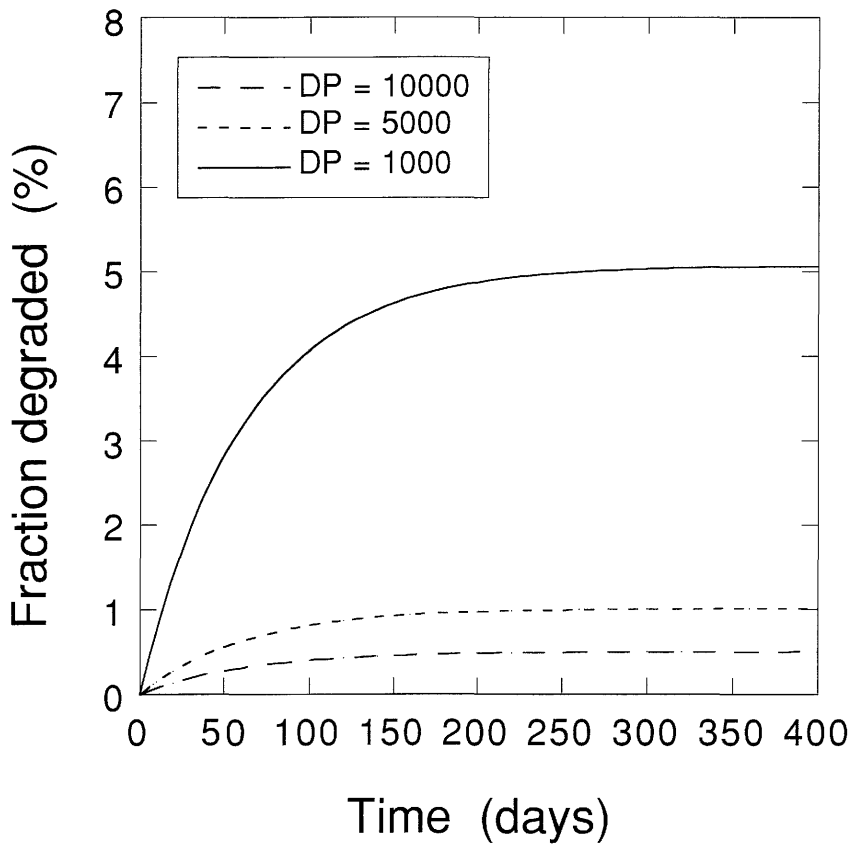

Figure 9: Degradation of cellulose as a function of time at 0.3 M OH^- and 25 °C for different degrees of polymerisation (DP). The solid lines were calculated using equation (28) with $k_1 = 3.4 \cdot 10^{-2}$ h^{-1} and $k_t = 6.8 \cdot 10^{-4}$ h^{-1} (values of k_1 and k_t taken from Table 2).

The effect of the degree of polymerisation (DP) on the extent of degradation is clearly demonstrated by experiments performed by RICHTZENHAIN et al. (1954). They prepared hydrocellulose from native cotton by treating the cotton with 1 M HCl at 50 °C for different periods of time, ranging from 1 hour to 480 hours. The treatment resulted in hydrolysed cellulose samples with a different degree of polymerisation ranging from 130 to more than 3000. After preparation, the hydrolysed cotton samples were degraded in 0.5 M NaOH at 100 °C. The extent of degradation of the samples was calculated from the amount of acids produced. The results are summarised in Figure 10, showing a plot of the extent of degradation, $(celdeg)_{max}$, against the degree of polymerisation. The relative standard uncertainty on $(celdeg)_{max}$ was estimated to be 10%.

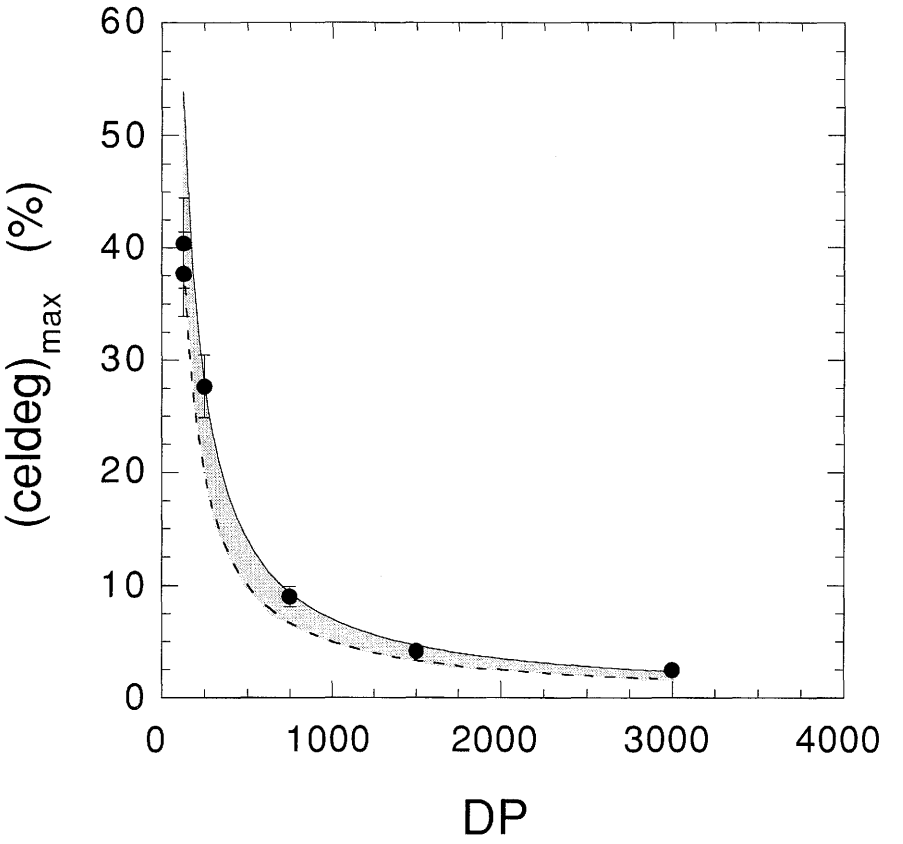

Figure 10: Dependence of the extent of degradation of hydrocellulose on the degree of polymerisation. Filled symbols represent the experimental data of RICHTZENHAIN et al. (1954). The curves were calculated using equation (34) with $k_1/k_t = 50$ (dashed line) and $k_1/k_t = 70$ (solid line).

The solid lines in Figure 10 were calculated using equation (34) with k_1/k_t = 50-70, under the assumption that $(G_r)_o$ = 1/DP. The figure clearly shows the dependence of the extent of degradation on the degree of polymerisation (or on the mole fraction of reducing end groups).

4.1.2.2 Effect of temperature on the reaction kinetics

The reaction rate constants k_1, k_2, k_{cr} and k_t were determined by HAAS et al. (1967) at different temperatures between 65 °C and 132 °C and an hydroxyl concentration of 1.25 M. The authors used hydrocellulose with DP = 166. The values are summarised in Table 1.

Table 1: Overview of the reaction rate constants for cellulose degradation (peeling off reaction) at different temperatures in 1.25 M NaOH (from HAAS et al. 1967).

T (°C)	k_1 (h^{-1})	k_2 (h^{-1})	k_{cr} (h^{-1})	k_t (h^{-1})	k_1/k_t
[1)]25	0.037	0.000013	[2)]0.00072	0.00073	51
65	4	0.004	0.057	0.06	67
78	17.8	0.03	0.26	0.29	61
87	46.3	0.1	0.64	0.74	63
100	147	0.50	1.60	2.1	70
132	1550	7	13.0	20	78

[1)] extrapolated by the Arrhenius equation (38):

$\log k_1 = 16.2 + 5257 \cdot T^{-1}$ → $k_1(25°C) = (3.7 \pm 2.6) \cdot 10^{-2}\ h^{-1}$

$\log k_2 = 17.2 + 6564 \cdot T^{-1}$ → $k_2(25°C) = (1.3 \pm 1.1) \cdot 10^{-5}\ h^{-1}$

$\log k_t = 13.9 + 5069 \cdot T^{-1}$ → $k_t(25°C) = (7.3 \pm 3.7) \cdot 10^{-4}\ h^{-1}$

[2)] the value of k_{cr} at 25 °C was calculated from the extrapolated values k_t and k_2 by using the equation $k_{cr} = k_t - k_2$ because k_{cr} is not a measured value but calculated from k_t and k_2

Values of these constants at lower temperatures can be estimated by applying the Arrhenius equation:

$$k = A \cdot e^{-E_a / R \cdot T} \qquad (37)$$

or in the linear form:

$$\log k = \log A - 0.434 \cdot \frac{E_a}{R \cdot T} \qquad (38)$$

with:

A	=	Arrhenius parameter (h^{-1})
k	=	reaction rate constant (h^{-1})
E_a	=	activation energy ($J \cdot mol^{-1}$)
R	=	universal gas constant ($J \cdot mol^{-1} \cdot K^{-1}$)
T	=	absolute temperature (K)

A logarithmic plot of k versus the reciprocal absolute temperature yields a straight line. Figure 11 illustrates the Arrhenius equation for the different reactions of the peeling off process.

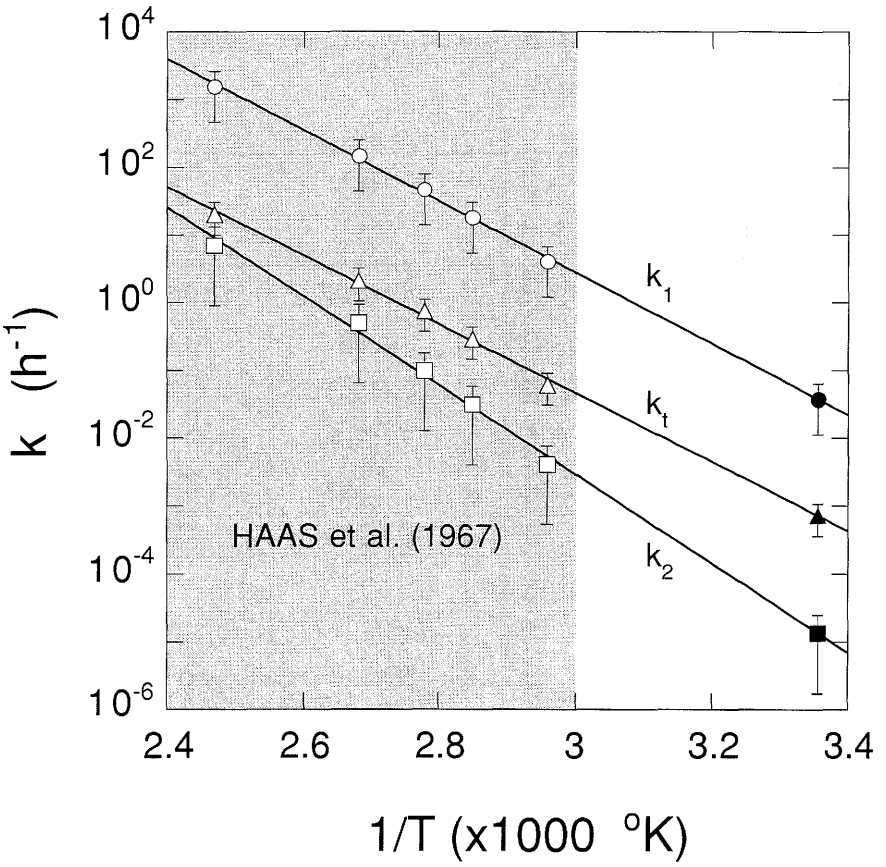

Figure 11: Arrhenius plot for the peeling off reaction (k_1: chain propagation, k_2: chemical stopping reaction, k_t: overall stopping reaction) of cellulose in 1.25 M NaOH. Open symbols represent data from HAAS et al. (1967), closed symbols are extrapolated values.

It is clearly shown that the relationship between the logarithm of the rate constants and the reciprocal absolute temperature is a linear one according to equation (38). Values for k_1, k_2 and k_t at 25 °C were calculated using equation (38) and are also summarised in Table 1. The uncertainty on the rate constants of the overall stopping reaction was estimated by a re-evaluation of the original data of HAAS et al. (1967) using equation (28). Based on the scattering of the original data, the relative standard uncertainty of the rate constants for the overall stopping reaction (RSU_{kt}) is assumed here to be ca. 50%. Rate constants for the propagation reaction and chemical stopping reaction were calculated from equation (34) and (31) respectively. The RSU on the calculated constants are 70% and 87 % for k_1 and k_2 respectively. The uncertainty on the estimated values was assumed to be the same as for the measured data. The activation energy (E_a) of the different reactions can be calculated from the slope of the lines. The propagation reaction has an activation energy of 101 $kJ \cdot mol^{-1}$ and the activation energy of the overall stopping reaction is 97 $kJ \cdot mol^{-1}$. The extent of cellulose degradation by the peeling off reaction depends on the ratio of the rate constants k_1/k_t (equation 34) and consequently on the reaction temperature. At lower temperatures, the degree of degradation is smaller than at higher temperatures. This can be explained properly by the slightly higher activation energy of the propagation reaction compared to the overall stopping reaction, resulting in a higher ratio at higher temperatures. The effect of temperature, however, is relatively small and of minor importance.

From Table 1 it can be derived that at high temperature, chemical and physical stopping reactions are equally important ($k_2 \leq k_{cr}$), whereas at low temperatures, the physical stopping reaction seems to be the dominating stopping mechanism ($k_2 << k_{cr}$).

4.1.2.3 Effect of hydroxyl concentration on the peeling off reaction kinetics

The concentration of OH^- in the cement pore water in the initial stage of cement degradation is about 0.3 M (see chapter 2), and the Ca level is about 2 mM. To evaluate the degradation of cellulose under such repository conditions, the effect of pH (or OH^- concentration) and the effect of Ca^{2+} on the

peeling off reaction have to be discussed. The rate constants discussed in the previous section were derived for reaction conditions of 1.25 M NaOH in the absence of Ca. No further systematic studies on the effect of $[OH^-]$ and $[Ca^{2+}]$ on the rate constants (k_1, k_2, k_{cr} and k_t) have been found in the literature for cellulose. Although no experimental data on the effect of OH^- and Ca^{2+} are available for cellulose, some data exist for other polymeric materials. Studies on amylose (LAI & SARKANEN 1969) and β-(1-3)-glucans (YOUNG et al. 1972) showed that the hydroxyl ion does not participate in the rate determining reaction step and that anionic species are involved in the peeling off and chemical stopping reaction for these polysaccharides. It was further shown that the alkaline degradation of amylose with α-(1-4)-glycosidic bonds (at temperatures < 120 °C) proceeds by the same reaction mechanisms as the alkaline degradation of cellulose with β-(1-4)-glycosidic bonds (LAI & SARKANEN 1969), i.e.:

- a chain propagation reaction (peeling off reaction), resulting in the formation of isosaccharinic acid
- a chemical stopping reaction by which the reducing end group is transformed into an alkali-stable metasaccharinic acid end group

A physical stopping reaction does not occur because amylose does not have a microfibrillar structure such as cellulose. Conclusions drawn from the study on amylose (LAI & SARKANEN 1969) are, to a large extent, applicable to cellulose. Figure 12 shows the dependence of the rate constants (for alkaline degradation of amylose) on the OH^- concentration. The rate constant for the peeling off reaction (k_1) increases with the hydroxyl concentration up to 0.3 M. Beyond 0.3 M, k_1 stays constant. The rate constant for the chemical stopping reaction (k_2) is negligibly small for a concentration of OH^- below 0.1 M and could not be quantified. Beyond 0.3 M, k_2 increases until the concentration of OH^- reaches a value of 1.5 M. Beyond 1.5 M, k_2 stays constant. It was also observed that up to 0.1 M, amylose completely degrades and that for 0.1 M < $[OH^-]$ < 1.5 M, the extent of degradation decreases. Beyond 1.5 M, the extent of degradation stays constant (LAI & SARKANEN 1969).
In analogy to amylose, it is assumed that the reactivity of the reducing end group in cellulose is proportional to its degree of deprotonation:

$$\text{cellulose} - G_r + OH^- \Leftrightarrow \text{cellulose} - G_r^- + H_2O \qquad (39)$$

The deprotonation constant is defined as:

$$K_1 = \frac{(G_r^-)}{(G_r)\cdot[OH^-]} \tag{40}$$

where (G_r^-) is the mole fraction of deprotonated reducing end groups and (G_r) is the mole fraction of protonated reducing end groups.

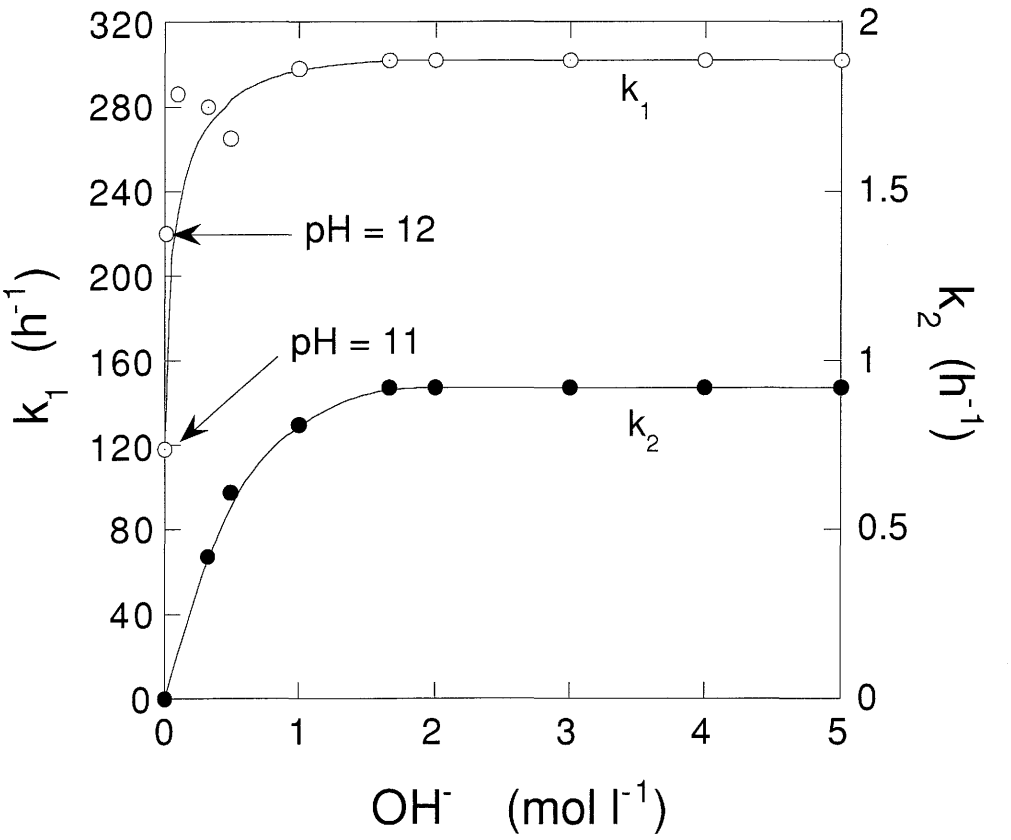

Figure 12: Dependence of the reaction rate constants for the peeling off reaction (k_1) and chemical stopping reaction (k_2) of amylose on the hydroxyl concentration at 100 °C (LAI & SARKANEN 1969).

From the mass balance:

$$(G_r)_{tot} = (G_r) + (G_r^-) \tag{41}$$

and equation (40), it can be shown that:

$$(G_r^-) = \frac{K_1 \cdot [OH^-]}{1 + K_1 \cdot [OH^-]} \cdot (G_r)_{tot} \quad (42)$$

where $(G_r)_{tot}$ represents the total mole fraction of reducing end groups. The rate equation for the propagation reaction can be written as:

$$\frac{d(G_e)}{dt} = k_1' \cdot (G_r^-) \quad (43)$$

where k_1' is the OH-independent first order rate constant for the peeling off reaction. Combining equation (42) and (43) results in:

$$\frac{d(G_e)}{dt} = k_1' \cdot \frac{K_1 \cdot [OH^-]}{1 + K_1 \cdot [OH^-]} \cdot (G_r)_{tot} \quad (44)$$

With:

$$k_1 = k_1' \cdot \frac{K_1 \cdot [OH^-]}{1 + K_1 \cdot [OH^-]} \quad (45)$$

equation (44) can be written as:

$$\frac{d(G_e)}{dt} = k_1 \cdot (G_r)_{tot} \quad (46)$$

where k_1 is the "conditional" OH-dependent rate constant. Equation (46) is very similar to equation (21). The formalism developed by HAAS et al. (1967) for the peeling off reaction was a special case of the more general formalism presented by equation (46) because their studies were performed at a high and constant concentration of OH^-.

For the stopping reaction, a further deprotonation of the reducing end group is required so that a second deprotonation step has to be introduced. The rate equation for the chemical stopping reaction can be written as:

$$\frac{d(MSA)}{dt} = k_2' \cdot (G_r^{2-}) \quad (47)$$

where k_2' is the OH-independent first order rate constant for the chemical stopping reaction and (G_r^{2-}) the mole fraction of twofold deprotonated

reducing end groups. Since, at low temperatures, the chemical stopping reaction plays a minor rôle in the overall stopping reaction of the alkaline degradation of cellulose (see Table 1, $k_2 << k_{cr}$), the dependence of k_2 on the hydroxyl concentration is not further discussed here.

The effect of $[OH^-]$ on the physical stopping reaction was not studied by LAI & SARKANEN (1969) because, as already mentioned, such a stopping process does not occur in amylose. For cellulose, however, the following rate equation – based on equation (24) – can be written assuming that the reaction rate is proportional to the mole fraction of deprotonated end groups:

$$\frac{d(G_{r,c})}{dt} = k'_{cr} \cdot \frac{K_1 \cdot [OH^-]}{1 + K_1 \cdot [OH^-]} (G_r)_{tot} \tag{48}$$

with:

$$k_{cr} = k'_{cr} \cdot \frac{K_1 \cdot [OH^-]}{1 + K_1 \cdot [OH^-]} \tag{49}$$

Equation (48) is similar to equation (44) for the peeling off reaction. This similarity can be justified as follows. Since the physical stopping reaction occurs when a reducing end group reaches the crystalline region of the cellulose fiber, its rate will depend strongly on the rate of the peeling off reaction. The faster the peeling off reaction, the faster a reducing end group will reach the crystalline region. Consequently, the rates of both reactions should be strongly correlated. The ratio k'_1 / k'_{cr} is constant and equals k_1 / k_{cr}.

From the considerations made above, the maximum amount of cellulose that will be degraded can be written as:

$$(\text{cel deg})_{max} = (G_e)_{max} = \frac{k'_1}{k'_t} \cdot (G_r)_o \tag{50}$$

where k'_1 and k'_t are the intrinsic (i.e. OH-independent) rate constants. Because of the assumption that the rate of stopping is proportional to the rate of degradation, the extent of cellulose degradation is independent of the OH^- concentration. This was experimentally confirmed by MACHELL & RICHARDS (1958) who did not see any effect of the alkali concentration on the extent of cellulose degradation in the range $0.125\ M < [OH^-] < 1.25\ M$. For a concentration of OH^- larger than 2 M, a significant effect of OH^- on the extent of degradation was observed. At these concentrations, however, the structure of

cellulose is changed (transition of crystalline to amorphous cellulose) resulting in a higher accessibility of the cellulose to OH^- (LAI & ONTTO 1979). The reaction rate, however, depends on the concentration of OH^-.
The values of the first order rate constants for cement pore water conditions (i.e. $[OH^-] = 0.3$ M) can be calculated by applying the following equation:

$$k_{i,0.3} = k_i' \cdot \frac{K_1 \cdot [OH^-]}{1 + K_1 \cdot [OH^-]} \qquad (51)$$

with:

$k_{i,0.3}$ = rate constant for $[OH^-] = 0.3$ M
k_i' = intrinsic rate constant
$[OH^-]$ = concentration of OH^- (M)
K_1 = deprotonation constant for the deprotonation of C_1-OH of the reducing end group ($K_1 \approx 30$, VUORINEN 1988)

The values of k_i' were calculated by applying equation (51) for $[OH^-] = 1.25$ M and the values of $k_{i,1.25}$ at 25 °C as summarised in Table 1.

Table 2: Overview of the reaction rate constants for cellulose degradation by the peeling off reaction extrapolated for 25 °C and recalculated for 0.3 M OH^-.

$[OH^-]$ (M)	**k_1** (h^{-1})	**k_2** (h^{-1})	**[2)] k_{cr}** (h^{-1})	**k_t** (h^{-1})
1.25	$3.7 \cdot 10^{-2}$	$1.3 \cdot 10^{-5}$	$7.2 \cdot 10^{-4}$	$7.3 \cdot 10^{-4}$
[1)] 0.3	$3.4 \cdot 10^{-2}$	$1.2 \cdot 10^{-5}$	$6.7 \cdot 10^{-4}$	$6.8 \cdot 10^{-4}$

[1)] calculated by equation (51)

[2)] $k_{cr} \approx k_t - k_2$

The values of the different rate constants for 0.3 M OH^- and 25 °C are summarised in Table 2. The difference in rate constant between 1.25 M and 0.3 M OH^- is very small because K_1 of the reducing end group is ≈ 30 or the deprotonation constant $pK_a \approx 12.5$ (LAI & SARKANEN 1969, YOUNG et al. 1972, VUORINEN & SJÖSTRÖM 1982, VUORINEN 1988). Hence beyond pH 13, the reducing end groups are almost completely deprotonated.

4.1.2.4 Effect of Ca^{2+} on the peeling off reaction kinetics

Ca^{2+} has a significant effect on the peeling off reaction (BLEARS et. al. 1957, MACHELL & RICHARDS 1958, MACHELL & RICHARDS 1960, COLBRAN & DAVIDSON 1961). Ca^{2+} seems to catalyse the benzilic acid type of rearrangement leading to the formation of ISA. Also the chemical stopping reaction is catalysed. The overall effect of the presence of Ca^{2+} is a lower degree of degradation and the formation of relatively more ISA at the expense of side products. No systematic kinetic studies on the alkaline degradation of cellulose in presence of Ca^{2+} have been performed.

4.2 Alkaline hydrolysis of cellulose

4.2.1 General reaction mechanisms

A second important process in alkaline degradation is the base-catalysed cleavage of glycosidic bonds (alkaline hydrolysis). Alkaline hydrolysis of cellulose cannot be studied separately from the peeling off reaction because hydrolysis produces new reducing end groups initiating a peeling off reaction. As illustrated in Figure 13, the degradation is initiated by cleavage of a glycosidic bond. The newly-formed reducing end groups give rise to a chain degradation (peeling off) process by progressively converting the terminal units to isosaccharinic acid and other products (see previous section).

4.2.2 Kinetic aspects of alkaline hydrolysis

4.2.2.1 General reaction kinetics

A few mechanisms are known for the base catalysed cleavage of glycosidic linkages. For cellulose, an internal nucleophilic substitution (SN_i) was found to

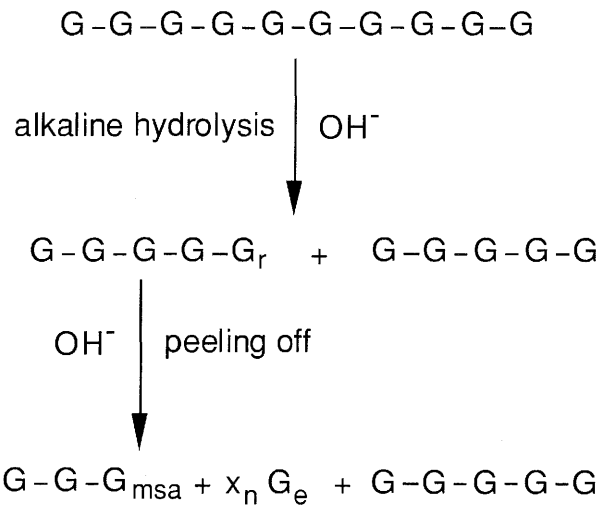

Figure13: Schematic overview of the alkaline degradation of cellulose by the base-catalysed cleavage of glycosidic bonds and the peeling off reaction. G_r = reducing end group, G_{msa} = alkali-stable meta-saccharinic acid end group, G_e = glucose units eliminated as ISA or other products, x_n = the number of the peeled off glucose units.

be the most evident one (LAI 1981). The SN_i-mechanism for base-catalysed cleavage of glycosidic bonds can be divided in two processes (LAI 1972). In a first step, a deprotonation reaction occurs:

$$GlcOH + OH^- \overset{K}{\longleftrightarrow} H_2O + GlcO^- \qquad (52)$$

In a second step, the intermediate product ($GlcO^-$) is transformed:

$$GlcO^- \xrightarrow{k} \text{degradation products (P)} \qquad (53)$$

Where GlcOH is the glycoside (cellulose in our case) and $GlcO^-$ is the anionic intermediate. K is the equilibrium constant between neutral and ionic glycosides (deprotonation constant) and k is the specific rate constant in the conversion of anionic intermediates to degradation products. The latter is the rate determining step in the overall reaction. The rate of alkaline degradation of glycosides can be expressed as:

$$\frac{d(P)}{dt} = k \cdot (GlcO^-) \tag{54}$$

where (P) represents the mole fraction of glycosides reacted after time t (or the mole fraction of degradation products formed) and ($GlcO^-$) is the mole fraction of ionised, intermediate glycosides at time t.
The "deprotonation" constant K is defined as:

$$K = \frac{(GlcO^-)}{\left\{(GlcOH)_o - (GlcO^-) - (P)\right\} \cdot [OH^-]} \tag{55}$$

where $(GlcOH)_o$ is the mole fraction of glycosides at t=0. Combination of equation (54) and (55) yields a rate equation which is integrated to give:

$$\ln \frac{(GlcOH)_o - (P)}{(GlcOH)_o} = -\frac{K \cdot k \cdot [OH^-]}{1 + K \cdot [OH^-]} \cdot t \tag{56}$$

If:

$$k_{obs} = \frac{K \cdot k \cdot [OH^-]}{1 + K \cdot [OH^-]} \tag{57}$$

where k_{obs} is the pseudo-first-order reaction rate constant, equation (56) becomes:

$$\ln \frac{(GlcOH)_o - (P)}{(GlcOH)_o} = -k_{obs} \cdot t \tag{58}$$

FRANZON & SAMUELSON (1957) studied the alkaline degradation of cellulose at 170 °C in 1.25 M NaOH. They observed a change in DP of the cellulose and a weight loss. The overall degradation was found to be the result of two processes: the cleavage of glycosidic bonds (resulting in a decrease of DP) followed by a peeling off reaction starting from the newly created reducing end group (resulting in weight loss). The amount of cellulose units peeled off after each chain break (x_n) was shown to be constant (x_n = 65) and independent of the DP within a wide range. The rate controlling step in the overall degradation process is the cleavage reaction.

The amount of cellulose left after degradation (Y) was found to be related to the degradation time (t) by the following equation:

$$\ln(Y) = -k \cdot t \tag{59}$$

with:
Y = fraction of cellulose left
k = rate constant (h^{-1})
t = time (h)

LAI & SARKANEN (1967) studied the alkaline degradation of cellulose at different temperatures between 146 and 186 °C in 1.25 M NaOH. They came to similar conclusions as FRANZON & SAMUELSON (1957) and showed that the rate of degradation was conform with the following equation:

$$\ln(Y) = -k_{obs} \cdot x_n \cdot t \tag{60}$$

with:
Y = fraction of unreacted cellulose
t = time (h)
k_{obs} = rate constant (h^{-1})
x_n = average number of glucose units peeled off (x_n = 65)

Equations (59) and (60) are very similar. Since the number of glucose units peeled off for each chain break (x_n) is constant, it can be integrated in the rate constant as was done by FRANZON & SAMUELSON (1957):

$$k_{obs} \cdot x_n = k \tag{61}$$

4.2.2.2 Effect of temperature on reaction kinetics

LAI & SARKANEN (1967) measured the rate constants for the degradation of cellulose (cotton and mercerised cotton) in 1.25 M NaOH at different temperatures between 146 °C and 185 °C. Table 3 summarises their results.

Although it is known that mercerisation[1] changes the structure of cellulose, this process seems to have only a minor effect on alkaline hydrolysis. The difference in rate constants between native cotton and mercerised cotton is very small.

Table 3: Reaction rate constants for degradation of cellulose in 1.25 M OH^- (from LAI & SARKANEN 1967) with exception of the data for 170 °C originating from FRANZON & SAMUELSON 1957).

Temperature (°C)	$k_{obs} \cdot x_n$ (h^{-1})
1)25	$3.6 \cdot 10^{-10}$
146	$4.0 \cdot 10^{-3}$
2)148	$5.8 \cdot 10^{-3}$
156	$9.8 \cdot 10^{-3}$
165	$23 \cdot 10^{-3}$
2)167	$28 \cdot 10^{-3}$
170	$16 \cdot 10^{-3}$
2)170	$34 \cdot 10^{-3}$
175	$65 \cdot 10^{-3}$
185	$129 \cdot 10^{-3}$
2)187	$162 \cdot 10^{-3}$

1) extrapolated by applying the Arrhenius equation (38):

$\log(k_{obs} \cdot x_n) = 14.9 - 7260 \cdot T^{-1} \quad \rightarrow k_{obs} \cdot x_n = 3.6 \cdot 10^{-10}\ h^{-1}$

2) mercerised cotton

Figure 14 illustrates the temperature dependence of the rate constants for both native and mercerised cotton. The relative standard uncertainty on the rate constants was estimated to be 70%. The plot of logk against the reciprocal absolute temperature results in a linear curve. A reaction rate constant for 25 °C was calculated by applying the Arrhenius formalism (see equation 38). This value is also given in Table 3. At a temperature of 25 °C, the rate constant is about 7 orders of magnitude lower than the one at 146 °C. Alkaline

[1] Mercerisation is the treatment of cellulose with an aqueous NaOH solution (e.g. 18 %). Mercerisation changes the supramolecular structure of a cellulose fiber (cotton) resulting in an increased reactivity (accessibility) of the cotton.

hydrolysis seems to be a process of minor importance in alkaline degradation of cellulose at low temperatures. The activation energy for alkaline hydrolysis was derived from the slope of the regression line in Figure 14, and equals 140 $kJ \cdot mol^{-1} \cdot K^{-1}$. The base-catalysed cleavage of glycosidic bonds is very sensitive to temperature. When the kinetic data of the peeling off reaction are compared with those of alkaline hydrolysis, it is obvious that alkaline hydrolysis is a relatively slow process even at higher temperatures. For example, at 25 °C (k_1 in Table 1) the rate of the peeling off reaction is 10^8 times faster than the rate of alkaline hydrolysis at 25 °C (Table 3). It can therefore be concluded that alkaline hydrolysis is a process of minor importance for alkaline degradation of cellulose under the temperature conditions of a cementitious (L/ILW) repository as planned in Switzerland (T = ~ 25 °C).

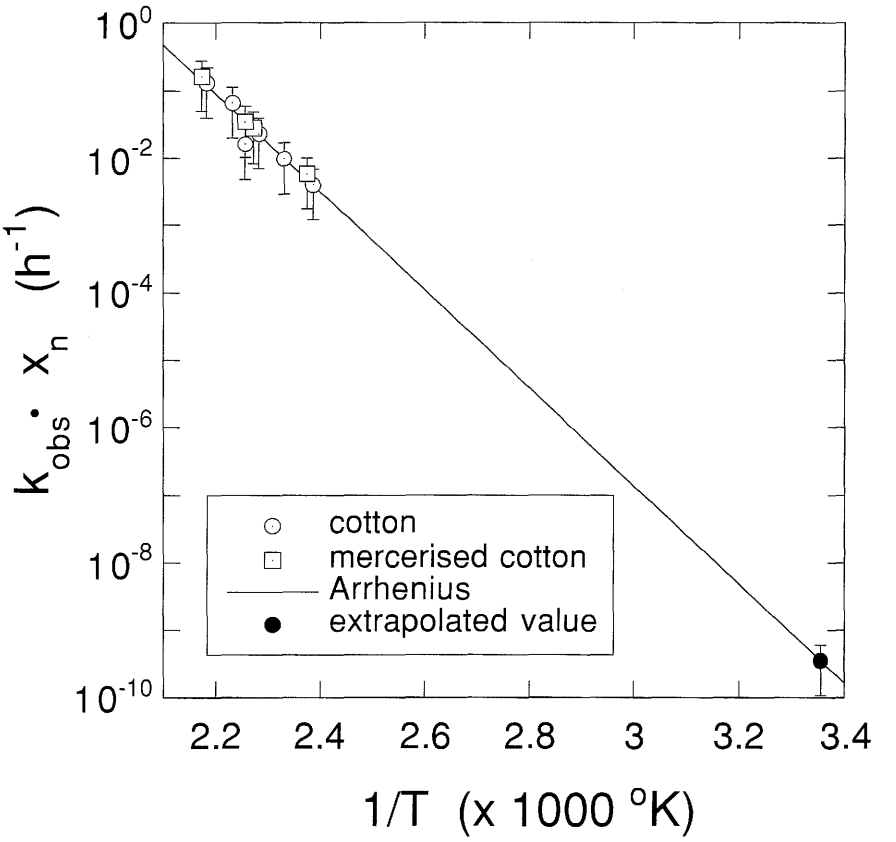

Figure 14: Arrhenius plot for alkaline hydrolysis of cellulose in 1.25 M NaOH (FRANZON & SAMUELSON 1957, LAI & SARKANEN 1967).

4.2.2.3 Effect of hydroxyl concentration on reaction kinetics

LAI & SARKANEN (1967) found a linear dependence of $k_{obs} \cdot x_n$ on the concentration of OH^- for 0 M < $[OH^-]$ < 2 M. Figure 15 illustrates this dependence for the degradation of cellulose at 185 °C. Assuming that a similar linear relationship is valid for lower reaction temperatures, a rate constant for the degradation of cellulose in 0.3 M OH^- at 25 °C can be calculated by applying the following equation:

$$k_{obs,0.3} \cdot x_n = \frac{k_{obs,1.25} \cdot x_n}{1.25} \cdot 0.3 \qquad (62)$$

and results in a value of $k_{obs} \cdot x_n = 8.6 \cdot 10^{-11}\ h^{-1}$ for 25 °C.

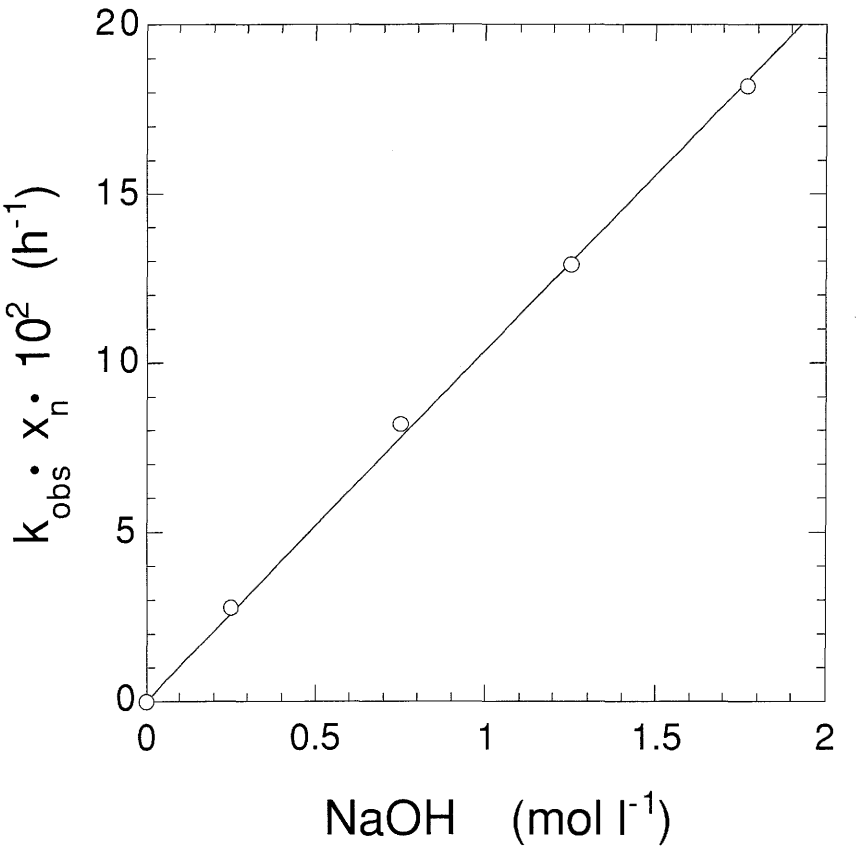

Figure 15: Dependence of $k_{obs} \cdot x_n$ on the concentration of OH^- at 185 °C (LAI & SARKANEN 1967).

4.2.2.4 Effect of Ca^{2+} on the reaction kinetics

No information is available on the possible effect of Ca^{2+} on the base catalysed hydrolysis of cellulose.

4.3 Summary

Under the physico-chemical conditions expected for the L/ILW cementitious repository in the Wellenberg site (T = 25 °C, pH = 13.4), the peeling off reaction is proposed to be the main degradation process for cellulosic materials. Based on the different reaction mechanisms published in the literature, it can be concluded that only a part of the cellulose will degrade by this fast peeling off reaction. The extent of degradation depends mainly on the number of reducing end groups, and hence on the degree of polymerisation of the cellulose present in the waste, and on the accessibility. The most important degradation products likely to be formed are α- and β-ISA and, to a much lower extent, small organic acids such as lactic acid, formic acid and glycollic acid.

These conclusions are mainly based on experimental evidence obtained under completely different conditions of temperature and alkali concentrations. A justification of the extrapolation of literature data, obtained under different conditions, to relevant conditions is not evident and therefore such a procedure might be rightly criticised. Justification can only be obtained by experimental evidence. The following chapter (chapter 5) describes experiments on alkaline degradation of different cellulosic materials performed under relevant conditions for waste disposal, i.e low temperature (25 °C) and an alkali concentration of 0.3 M and the presence of Ca. The results of these experiments will be compared with the conclusions drawn here and might be used to get confidence in the extrapolation procedures used before.

5 EXPERIMENTAL STUDIES ON ALKALINE DEGRADATION OF CELLULOSE

5.1 Materials and methods

5.1.1 Cellulosic materials used

The type of cellulose has a large impact on the extent of degradation and consequently on the amount of degradation products that will be formed (VAN LOON & GLAUS 1997b, see also chapter 4). Especially the amount of reducing end groups, the degree of polymerisation and the accessibility of the cellulose influence the extent of degradation. Different types of cellulose were therefore chosen for using in a long-term degradation experiment. The main degradation study was carried out with pure cellulose, denoted hereafter as series A. This cellulose was a powdered cellulose (Aldrich cellulose powder, 20 μm spheres, art. 31,069-7). In parallel, a few systems, containing other cellulose forms, were set up. The cellulose forms used were:

- Tela tissues (Tela Papierfabrik AG, Balsthal, Switzerland), denoted hereafter as series C1.
- cotton (Migros, Switzerland), denoted hereafter as series C2.
- recycling paper, (Recycling Copy, Steinbeis Temming Papier GmbH, Glückstadt, Germany), denoted hereafter as series C3.

5.1.2 Experimental conditions

The degradation was studied under near field conditions representing those of the early stage of cement degradation. The artificial cement pore water (denoted hereafter as ACW-I) used was a NaOH/KOH solution saturated with respect to $Ca(OH)_2$ (BERNER 1990). The composition of the ACW-I, with respect to its main constituents, is the following:

Na : 114 mM	Ca : 2.3 mM
K : 180 mM	pH : 13.3

The ACW-I was prepared in a glove box under a controlled N_2 atmosphere (O_2, CO_2 < 5 ppm) by mixing 4.56 g NaOH (Merck, 100%), 11.61 g KOH (Merck, 87%) and 10 g $Ca(OH)_2$ (Merck, 100%) in one liter of demineralised water. All chemicals used were of analytical grade quality. The water was flushed with argon for half an hour before transferring it into the glove box. For the degradation experiments the solid $Ca(OH)_2$ was left in the solution to maintain saturation w.r.t. portlandite during the whole degradation process.

The cellulose to liquid ratio used was estimated from an operational cellulose loading of 1% (cement porosity 20%, density 1.8 $kg \cdot dm^{-3}$). A solid:liquid ratio of 0.1 (100 $g \cdot l^{-1}$) was found to be representative. To check whether the amount of degradation products formed is proportional to the solid:liquid ratio, a few systems with a ratio of 0.01 (10 $g \cdot l^{-1}$), denoted hereafter as series B1 and 0.001 (1 $g \cdot l^{-1}$), denoted hereafter as series B2, were set up in parallel.

The degradation was carried out under anoxic conditions in a glovebox with a controlled N_2 atmosphere. The effect of reducing conditions was studied in a few parallel systems containing Fe(II) in a concentration of 10^{-7} M, denoted hereafter as series D.

The temperature in the planned L/ILW repository (Wellenberg) lies around 20-25 °C (J. Pöttinger, personal communication). Degradation experiments were therefore carried out at a temperature of 25 ± 2 °C.

The degradation studies were carried out in Teflon containers (volume 2 l) and were kept in the dark to avoid photoinduced reactions.

Because of the high pH of the solutions and the lack on major nutrients such as P, N and S, the microbial activity was expected to be very low. No special precautions were taken to keep the systems sterile.

A series of 15 batch systems containing the Aldrich cellulose (series A) were set up simultaneously. As a function of time, the liquid phase of these batch systems was sampled by filtering as described in 5.1.3. The time schedule of this experiment is given in Table 4. The kinetics of the degradation of the other cellulosic materials (series C1, C2 and C3) was studied less intensively. The time schedules for series B1, B2, C1, C2, C3 and D are also summarised in Table 4. The total duration of the experiments will be four years.

Table 4: Time schedule of the long term degradation experiment

	Series A					Series B			Series C				Series D	
Sampling time	Batch Nr	Total [a]	Ni,Th[b]	Stability	Cement sorption	Batch Nr.		Total[a]	Batch Nr			Total[a] / Ni,Th[b]	Batch Nr.	Total[a]
1 week	A1	+				B1.1	B2.1	+	C1.1	C2.1	C3.1	+	D1	+
2 weeks	A2	+	+											
1 month	A3	+												
2 months	A4	+												
4 months	A5	+	+	+	+	B1.2	B2.2	+	C1.2	C2.2	C3.2	+	D2	+
6 months	A6	+												
8 months	A7	+												
10 months	A8	+												
12 months	A9	+	+	+	+	B1.3	B2.3	+	C1.3	C2.3	C3.3	+	D3	+
18 months	A10	+												
24 months	A11	+							C1.4	C2.4	C3.4	+		
30 months	A12	+												
36 months	A13	+												
42 months	A14	+												
48 months	A15	+	+	+	+	B1.4	B2.4	+	C1.5	C2.5	C3.5	+	D4	+

[a] Analysis of parameters described in section 5.1.4 and sorption of Eu(III) on feldspar described in section 8.1.2.

[b] Sorption of Ni(II) and Th(IV) described in section 8.1.3 and 8.1.4.

Series A: Aldrich cellulose ; **Series B**: Aldrich cellulose + variation of solid:liquid ratio ; **Series C**: variation of cellulose type ; Series D: **Series A** + Fe(II)

5.1.3 Sampling of the degradation products

The degradation products were sampled by filtering the degradation solutions through a membrane filter (Teflon membrane filter, type FH, 0.5 μm, Millipore). The filter was prewashed with 50 ml ACW-I to remove soluble organic carbon from the filter. All manipulations were carried out in a glove box under N_2 atmosphere. After filtering, the solutions were stored in Teflon containers in the dark under N_2 atmosphere at 25°C till further experiments and/or analysis.

5.1.4 Analytical

A series of analysis were carried out on the solutions containing the degradation products and on the cellulosic materials used.

5.1.4.1 pH

The pH of the solutions was measured by a WTW pH-meter with an Ingold combined electrode. The electrode was calibrated with Titrisol buffers at pH 7 and 10. Since the pH of the samples (pH ± 13.3) was beyond the calibration range, and the ionic strength of the samples (I ± 0.3 M) was not identical to the ionic strength of the standards, the pH-measurements were not very accurate. An error of ± 0.05 pH units might result from the procedure applied. The pH, however, was used only as an indicator of the rate of change of the chemical conditions as degradation proceeds.

5.1.4.2 DOC (dissolved organic carbon)

The total dissolved organic carbon was measured by a carbon analyzer (Dohrmann DC-180) with a UV-promoted persulphate oxidation. The apparatus was calibrated with standard solutions of potassium biphthalate in a concentration range between 0.5 and 40 ppm dissolved organic carbon. The alkaline solutions, containing the degradation products, were diluted so that the concentration of DOC was covered by the calibration range. The solutions

were neutralised before analysis by adding 0.5 ml concentrated phosphoric acid (H_3PO_4 85 %, Merck) to 20 ml of the degradation solutions.
The average relative standard uncertainty (RSU) on the DOC measurements was 3%.

5.1.4.3 Ca, Na, K

Na, K and Ca were measured by ICP-AES. The solutions were diluted four times and acidified with concentrated HNO_3 before analysis. The relative standard uncertainties on the measurements were 2%, 4% and 5% for Na, K and Ca respectively.

5.1.4.4 Total amount of acids produced

The total amount of acids produced was measured by acid/base titration. 50 ml of demineralised water were placed in a titration vessel and purged with N_2 for 15 minutes. 5 ml of the alkaline degradation solutions or ACW-I were added and the mixture was purged with N_2 for another two minutes. The mixture was then titrated automatically with 0.1 M HCl under a N_2-atmosphere until pH = 8 (Titroprocessor 610, Metrohm). The total amount of acids produced was calculated by the difference in OH-concentration of the artificial cement pore water and the solutions containing the degradation products:

$$C_p = \frac{(V_{ACW} - V_s) \cdot C_{HCl}}{V_p} \qquad (63)$$

where:
V_{ACW} = amount of HCl used to titrate the ACW-I (ml)
V_s = amount of HCl used to titrate degradation products (ml)
V_p = the volume of the sample titrated (ml)
C_{HCl} = concentration of HCl (mM)
C_p = concentration of acids in solution (mM)

The relative standard uncertainty on the total amount of acids was 5%.

5.1.4.5 Organic acids

The organic acids formed during the alkaline degradation of cellulose were analysed by ion exclusion chromatography (at GSF, München) and by ion exchange chromatography.

Short chain aliphatic acids such as acetic acid, formic acid, lactic acid etc. were analysed by ion exclusion chromatography. The ion exclusion chromatography was performed with a Dionex DX-500 system comprising a quaternary gradient pump (GP40), a HPICE-AS6 separation column, a AMMS-ICE micromembrane suppressor and an electrochemical detector (ED 40) in the conductivity mode. The eluent contained 1.6 mM PFBA (perfluoro-butyric acid). The acids were detected by suppressed conductivity using 5mM TBAOH (tetrabutylammonium hydroxide) as suppressor regenerant. The column temperature was held at 20 °C. The standards used were made up from pure commercial products (FISCHER et al. 1996).

The isomers of isosaccharinic acid (α- and β-isosaccharinic acid) were analysed with ion exchange chromatography. The ion exchange chromatography was performed with a Dionex DX-500 system (Dionex, Switzerland) comprising a quaternary gradient pump (GP40), a Carbopac PA-100 separation column and an electro-chemical detector (ED 40) in the pulsed amperometric mode. The eluent contained 0.1 M NaOH and a gradient of NaOAc. Isosaccharinic acid was detected with pulsed amperometry using a golden working electrode and a Ag/AgCl reference electrode. The column temperature was maintained between 18 °C and 23 °C. The Ca salt of α-ISA was synthesised as described in 5.1.5 and was used to prepare standards. A typical value for the relative standard uncertainty on the ISA measurements was 5 %.

5.1.5 Synthesis of $Ca(\alpha\text{-ISA})_2$ and $Na(\alpha\text{-ISA})$

$Ca(ISA)_2$ was synthesised by contacting lactose with limewater as described in WHISTLER & BeMILLER (1963) and transformed into NaISA by treating the $Ca(ISA)_2$ with an ion exchange resin in the Na^+-form: 8 g of $Ca(ISA)_2$ were mixed with 200 g Chelex-100 (BioRad) in 1000 ml of demineralised water. After mixing the suspension for three hours, the resin was filtered off with a

membrane filter (Millipore 0.2 μm) and the filtrate was concentrated by boiling to a volume of about 100 ml. The solution was further evaporated in an oven at 80 °C till a thick syrup was obtained. The syrup was cooled and left standing at room temperature (20 °C) to crystallise. The obtained crystals were triturated in the presence of water-free diethylether to remove remaining water, filtered off, washed again with water-free diethylether and finally dried under reduced pressure in a vacuum oven at 55 °C. HPLC analysis on a Carbopac PA-100 column (Dionex, amperometric detection using a gold working electrode) showed the presence of two peaks in the NaISA salt. The peak area of ISA contributed to 98 % of the total peak area. The Ca level in the product obtained was ~0.01 %.

5.1.6 Isolation of β-ISA

β-ISA was isolated from a mixture of α-, β-ISA and other unknown substances, obtained by contacting 100 g of pure cellulose with 1 l of lime water for approximately 6 months. The isolation was performed by fractionation of the cellulose degradation solution on a 9x250 mm Carbopac PA-100 column (equipped with a 4x50 mm Carbopac PA-100 guard column). The HPLC system was a Dionex DX-500 (Dionex, Switzerland) consisting of a metal-free GP 40 quaternary gradient pump, an ED 40 electrochemical detector (not in use for the semi-preparative application due to signal overload) and an AS3500 SpectraSYSTEM autosampler (Thermo Separation Products), equipped with a 9010 motor-driven Rheodyne injection valve, a 500 μl PEEK injection loop and a 2.5 ml sample syringe. The peaks of interest were collected by switching a column switching valve (P/N 044858, Dionex), installed immediately after the column outlet. The time for switching the valve was determined in a prior test injection of the cellulose degradation solution. Upon this injection, the fractions eluting from the column were manually collected at intervals of 30 seconds and separately analysed on the 4x250 mm Carbopac PA-100 column.

The hydroxide ion concentration in the cellulose degradation solution injected in the column had to be adjusted (by addition of a strong cation exchanger in the H^+ form) to a value lower than 10 mM for obtaining optimal peak resolution. In order to obtain workable amounts of pure β-ISA within a

reasonable time, relatively large amounts of the cellulose degradation solution had to be brought on the column. However, it was not possible to simultaneously fulfill the requirements of "reasonable time" and "optimal separation performance". The reason was mainly the presence of substances in the cellulose degradation solution that were sticking to the column and thereby impaired the separation performance. These substances had to be washed out from the column after each injection by applying a step gradient to 1 M NaOH for 15 minutes after elution of the peaks of interest.

In order to optimise the effort for the isolation of workable amounts of β-ISA, the isolation of β-ISA had to be performed in two separation steps. In a first step, α- and β-ISA together with two unknown impurities were separated from all the other substances present in the degradation solution. These impurities eluted between the peaks of the two ISA isomers. For this first step, approximately 60 µmol of β-ISA applied in a volume of 500 µl were repetitively injected and fractionated at a flow rate of 4 $ml \cdot min^{-1}$ using 70 mM NaOH as an eluent (followed by 1 M NaOH for regenerating the column). Within several days, a total amount of approximately 1.5 g of β-ISA was thereby collected in a volume of approximately 750 ml. Prior to further fractionation, the hydroxide ion concentration was adjusted in this solution to 10 mM (by addition of a strong cation exchanger in the H^+ form). For the second isolation step, approximately 5 µmol of β-ISA applied in a volume of 500 µl were repetitively injected and fractionated at a flow rate of 2 $ml \cdot min^{-1}$ using 60 mM NaOH as eluent (regeneration of the column after each injection was not necessary). Due to partial overlapping of the peaks of one of the impurities and β-ISA, only 50% of the amount of β-ISA applied to the column could be obtained in pure form. After a total of 450 injections, approximately 220 mg of pure β-ISA could be isolated (i.e. total peak height of impurities is less than 2% of the peak height of β-ISA).

In an earlier attempt, approximately 1 g of β-ISA were enriched by a similar procedure (by applying more β-ISA in the second isolation step to the column). However, this product contained more impurities (total peak height of impurities ≈10% of the peak height of β-ISA).

The β-ISA was transformed to the lactone form by the same procedure as described by WHISTLER & BeMILLER (1963). The obtained lactone was an oily substance, which was used as such for characterisation purposes. The results of the characterisation can be found in FISCHER et al. (1997).

5.1.7 Degree of polymerisation of cellulose

The measurements of the degree of polymerisation of the different cellulosic materials were performed by a cellulose manufacturer in Switzerland (Cellulose Attisholz AG). The method used implies the determination of the intrinsic viscosity of a solution of cellulose dissolved in Cu-ethylenediamine. The viscosity of such solutions is proportional to the molecular weight of the solute when its concentration is very low. The relationship between the intrinsic viscosity and the degree of polymerisation is given by (SIHTOLA et al. 1963):

$$DP^{0.905} = 0.75 \cdot [\eta] \qquad (64)$$

where:

DP = degree of polymerisation

$[\eta]$ = intrinsic viscosity ($cm^3 \cdot g^{-1}$)

The relative standard uncertainty on the viscosity measurements and consequently on the DP was 2%.

5.1.8 Number of reducing end groups in cellulose

The number of reducing end groups is a key parameter in alkaline degradation of cellulose since it affects the extent of degradation by the peeling off reaction. A theoretical (maximum) value for the number of reducing end groups can be estimated from the degree of polymerisation. To evaluate whether this theoretical value is a realistic one, a direct measurement of the number of reducing end groups was performed. Note that no standard methods for the determination of reducing end groups in cellulose exist.

5.1.8.1 Principle of determination of reducing end groups

The method used to measure the number of reducing end groups of cellulose (GLAUS et al. 1997a) is based on a method described in the literature

(REHDER et al. 1965), further developed and tested by TÖPPEL (1967), ZWAHLEN et al. (1967) and BUCHER-JOHNSSON et al. (1970). Cellulose is brought into contact with a solution of hydroxylamine, whereby the amino-group of hydroxylamine reacts with the reducing end group of cellulose resulting in the formation of an oxime (cf. Figure 16). The reactivity of hydroxylamine under the given conditions is more or less specific for aldehydo functional groups. It has been shown (REHDER et al. 1965) that e.g. carboxylic groups or carboxylate-esters (including lactones) do not react with hydroxylamine under the reaction conditions given, due to the presence of large amounts of Zn^{2+}. After washing out the excess of non-reacted hydroxylamine, the oximated cellulose is submitted to Kjeldahl digestion, and the ammonia produced is quantitatively determined after steam distillation of the digestion mixture. The amount of nitrogen recovered as ammonia is thus a direct measure for the content of reducing end groups originally contained in the cellulose.

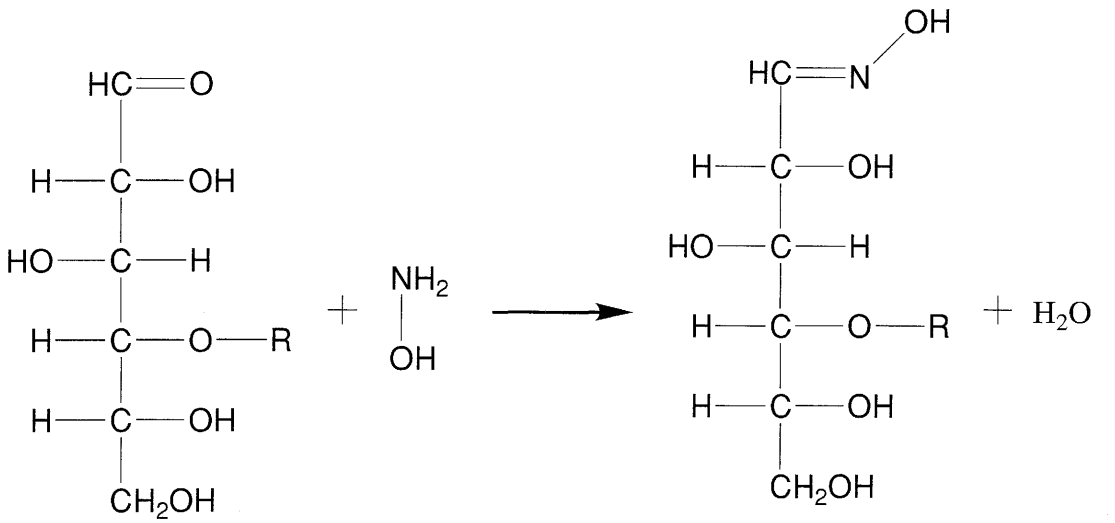

Figure 16: Formation of an oxime (right-hand formula) by reaction of the reducing end of a cellulose chain (left hand formula) with hydroxylamine (R = cellulose chain).

5.1.8.2 Experimental

Cellulose samples (cotton, paper, Tela tissues) were cut into small pieces of an edge-length of less than 5 mm and were stored in a desiccator (filled with silicagel) under atmospheric pressure for at least 1 week before use. The dry weight of the samples was measured. Triplicate samples of approximately 1 g were heated in an oven at 105 °C for 1 h. After cooling down to room temperature in a desiccator (filled with dry silicagel), the samples were weighted. This procedure was repeated until a constant weight was obtained.
A weighted amount of cellulose (approximately 0.2 g in the case of pure cellulose, Tela and paper; approximately 2 g in the case of cotton) was suspended in approximately 100 ml of 0.01 M zinkacetate solution in a 300 ml Erlenmeyer flask and well mixed using a magnetic stirrer. After standing for 2 h, the suspension was filtered using a porous glass filter (porosity 4), and the filter residue was washed twice with fresh zinkacetate solution. The washed filter residue was quantitatively brought back into the Erlenmeyer flask, followed by the addition of 100 ml oximation reagent. The oximation reagent was a solution containing per liter 55 g of zinkacetate-dihydrate, 160 ml of 1 M NaOH, 35 g of hydroxylammoniumchloride, and 1.6 ml of 100% acetic acid. After standing for 20 h at room temperature, the oximated sample was filtered using the same glass filter as before. The Erlenmeyer was washed twice with water, which in turn was used to wash the filter residue. The washed filter residue was again brought back into the Erlenmeyer flask and suspended in approximately 100 ml of 0.01 M zinkacetate solution for another 2 h. After filtering and washing by the same procedure as in the first step, the nitrogen in the samples was measured using Kjeldahl digestion followed by NH_4-determination.
The apparatus used for digestion of the samples was a Kjeldahl digestion unit 426 (Büchi AG, Switzerland). The sample (not exceeding a weight of 2 g and not exceeding a nitrogen content of 10^{-4} mol) was added as a solution or as a solid to 20 ml of 98% H_2SO_4 (Merck Art. Nr. 748, special quality for determination of nitrogen). After addition of one tablet of catalyst (Merck, Art. Nr. 15348, containing K_2SO_4, TiO_2 and $CuSO_4$), the mixture was boiled until a transparent light-green solution was obtained. In the case of oximated cellulose, the time for complete digestion was of the order of two hours. After

cooling the mixture down to room temperature, it was diluted with 80 ml of water.

The sample obtained after Kjeldahl digestion was mixed with 100 ml of NaOH 32% (Merck Art. Nr. 5590, special quality for nitrogen determination) and submitted to steam distillation in a steam distillation apparatus (distillation unit Nr. 315 from Büchi AG, Switzerland). The distillate was sampled in a 100 ml volumetric flask containing 50 ml of 0.005 M H_2SO_4, until a volume of approximately 95 ml was reached. Finally the volume was brought to 100 ml by adding Milli-Q water. Ammonium was analysed by high performance cation exchange chromatography using a 4x250 mm CS-14 IonPac column equipped with a 4x50mm CG-14 guard column (Dionex, Switzerland). The HPLC system was a Dionex DX-500 (Dionex, Switzerland) comprising a metal-free GP 40 quaternary gradient pump, an ED 40 electrochemical detector and an AS3500 SpectraSYSTEM autosampler (Thermo Separation Products), equipped with a 9010 motor-driven Rheodyne injection valve. A conductivity cell in combination with a CSRS-I auto-suppressor operating in recycling mode was used for detection of ammonium. Samples were injected in the full-loop mode from a 20 µl sample loop. The samples were eluted at a flow rate of 1 $ml \cdot min^{-1}$ using 0.01 M methanesulfonic acid as an eluent. Since the calibration curve is non-linear, at least six standards, containing NH_4Cl between 20 and 800 µM and 5 mM of H_2SO_4, were used for calibration. If necessary, samples were diluted to keep the nitrogen concentration within the same concentration range as covered by the calibration standards. The samples contained the same concentration of H_2SO_4 as the calibration standards.

The relative standard uncertainty on the determination of reducing end groups is relatively large and varies from 10% to 90 %, depending on the cellulosic material used.

5.1.9 Hemicellulose

5.1.9.1 Extraction of hemicellulose from cellulose

The extraction of hemicelluloses was performed by a procedure, slightly modified from the one as described in DIN 54 356 (1977). 100 g of cellulosic

material was extracted with one liter of ACW-I for one hour under air atmosphere. The extracts were centrifuged for 1 hour at 30000 x g and filtered through a 0.2 μm filter. The DOC in the extracts was measured as described in 5.1.4.2. ISA was measured by HPLC as described in 5.1.4.5.

5.1.9.2 Composition of hemicellulose in alkaline extracts

The composition of the hemicelluloses in the alkaline extracts was determined by a method described in PAZUR (1994). The polysaccharides were first hydrolysed to its monomeric units by treating them with 2 M HCl at 100 °C for 2-3 hours. Under these conditions, hydrolysis of the polysaccharides was complete. Hereafter, the samples were diluted with demineralised water and analysed for its composing monosaccharides by HPLC (Carbopac PA-100, 10 mM NaOH eluent, 1ml·min^{-1}, pulsed amperometric detection). Standard solutions were made up from pure monosaccharides.

5.1.10 Uncertainty estimation

The relative standard uncertainties (RSU) given for the different analytical methods are empirical values and represent typical values observed for a large amount of measurements made in the laboratory.

5.2 Results and discussion

5.2.1 Degree of polymerisation and reducing end groups

Table 5 shows the degree of polymerisation and the number of reducing end groups for the 4 cellulose materials used in the long-term degradation experiment. The number of reducing end groups measured are compared with the theoretical value. As discussed in chapter 4, the concentration of reducing end groups is given by equation (36):

$$0 \leq (G_r)_o \leq \frac{1}{DP}$$

The maximum concentration of reducing end groups is the reciprocal of the degree of polymerisation (1/DP). With respect to the uncertainty of $(G_r)_o$ and with respect to the fact that the uncertainty of DP is unknown, measured and theoretical values are in good agreement for pure cellulose, cotton and Tela tissues. The value for paper deviates from the theoretical value. This deviation might be explained by the presence of more *oximation reactive* groups other than reducing end groups.

Table 5: Overview of degree of polymerisation (DP), measured and theoretical values of reducing end groups in cellulosic materials.

Cellulose	DP	* $(G_r)_o$	$(G_r)_o$
Aldrich cellulose	117	$8.6 \cdot 10^{-3}$	$(7.8 \pm 0.8) \cdot 10^{-3}$
Tela tissues	1110	$9.0 \cdot 10^{-4}$	$(2.4 \pm 1.1) \cdot 10^{-3}$
Cotton	1800	$5.6 \cdot 10^{-4}$	$(3.2 \pm 3.0) \cdot 10^{-4}$
Recycling paper	290	$3.5 \cdot 10^{-3}$	$(1.2 \pm 0.4) \cdot 10^{-2}$

* $(G_r)_o = 1/DP$

Measurements of reducing end groups, $(G_r)_o$, in cellulose do not give more accurate values than the theoretical values based on DP. Therefore, the reciprocal value of DP will be used as a good approximation for $(G_r)_o$.

5.2.2 Characterisation of degradation products and alkali-soluble organic substances

5.2.2.1 Alkali soluble organic compounds

The results of the short term extraction of the cellulosic materials is given in Table 6. Paper shows a large amount of alkali soluble compounds, whereas cotton has only a small amount of such organics.
These data show that the amount of extractable material is not a constant, but varies with the type of cellulosic material. It is also not possible to predict a priori the amount of extractable material.

Table 6: Amount of extractable organic material in different cellulosic materials.

Sample	DOC in extract (ppm)	extractable (%)	Type DOC
Aldrich	199	0.5	unknown
Tela tissues	841	2.1	xylan
Cotton	48	0.1	unknown
Paper	2877	7.2	unknown

The type of extractable material is, apart from the Tela tissues, still unknown. Hydrolysis of the Tela extract yields only xylose. This is an indication that xylan is the only hemicellulose extracted from Tela. About 70 % of the organic carbon in the hydrolysed sample could be identified as xylose. Since xylan contains only 80 % of xylose (see section 3.2), it can be concluded that about 90 % of the organic carbon in the alkaline Tela extract is xylan.

5.2.2.2 Degradation products of pure cellulose (Aldrich)

Fig. 17 shows a typical chromatogram of cellulose degradation products (Aldrich cellulose degraded in ACW-I under N_2 atmosphere at 25 °C) analysed by Ion Pac ICE-AS6 (ion exclusion chromatography). The most important degradation products detected by this method were isosaccharinic acid, lactic

acid, formic acid, acetic acid, glycollic acid etc.. The chromatogram clearly shows that isosaccharinic acid is the main component in the cellulose degradation solution (assuming the response factor being identical for all compounds).

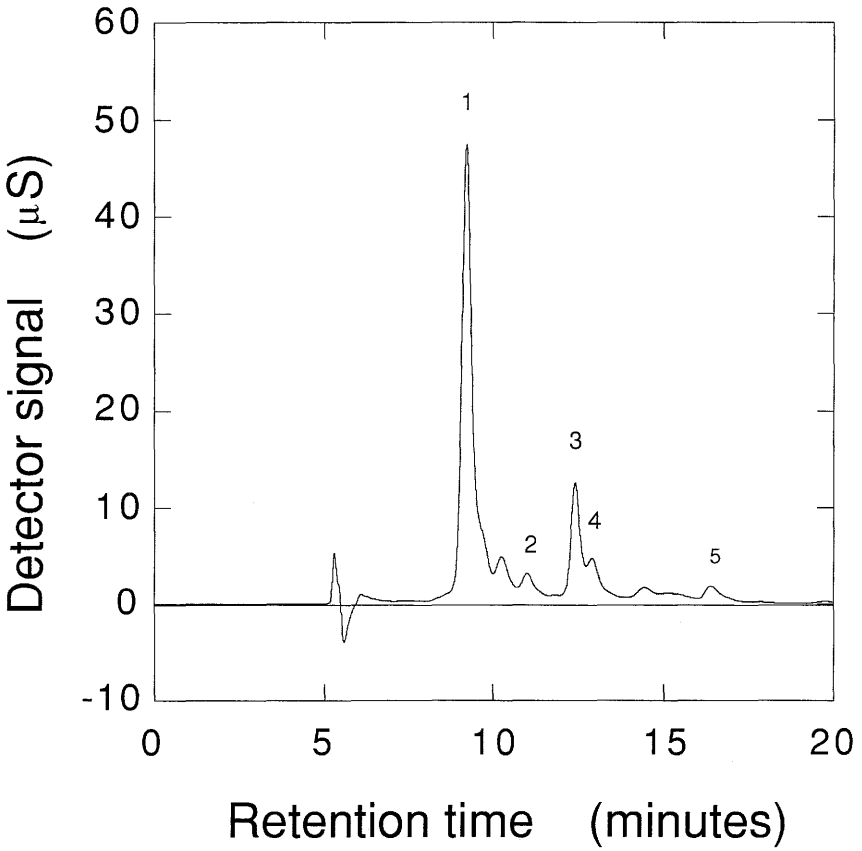

Figure 17: Chromatogram of a cellulose degradation solution (Aldrich cellulose degraded for 1 month in ACW-I). Column: Dionex Ion Pac ICE-AS6, T=20°C, flow rate: 1 ml·min^{-1}; eluent: 1.6 mM perfluorbutyric acid; detection: suppressed conductivity. Peak identification: 1= Isosaccharinic acid (α+β-ISA), 2 = glycollic acid, 3 = formic acid, 4 = lactic acid, 5 = acetic acid.

Figure 18 gives a typical chromatogram of cellulose degradation products analysed by Carbopac PA-100 (ion exchange chromatography) combined with the pulsed amperometric detection mode. With this detector, only molecules that can be oxidised at the gold working electrode are detected.

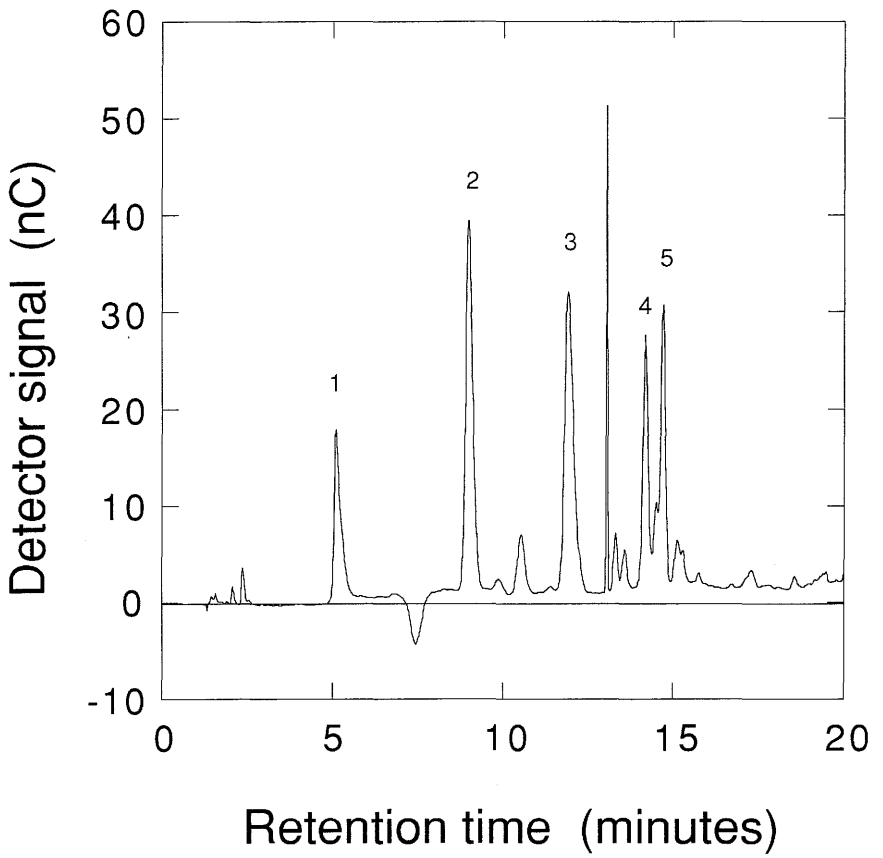

Figure 18: Chromatogram of cellulose degradation products (Aldrich cellulose degraded for 1 month in ACW-I: A3). Column: Dionex Carbopac PA-100, T=20 °C, flow rate: 1 ml·min^{-1}, eluent: 0.1 M NaOH + gradient of NaOAc; detector: pulsed amperometric detection. Peak identification: 1 = unknown, 2 = α-ISA, 3 = β-ISA, 4 = (probably) α-glucometasaccharinic acid, 5 = β-glucometasaccharinic acid.

In this case, only compounds with primary or secondary hydroxyl groups such as carbohydrates (sugars, sugar acids) can be analysed. Five main peaks can be observed in this chromatogram. Peak 2 (RT = 9 minutes) was identified as α-ISA. Peak 3 (RT = 12 minutes) was identified as β-ISA. The Carbopac PA-100 thus separates the two isomers of ISA. Both isomers are present in roughly the same concentration in the degradation solution. GREENFIELD et al. (1993) also observed the formation of these two isomers of ISA during alkaline degradation of cellulosic materials. Peak 5 could be identified as β-glucometasaccharinic acid. Peak 4 is probably the α-isomer of glucometa-

saccharinic acid. Peak 1 is an unknown component. Average concentrations of the degradation products as measured with both analytical systems are summarised in Table 7. ISA is the main degradation product formed during the alkaline degradation of cellulose and contributes to approximately 90 % of the total dissolved organic carbon (DOC). The other products such as lactic acid, formic acid etc. only form a minor, negligible part of the DOC (Σ = ~5 %). Alkali extractable organics contribute to ~ 5 % to the DOC. This means that during the degradation of cellulose in ACW-I, the intermediate product split off from the cellulose chain is transformed mainly by the benzilic acid type of rearrangement to isosaccharinic acid. The fragmentation reaction (Figure 8) can be neglected. This is due to the presence of Ca^{2+} in the artificial cement pore water. Ca^{2+} is known to catalyse the benzilic acid type of rearrangement at the expense of the fragmentation reaction (BLEARS et al. 1957, MACHELL & RICHARDS 1958, MACHELL & RICHARDS 1960, COLBRAN & DAVIDSON 1961) as discussed in chapter 4. Similar results were obtained for the other samples of series A. On an average, ISA contributes to ~80 % to the DOC (see Table 8). The other organic acids contribute to ~5 %. Roughly 15 % of the DOC remains unidentified.

Table 7: Overview of the different substances in a cellulose degradation solution after one month degradation time (A3), as analysed by ion exclusion chromatography[1] and ion exchange chromatography[2].

Component	Concentration (mM)	% of DOC
DOC	317	100
alkali extractable DOC	16.6	5.2
[1]Oxalic acid	n.m.	-
[1]Formic acid	3.9	1.2
[1]Acetic acid	2.3	1.5
[1]Glycollic acid	1.1	1.0
[1]Lactic acid	1.9	0.9
[1]Succinic acid	0.1	0.1
[2]α-Isosaccharinic acid	24.5	46
[2]β-Isosaccharinic acid	20.3	39

n.m: detected but not quantified

Table 8: Overview of the analysis of the degradation solutions.

Sample	Time (days)	pH	DOC (mM)	α-ISA (mM)	β-ISA (mM)	*ISA (mM)	α/β (mM)	H^+ (mM)	Ca (mM)
ACW-I	0	13.40	0	0	0	0	–	0	1.83
A1	7	13.37	123	6.23	5.36	11.6	1.16	36	3.59
A2	14	13.36	181	12.9	11.3	24.2	1.14	37	4.99
A3	40	13.23	317	24.5	20.4	44.9	1.20	62	8.56
A4	62	13.31	471	32.1	27.6	59.7	1.16	82	10.9
A5	119	13.25	685	45.6	38.9	84.5	1.17	105	16.8
A6	181	13.26	784	54.2	47.6	102	1.14	119	22.0
A7	239	13.13	910	62.2	54.9	117	1.13	126	28.1
A8	301	13.12	951	66.8	59.0	126	1.13	126	33.2
A9	378	13.04	996	73.8	63.1	137	1.17	129	36.9
A10	595	13.04	1070	77.0	66.9	144	1.15	127	47.3
A11	734	13.06	1179	79.2	68.7	148	1.15	112	54.6
A12	966	13.07	1125	79.5	68.4	148	1.16	120	52.4
B1.1	14	13.4	22.5	1.64	1.36	3.00	1.21	2.0	2.28
B1.2	118	13.4	73.1	4.83	4.47	9.30	1.08	n.m.	2.59
B1.3	377	13.3	107	7.84	7.03	14.9	1.12	22	2.94
B2.1	14	13.4	1.95	0.14	0.10	0.24	1.40	n.m.	1.93
B2.2	118	13.4	2.60	0.49	0.40	0.89	1.23	1.0	1.95
B2.3	377	13.3	10.3	0.78	0.59	1.37	1.32	1.0	1.83
C1.1	14	13.4	76.9	1.51	1.33	2.84	1.14	31	2.44
C1.2	118	13.3	149	6.18	5.37	11.6	1.15	44	3.24
C1.3	378	13.3	189	9.08	8.22	17.3	1.10	55	3.27
C1.4	734	13.20	229	10.8	9.82	20.6	1.10	56	4.32
C2.1	14	13.4	6.26	0.16	0.14	0.30	1.14	16	1.84
C2.2	118	13.3	16.8	0.68	0.68	1.36	1.00	22	1.22
C2.3	378	13.3	26.5	1.06	0.98	2.04	1.08	22	1.61
C2.4	734	13.3	36.4	1.28	1.13	2.41	1.13	23	1.99
C3.1	14	13.3	208	3.39	3.21	6.60	1.06	44	5.71
C3.2	118	13.3	285	7.46	7.24	14.7	1.03	56	7.11
C3.3	378	13.3	380	10.7	10.6	21.3	1.01	72	7.36
C3.4	734	13.2	439	12.7	12.4	25.1	1.02	110	9.71
D1	14	13.4	175	13.1	10.6	23.7	1.24	42	4.64
D2	118	13.2	742	49.2	43.0	92.2	1.14	111	17.7
D3	374	13.1	973	71.1	61.5	133	1.16	136	33.4

A: Aldrich pure cellulose (100 $g \cdot l^{-1}$)

B1: Aldrich cellulose (10 $g \cdot l^{-1}$) B2: Aldrich cellulose (1 $g \cdot l^{-1}$)

C1: Tela tissues (100 $g \cdot l^{-1}$) C2: cotton (100 $g \cdot l^{-1}$) C3: recycling paper (100 $g \cdot l^{-1}$)

D: Aldrich pure cellulose (100 $g \cdot l^{-1}$), reducing conditions

*ISA: $\Sigma(\alpha+\beta)$, n.m: not measured

5.2.2.3 Degradation products of other cellulosic materials

For the other cellulosic materials, identical compounds could be detected by ion exclusion chromatography and ion exchange chromatography, i.e. formic acid, acetic acid, glycollic acid and isosaccharinic acid. The main difference with respect to the pure cellulose is that isosaccharinic acid contributes much less to the DOC. Whereas for the pure cellulose (Aldrich), ISA contributes to ~80% to the DOC, this contribution decreases to approximately 15-30% for the Tela tissues, 30% for the cotton and only 10-15% for the recycling paper. As was discussed briefly in 5.2.2.1, hemicelluloses are well soluble in alkali. They form the main part of DOC in the degradation solutions of the other cellulosic materials in the initial stage of degradation (Table 9). As degradation of cellulose proceeds, the relative contribution of alkali extractable organics to the DOC decreases, but still forms an important contribution.

Table 9: Relative distribution of DOC in cellulose degradation solutions. Organic carbon in solution (DOC_{tot}) originates from alkaline degradation of cellulose (DOC_{deg}) and from solubilisation of hemicelluloses (DOC_{sol}).

Cellulose	DOC_{tot} (mM)	DOC_{deg} (mM)	DOC_{sol} (mM)
Aldrich (14 days)	181 (100%)	164 (91%)	17 (9%)
Aldrich (2 years)	1179 (100%)	1162 (99%)	17 (1%)
Cotton (14 days)	6.3 (100%)	2.3 (36%)	4.0 (64%)
Cotton (2 years)	36 (100%)	32 (89%)	4.0 (11%)
Tela (14 days)	77 (100%)	7 (9%)	70 (91%)
Tela (2 years)	228 (100%)	158 (70%)	70 (30%)
Paper (14 days)	208 (100%)	-	240 (100%)
Paper (2 years)	438 (100%)	198 (45%)	240 (55%)

$DOC_{deg} = DOC_{tot} - DOC_{sol}$

Figure 19 shows the ion exchange chromatograms of the degradation products of the other cellulosic materials (after one year of degradation) as analysed with the Carbopac PA-100.

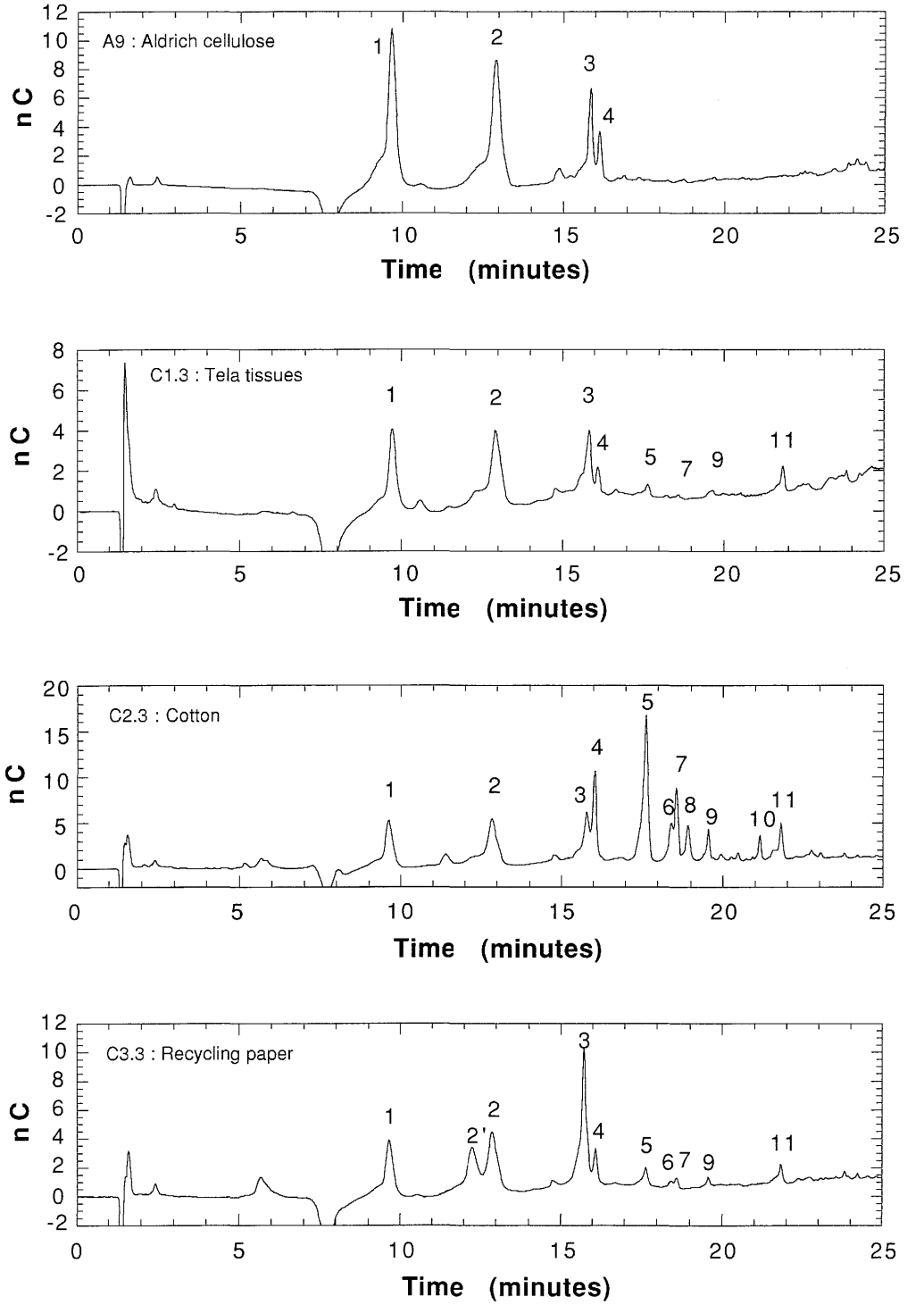

Figure 19: Chromatograms of the degradation products of different cellulosic materials degraded for one year in ACW-I at 25°C (Aldrich cellulose, Tela tissues, cotton and recycling paper).

These chromatograms are clearly different from the one obtained for the pure cellulose (Aldrich). For the pure cellulose, four main peaks could be detected. Peak 1 is α-ISA, peak 2 corresponds to β-ISA, peak 3 and 4 are isomers of metasaccharinic acid (MSA). These four peaks can be seen as a "fingerprint" for pure cellulose: α- and β-ISA are formed by the peeling off reaction of cellulose and MSA is formed by the removal of transformed reducing end groups from the cellulose. The same fingerprint can also be observed for the other cellulosic materials. However, additional peaks can be detected (peak 5-11). Especially the cotton shows a completely different chromatogram. These additional peaks are probably not formed by the alkaline degradation of cellulose, but by the degradation of non-cellulosic polysaccharides present in these materials (section 3.2). Hemicelluloses can be degraded by a similar peeling off reaction (LAI 1991) resulting in other degradation products than ISA.

5.2.2.4 Conclusions

Figure 20 gives a schematic overview of the origin of organic substances in a cellulose degradation solution. Organic compounds result from a *degradation process* and a *dissolution process*.

The *alkaline degradation* of cellulose under the conditions of a cementitious repository results in the formation of mainly isosaccharinic acid (ISA). Two isomers are formed in roughly equal amounts: α-ISA and β-ISA. Beside ISA, other small organic acids such as lactic, formic and acetic acid are produced, most probably by a fragmentation reaction of the intermediate product. The contribution of these organic acids to the total dissolved organic carbon is negligible.

The *amount of alkali soluble* organics (hemicellulose) depends on the type of cellulosic materials. Its contribution to the dissolved organic carbon can be large. The exact nature of the alkali soluble organics is still unknown for cotton and paper. For Tela tissues, xylan was found to be the main alkali soluble organic compound. Whether these alkali soluble organics in solution are stable or will further degrade, is unknown.

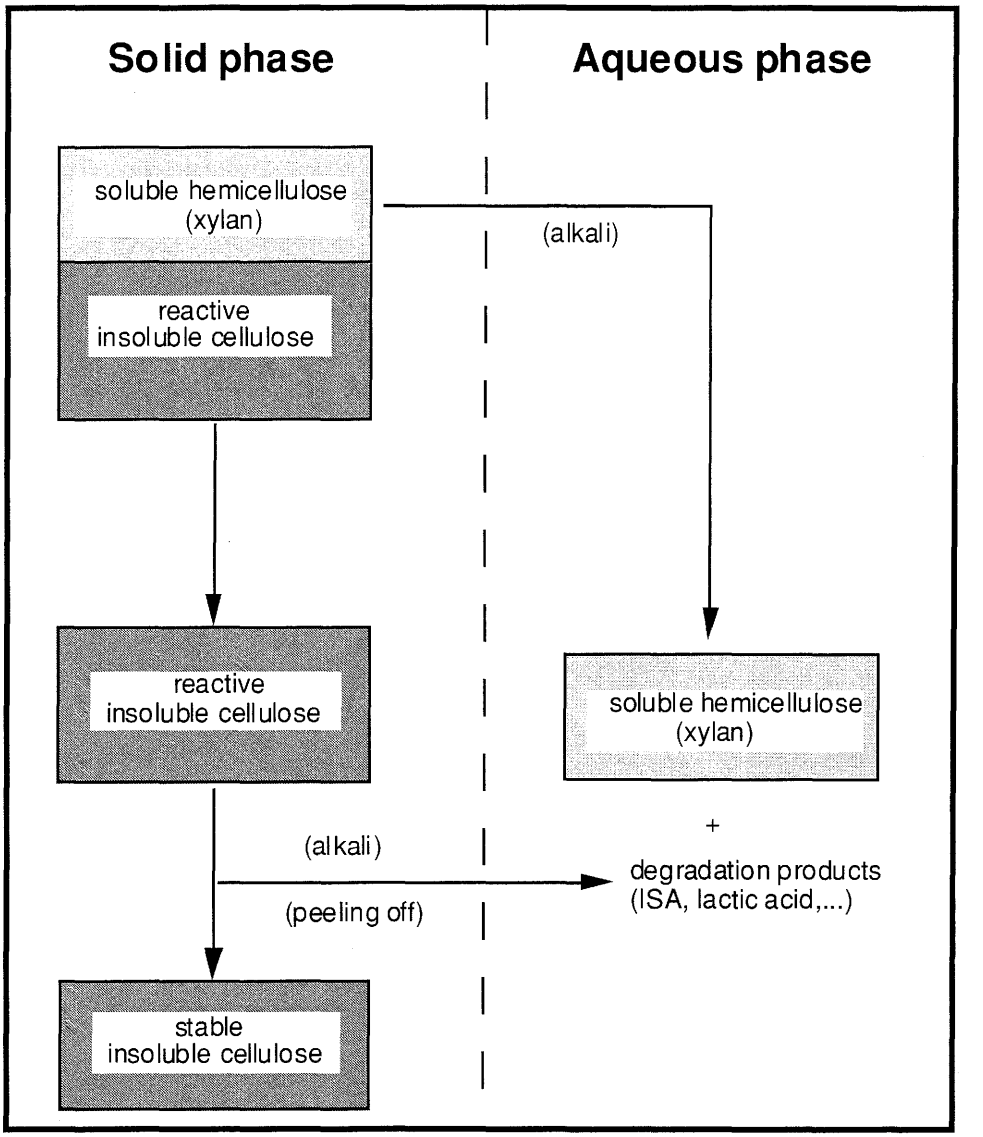

Figure 20: Schematic overview of degradation and solubilisation processes for cellulosic materials under alkaline conditions.

5.2.3 Effect of solid/liquid ratio on the degradation of cellulose

As can be seen from the data on DOC and ISA summarised in Table 8, changing the cellulose/solution ratio (series B1 and B2) results in a proportional change of the concentration of DOC and ISA in solution, i.e. when the ratio is changed by a factor of 10, the concentration of degradation products also changes with a factor of 10. This illustrates that the degradation rate is linearly proportional to the amount of cellulose in suspension. Figure 21

shows the concentration of DOC in the degradation solutions of pure Aldrich cellulose as a function of the amount of cellulose in suspension ($g \cdot l^{-1}$).

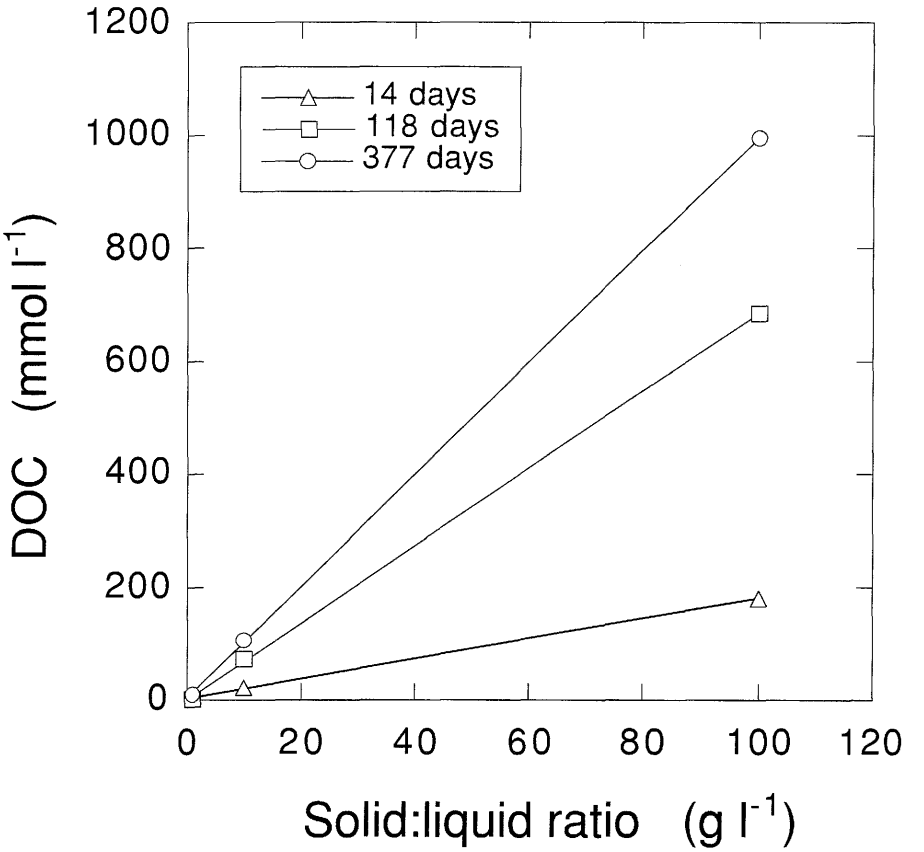

Figure 21: Effect of the amount of cellulose in suspension on the concentration of degradation products (DOC) in solution.

5.2.4 Kinetics of degradation

As discussed earlier, the total organic carbon in solution is the result of alkaline degradation of cellulose and solubilisation of hemicellulose (Figure 20) and is defined by:

$$DOC_{tot} = DOC_{sol} + DOC_{deg} \qquad (65)$$

The dissolvable organic carbon (DOC_{sol}) is a constant fraction of the cellulosic material. Since the solubilisation process is an effectively instantaneous

process, DOC_{sol} can be regarded as time independent. The carbon resulting from alkaline degradation, however, is time dependent since the degradation is a slow process.
Figure 22 shows the evolution of the total concentration of organic carbon (DOC_{tot}) and the carbon resulting from the degradation process (DOC_{deg}) as a function of time. DOC_{deg} was calculated as:

$$DOC_{deg} = DOC_{tot} - DOC_{sol} \tag{66}$$

where DOC_{tot} and DOC_{sol} are measurable parameters.
DOC_{deg} is a measure for the total amount of degradation products generated. DOC_{deg} increases quickly in the initial stage of degradation and slows down as the degradation proceeds. This observation is in agreement with the general accepted peeling off mechanism for cellulose degradation under alkaline conditions as discussed in chapter 4. Glucose units are progressively removed from the cellulose chain. As the reaction proceeds, reducing end groups are transformed to non-reducing end groups resulting in a degradation stop. The mole fraction of cellulose degraded (celdeg) can be expressed by the following equation (VAN LOON & GLAUS 1997b, see also equation 28):

$$(celdeg) = \frac{k_1}{k_t} \cdot (G_r)_o \cdot (1 - e^{-k_t \cdot t}) \tag{67}$$

where:

(celdeg) = the mole fraction of cellulose degraded
k_1 = first order rate constant for the peeling off reaction (h^{-1})
k_t = overall first order rate constant for the stopping reaction (h^{-1})
$(G_r)_o$ = the mole fraction of reducing end groups

The concentration of the DOC_{deg} in solution is proportional to the amount of cellulose degraded:

$$DOC_{deg} = f_{DOC} \cdot (celdeg) \tag{68}$$

where:

DOC_{deg} = the concentration of DOC_{deg} in solution (mM)
f_{DOC} = conversion factor (mM)

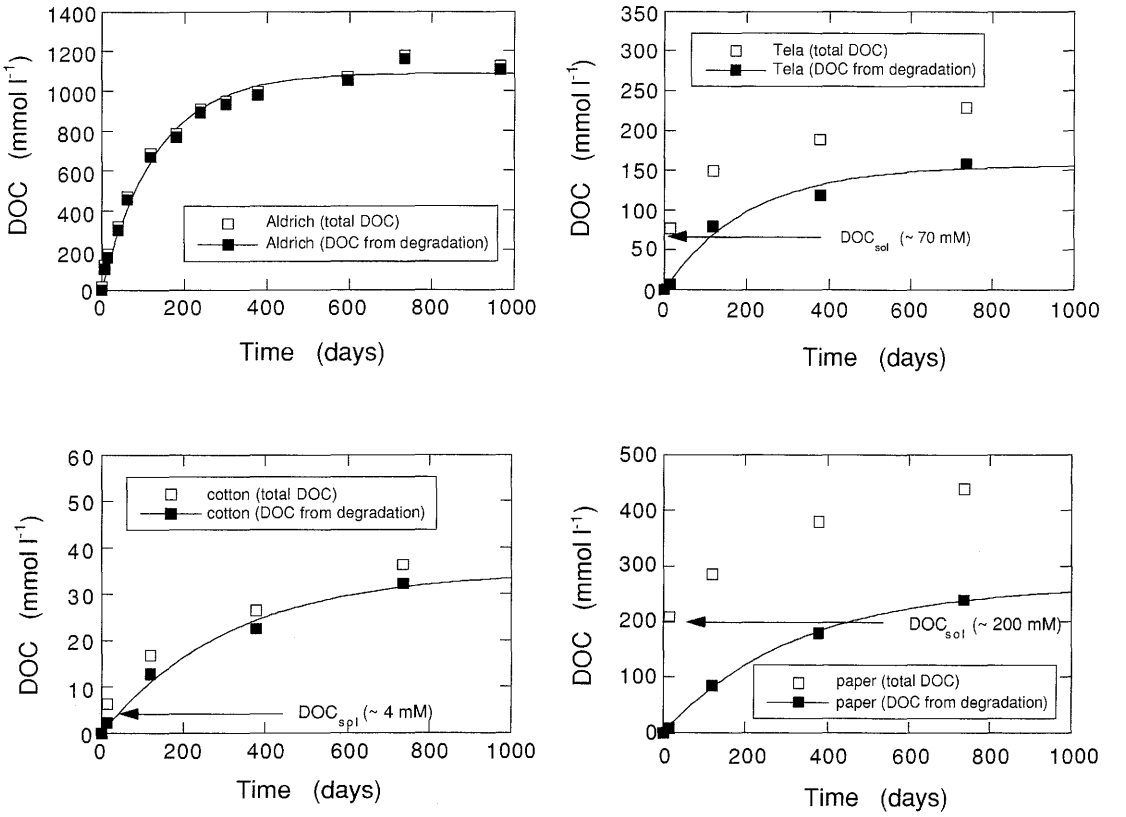

Figure 22: Evolution of total dissolved organic carbon (open symbols) and organic carbon from the alkaline degradation process (closed symbols) as function of time. Solid lines are fitted using equation (71).

Combining equation (67) and (68) results in:

$$DOC_{deg} = f_{DOC} \cdot \frac{k_1}{k_t} \cdot (G_r)_o \cdot (1 - e^{-k_t \cdot t}) \qquad (69)$$

Since f_{DOC}, k_1, k_t and $(G_r)_0$ are all constants, they can be combined in one constant. This constant represents the maximal concentration of DOC_{deg} that will be reached when the degradation reaction stops. For $t \rightarrow \infty$:

$$(DOC_{deg})_{max} = f_{DOC} \cdot \frac{k_1}{k_t} \cdot (G_r)_o \qquad (70)$$

Combining equation (69) and (70) gives:

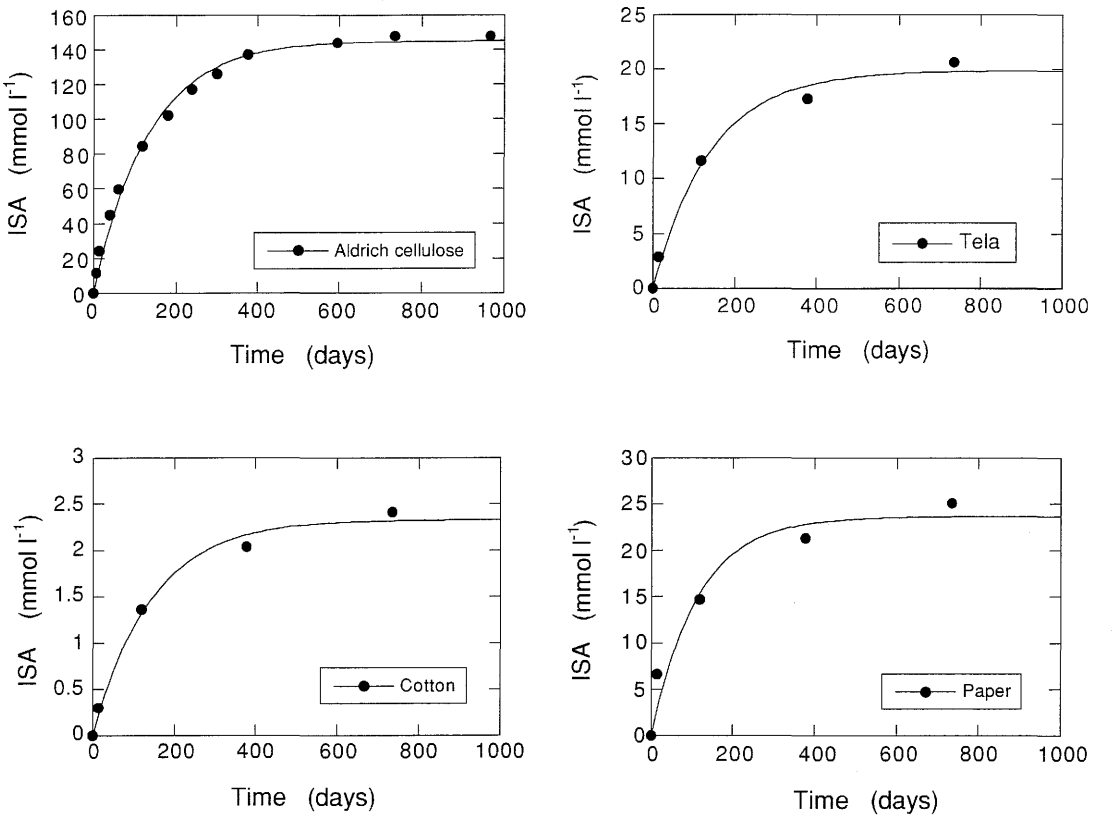

Figure 23: Evolution of the concentration of ISA in the degradation solutions of different cellulose materials as a function of pH. Solid lines are fitted using equation (74).

$$DOC_{deg} = (DOC_{deg})_{max} \cdot (1 - e^{-k_t \cdot t}) \qquad (71)$$

The experimental data (DOC_{deg}) given in Figure 22 could be fitted very well by equation (71). The values for $(DOC_{deg})_{max}$ and k_t are given in Table 10.
A similar picture is obtained for the concentration of ISA in solution. The experimental data for ISA (α- and β-ISA) are shown in Figure 23. The evolution of the concentration of ISA can be written as:

$$(ISA) = f_{ISA} \cdot (celdeg) \qquad (72)$$

where f_{ISA} is the conversion factor between the concentration of ISA in solution and the mole fraction of degraded cellulose. Combining equation (67) and (72) gives:

$$(ISA) = f_{ISA} \cdot \frac{k_1}{k_t} \cdot (G_r)_o \cdot (1 - e^{-k_t \cdot t}) \quad (73)$$

In analogy with equation (71):

$$(ISA) = (ISA)_{max} \cdot (1 - e^{-k_t \cdot t}) \quad (74)$$

where:

$$(ISA)_{max} = f_{ISA} \cdot \frac{k_1}{k_t} \cdot (G_r)_o \quad (75)$$

The data in Figure 23 could be fitted very well by equation (74). Values of ISA_{max} and k_t are given in Table 10. The conversion factors f_{ISA} and f_{DOC} depend on the amount of cellulose per volume unit of solution:

$$f_{ISA} = \frac{W_{cel} \cdot 1000}{162 \cdot V} \quad (76)$$

and

$$f_{DOC} = \frac{W_{cel} \cdot 1000 \cdot 6}{162 \cdot V} \quad (77)$$

where W_{cel} is the weight of cellulose (in g), V is the volume of solution available for the cellulose (in l) and 162 is the molecular weight of glucose (monomeric unit) in cellulose (in $g \cdot mol^{-1}$). The factor 1000 is introduced to give the results in mM. The factor 6 in f_{DOC} represents the number of carbon atoms in the degradation product ISA. The dimension of both conversion factors is mM. As an example: for a cellulose/liquid ratio of 0.1 (100 $g \cdot l^{-1}$), the conversion factor f_{ISA} is 617 mM and f_{DOC} is 3700 mM. When 10 % of the cellulose is degraded, the concentration of ISA in solution will be 61.7 mM and the concentration of DOC 370 mM.

The value for the kinetic parameter k_1 can be calculated from the plateau value of the curves depicted in Figure 22 and 23 respectively, by:

$$k_1 = \frac{(DOC_{deg})_{max}}{f_{DOC} \cdot (G_r)_o} \cdot k_t \quad (78)$$

when k_1 is calculated from the DOC data, and:

$$k_1 = \frac{(ISA)_{max}}{f_{ISA} \cdot (G_r)_o} \cdot k_t \qquad (79)$$

when k_1 is calculated from the ISA data. Note that $(ISA)_{max}$ is the plateau value for the total ISA in solution, i.e. the sum of α- and β-ISA. Since these isomers are produced in equal amounts, the kinetic parameter can also be calculated from only the α-ISA concentration or the β-ISA concentration. The conversion factor (f_{ISA}) to be used is then 309 mM.

Table 10 gives an overview of k_1 and k_t calculated from the DOC and ISA data for the four materials used. Within the experimental uncertainty, there is a good agreement between the kinetic constants extracted from both set of data (DOC_{deg} and ISA) for Aldrich cellulose and Tela tissues. This good agreement is not surprising since the major part (80 %) of the dissolved organic carbon formed by the peeling off process is α- and β-ISA.

Table 10: Overview of k_1 and k_t calculated from DOC_{deg} and ISA data for different cellulosic materials.

Material	**DOC-DATA**			
	$(DOC_{deg})_{max}$	k_1	k_t	k_1/k_t
	(mM)	(h^{-1})	(h^{-1})	
Aldrich	1089±24	$(1.1\pm0.2)\cdot10^{-2}$	$(3.1\pm0.3)\cdot10^{-4}$	35±4
Tela	156±13	$(9.6\pm2.6)\cdot10^{-3}$	$(2.1\pm0.5)\cdot10^{-4}$	45±6
Cotton	35±3	$(2.2\pm0.6)\cdot10^{-3}$	$(1.3\pm0.3)\cdot10^{-4}$	17±3
Paper	265±7	$(2.7\pm0.4)\cdot10^{-3}$	$(1.3\pm0.1)\cdot10^{-4}$	21±2
Material	**ISA-DATA**			
	ISA_{max}	k_1	k_t	k_1/k_t
	(mM)	(h^{-1})	(h^{-1})	
Aldrich	145±3	$(8.5\pm1.0)\cdot10^{-3}$	$(3.1\pm0.2)\cdot10^{-4}$	27±3
Tela	20±1	$(1.1\pm0.2)\cdot10^{-2}$	$(3.0\pm0.5)\cdot10^{-4}$	37±4
Cotton	2.3±0.1	$(2.0\pm0.4)\cdot10^{-3}$	$(2.9\pm0.5)\cdot10^{-4}$	7±1
Paper	24±3	$(4.1\pm1.6)\cdot10^{-3}$	$(3.7\pm1.3)\cdot10^{-4}$	11±2

For cotton and paper, the agreement between the two data sets is less good, probably due to the fact that for these materials only a part of the DOC (40-50%) could be explained by ISA.

The different cellulose materials give – within a factor of 2~3 – similar values for the kinetic constant of the overall stopping reaction (k_t). A larger discrepancy – up to a factor of 5 –, however, exists between the values for the kinetic constant of the propagation reaction (k_1). A possible explanation for this observation might be a difference in crystallinity of the cellulose materials. Since the peeling off reaction takes place in the amorphous region of the cellulose, the structure of this amorphous region is very important. When the amorphous region has a certain degree of crystallinity (semi-crystalline structure), it is possible that the peeling off reaction occurs slower, resulting in smaller kinetic constants. This could be observed especially in case of cotton and paper. Despite these differences apparently existing between the different cellulosic materials, it is clear that the values of the kinetic constants are of the same order of magnitude. A mean value for the rate constant for the overall stopping reaction is $(2.6\pm0.9)\cdot10^{-4}$ h^{-1}. For the propagation reaction, the mean value of the rate constant is $(6.4\pm4.0)\cdot10^{-3}$ h^{-1}.

Figure 24 shows the kinetic constants measured by HAAS et al. (1967) at different temperatures and the mean values of the kinetic constants of this work. The lines were calculated using the Arrhenius equation (38). The Figure clearly shows that the rate constants measured in this study at low temperature and low OH^- concentration are in agreement with those measured at higher temperature and higher OH^- concentration. It has to be mentioned that the comparison is not fully correct, since there is a difference in both temperature and OH^- concentration between the data of HAAS et al. (1967) and the data from this study. The effect of OH^-, however, is of minor importance so that a direct comparison is justified. The agreement between the data of this study and the literature data confirms the validity of the degradation model used.

The difference in DOC_{deg} between the various cellulosic materials is significant (see Figure 22). The lowest values are found for the cotton, followed by the Tela tissues and the recycling paper. The highest value is found for the pure cellulose. As already discussed in Chapter 4, the extent of degradation of cellulose depends strongly on the mole fraction of reducing end groups, $(G_r)_o$, in cellulose, and on the accessibility of the cellulose.

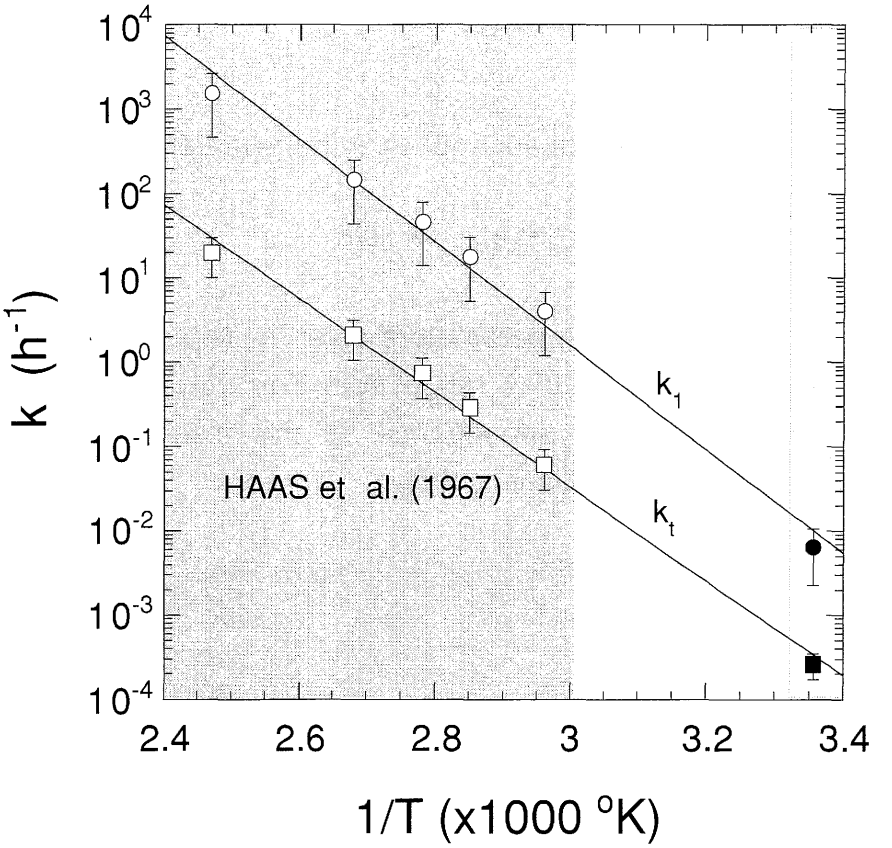

Figure 24: Arrhenius plot of rate constants measured by HAAS et al (1967) (open symbols) and values measured in this study (filled symbols).

The mole fraction of reducing end groups depends on the average number of reducing end groups per cellulose molecule and on the degree of polymerisation (DP). The maximum value of $(G_r)_o$ is given in equation (36) and equals the reciprocal value of the degree of polymerisation:

$$(G_r)_o = \frac{1}{DP} \tag{80}$$

For cellulose with the same average number of reducing end groups (N), the one with the higher DP will degrade less than the one with the lower DP. Combination of equation (34) and (80) gives the following expression for the extent of degradation:

$$(\text{cel deg})_{max} = \frac{k_1}{k_t} \cdot \frac{1}{DP} \qquad (81)$$

Since k_1 and k_t are constants, equation (81) can be rewritten as:

$$(\text{cel deg})_{max} = A / DP \qquad (82)$$

where $A = k_1/k_t$. From the kinetic parameters given in Table 10, a value for A can be calculated. The values of A range from 7 to 45 with an average of 25±13. Figure 25 shows the dependence of the extent of degradation, $(\text{celdeg})_{max}$, on the degree of polymerisation.

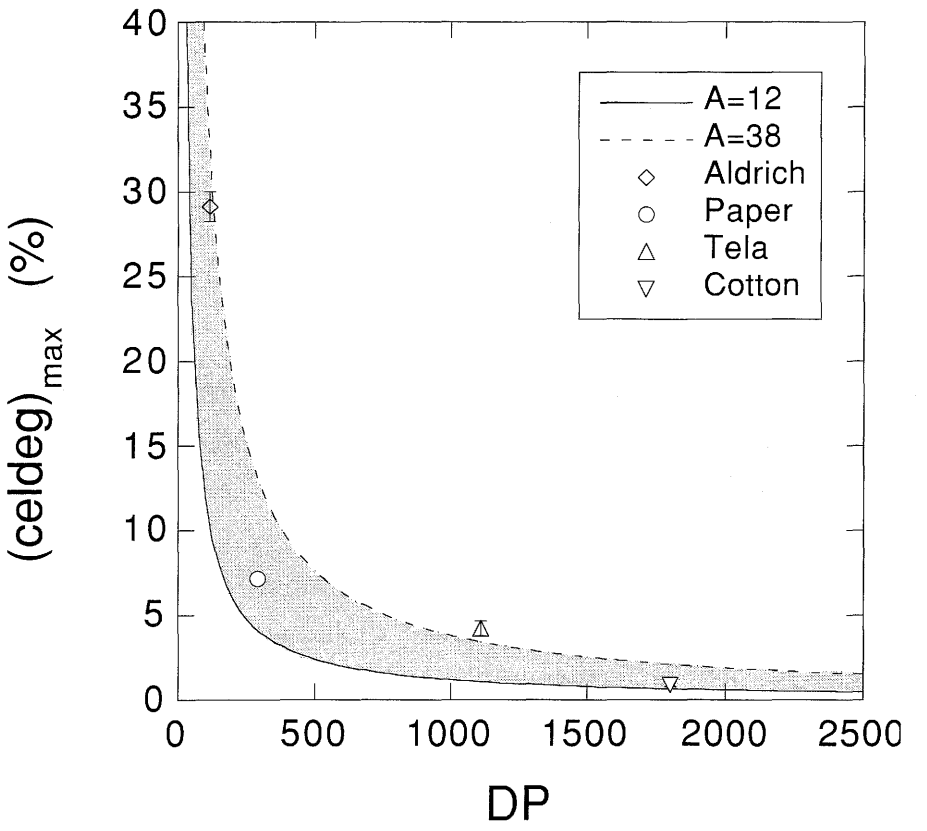

Figure 25: Dependence of the extent of degradation on the degree of polymerisation of cellulose. The curves shown were calculated using equation (82) with A = 25±13.

The shaded area represents the cases calculated with equation (82) for A = 25±13. This area can be regarded as the uncertainty area. The degree of

degradation of the four materials studied lies in this shaded area. The uncertainty range reflects the difference in accessibility (amorphicity) of the cellulosic materials used. The lowest accessibility could be observed for cotton, the highest accessibility for Tela tissues. The ratio k_1/k_t seems to reflect the accessibility of cellulosic materials. The higher this ratio, the higher the accessibility and the larger the extent of degradation. Figure 26 shows some indicative values for the fraction of amorphous material – a measure for accessibility – present in different cellulosic materials (JEFFRIES et al. 1969). Native cotton shows a relative low degree of amorphicity, indicating that the accessibility is low. Regenerated cellulose shows a relatively high degree of amorphicity. So, besides the degree of polymerisation, also the accessibility of cellulose determines the extent of degradation. It can be assumed that for cellulosic materials with a similar DP, the one with the higher accessibility will degrade to a larger extent.

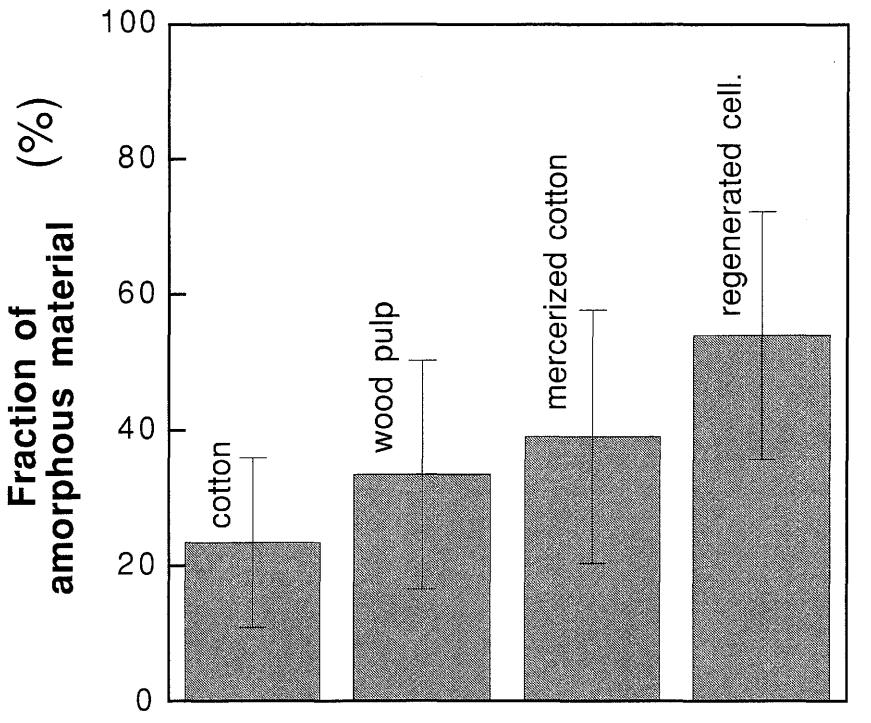

Figure 26: Fraction of amorphous (disordered) material in various cellulosic materials. The uncertainty bars reflect the differences observed using different techniques (Data taken from JEFFRIES et al. 1969).

5.2.5 Effect of degradation products on the composition of the cement pore water

The degradation of cellulose has an influence on the composition of the cement pore water. Since the extent of degradation is the largest for Aldrich cellulose, the largest effect will be observed for the systems containing this cellulose. In the following, only the systems containing Aldrich cellulose will be discussed (series A).

5.2.5.1 Na, K and Ca

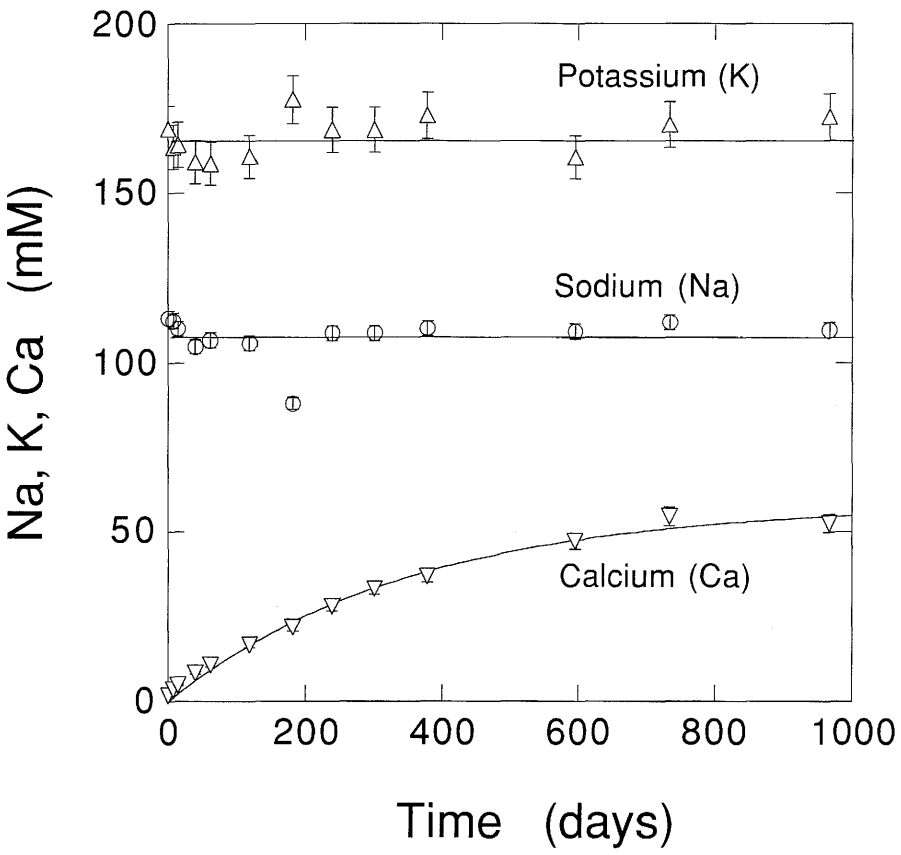

Figure 27: Evolution of the concentration of Na, K and Ca in the degradation solutions of Aldrich cellulose (Aldrich cellulose, Series A) as a function of time.

Figure 27 shows the concentrations of Na, K and Ca in solution as a function of time. The concentration of Na and K stays effectively constant. The concentration of Ca, however, increases with time. This increase of Ca cannot be explained only by the decrease in pH, causing a higher solubility of the $Ca(OH)_2$. This would lead to a much smaller increase than observed. The increase of Ca might be explained by a complexation reaction between ISA^- and Ca^{2+}.

According to VAN DUIN et al. (1989), alkaline earth metals can be coordinated by polyhydroxy carboxylic acids under alkaline conditions. Beyond pH 10, one carboxylic and one hydroxylic group of ISA (OH-group closest to the carboxylic group = α-OH group, see Figure 1) are involved in the complexation of Ca^{2+}. Since the α-hydroxylic group is not deprotonated at pH = 13.3, Ca^{2+} has to displace the proton from this hydroxylic group. The overall coordination reaction can be written as:

$$Ca^{2+} + H_4ISA^- \Leftrightarrow CaH_3ISA + H^+ \qquad (83)$$

H_4ISA^- used here corresponds to the ISA used throughout the text. "H_4" represents the protons of the 4 hydroxy-groups in ISA. Figure 28 shows the concentration of Ca as a function of the total ISA (α-ISA + β-ISA) in the degradation solutions. The symbols represent the experimental data. The dashed line is the total concentration of calcium calculated from the solubility of $Ca(OH)_2$ at the given pH of the solutions. The solid line represents the Ca-concentration calculated using equation (83) with a complexation constant $\log K_{CaISA} = -10.5$ (at I = 0).

The agreement between the calculated (solid line) and measured total concentrations of Ca in solution is very good as long as the total ISA concentration is lower than 130 mM. Beyond this concentration, measured values are significantly higher than calculated ones. This might be due to the formation of higher (1:2) Ca-ISA complexes. The complexation reaction decreases the concentration of free Ca^{2+} in solution. Due to coupled chemical equilibria, $Ca(OH)_2$ starts dissolving until its solubility equilibrium has been re-established.

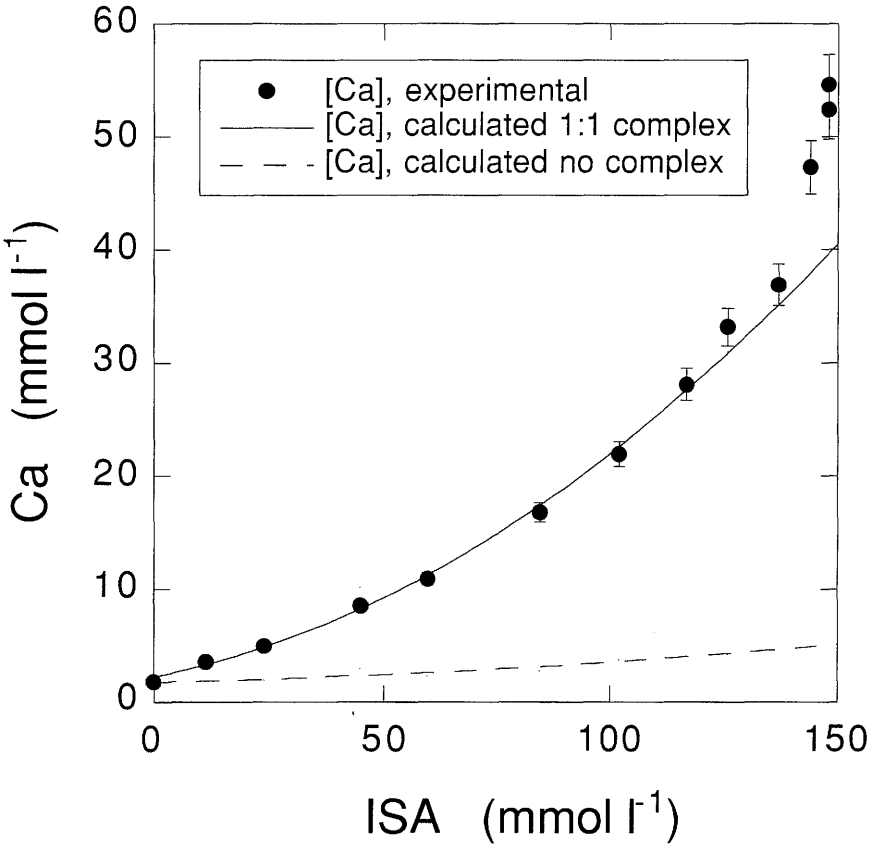

Figure 28: Dependence of the total Ca-concentration in the cellulose degradation solution (Aldrich cellulose, Series A) on the total concentration of ISA (α-ISA + β-ISA).

5.2.5.2 Organic acids produced

Figure 29 shows the evolution of the concentration of protons produced and of the pH as a function of time. The "protons produced" were calculated from the acid base titrations and the increase of Ca in the degradation solutions. The solubilisation of $Ca(OH)_2$ by ISA results in a net increase of OH^- equal to twice the increase of the Ca-concentration. Titrating the degradation solutions results in an underestimation of the protons produced by the peeling off process. The titration data were corrected for this effect by adding twice the increase in Ca concentration. The shape of the "proton curve" is similar to those for the evolution of DOC_{deg} (Fig. 22) and the formation of ISA (Fig. 23).

The data in Figure 29 could be fitted very well using an equation similar to equation (71) and (74):

$$[H^+]_{gen} = [H^+]_{max} \cdot (1 - e^{-k_t \cdot t}) \qquad (84)$$

The value of the kinetic constant k_t is $(3.8 \pm 0.4) \cdot 10^{-4}$ h^{-1} and is very similar to the values given in Table 10 for the Aldrich cellulose. The value for $[H^+]_{max}$ is 212 mM.

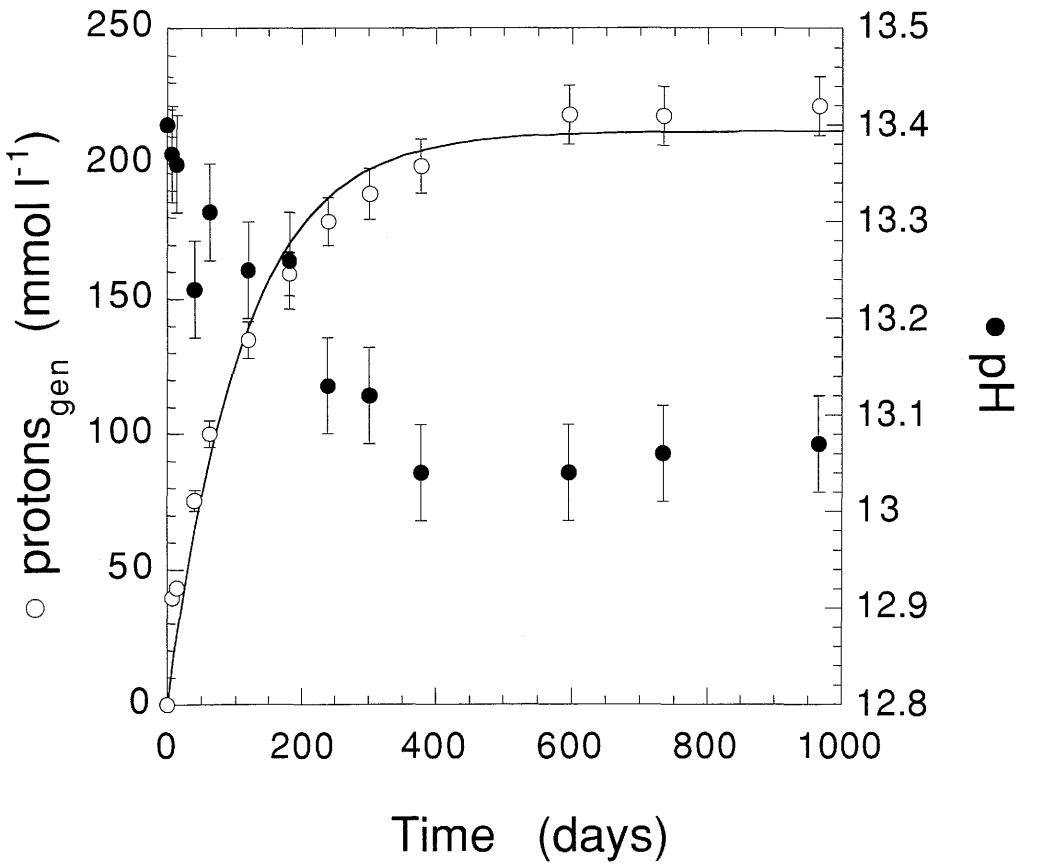

Figure 29: Concentration of protons generated (corrected for dissolution of $Ca(OH)_2$) and pH of cellulose degradation solutions (Aldrich cellulose, series A) as a function of time. The solid line was calculated using equation (84)

Plotting the concentration of protons produced against the concentration of glucose units peeled off (glucose units peeled off = $DOC_{deg}/6$) yields a straight line (Figure 30). The solid line in Figure 30 was calculated using least squares

linear regression. The curve was forced through the origin. The resulting slope of the line was nearly unity (slope = 1.2). This is in agreement with the observation that the main part of organic acids produced is ISA.The amount of moles of H^+ generated per mole of glucose split off is about 1. A value of one means that the glucose split off (G_e, see Figure 8) is transformed in a monoprotic acid (such as ISA) by e.g. the benzilic acid type of rearrangement.

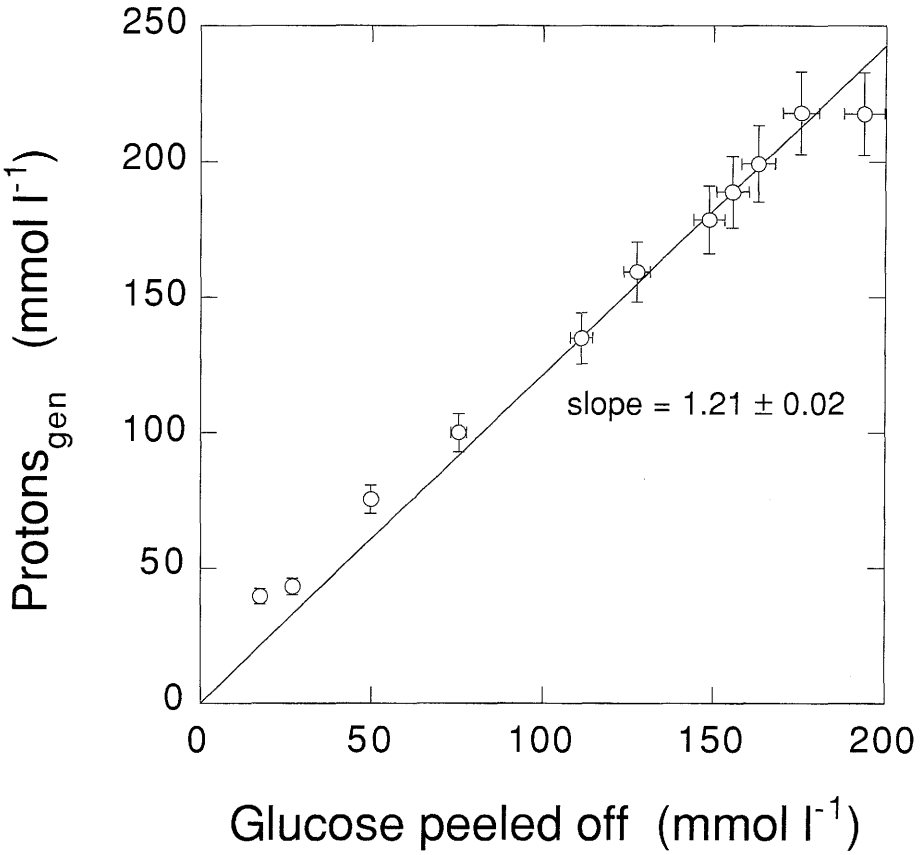

Figure 30: Correlation between amount of glucose units peeled off and the amount of protons produced for the alkaline degradation of pure cellulose in artificial cement pore water at pH = 13.3.

When the glucose split off (G_e) fragmentates to small organic acids, two protons per eliminated glucose are produced. The average amount of protons generated per glucose unit split off (P) is given by:

$$P = x_{br} \cdot 1 + x_{fr} \cdot 2 \qquad (85)$$

where x_{br} is the fraction of glucose units split off as ISA (as a result of the benzilic acid type of rearrangement of the intermediate G_e) and x_{fr} is the fraction of glucose units split off as smaller organic acids (as a result of the fragmentation reaction of the intermediate G_e). The numbers 1 and 2 represent the amount of protons generated by the removal of a glucose unit from the cellulose chain as ISA or as small acids respectively. In the literature, a value for P of 1.5 to 1.7 is reported for cellulose degraded in pure NaOH (RICHTZENHAIN et al. 1954, COLBRAN & DAVIDSON 1961, LAI & SARKANEN 1969, LAI 1991). This means that in a pure NaOH solution, 50-70% of the glucose split off, is transformed into smaller acids by the fragmentation reaction at expense of the benzilic acid type of rearrangement.

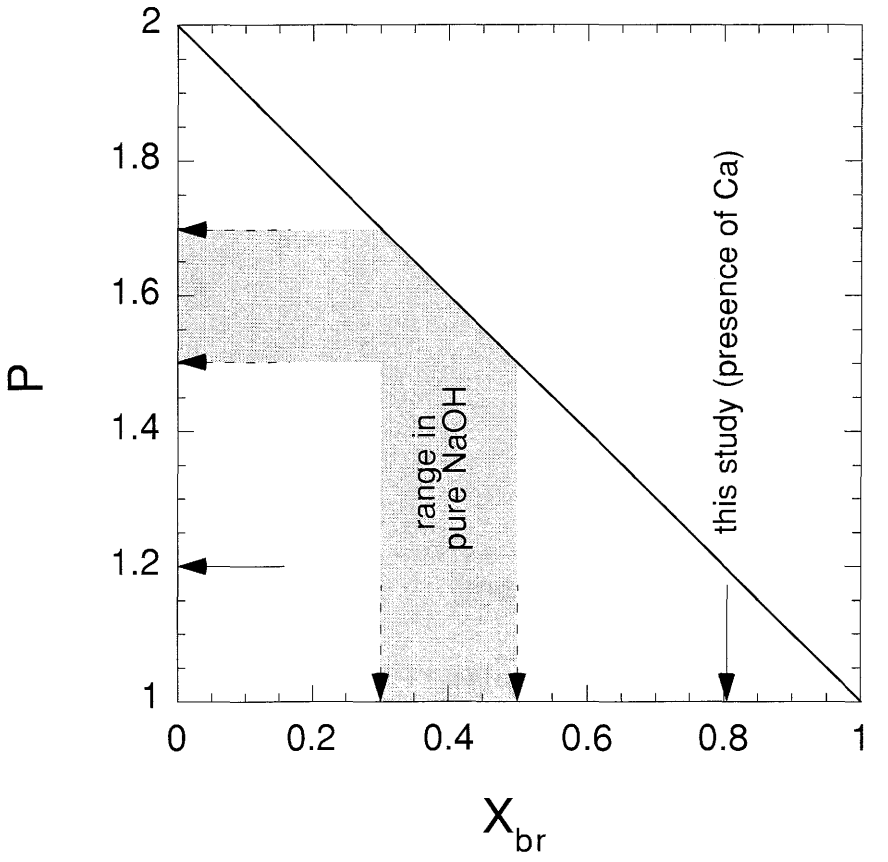

Figure 31: Relationship between the amount of protons generated per glucose unit split off (P), and the fraction of intermediate G_e transformed by the benzilic acid type of rearrangement (x_{br}).

Figure 31 represents the relationship between the amount of protons generated per glucose unit split off (P), and the fraction of intermediate G_e transformed by the benzilic acid type of rearrangement (x_{br}). It once again nicely illustrates the catalysing effect of Ca on the formation of isosaccharinic acid during alkaline degradation of cellulose.

5.2.6 Chemical stability of ISA under alkaline conditions

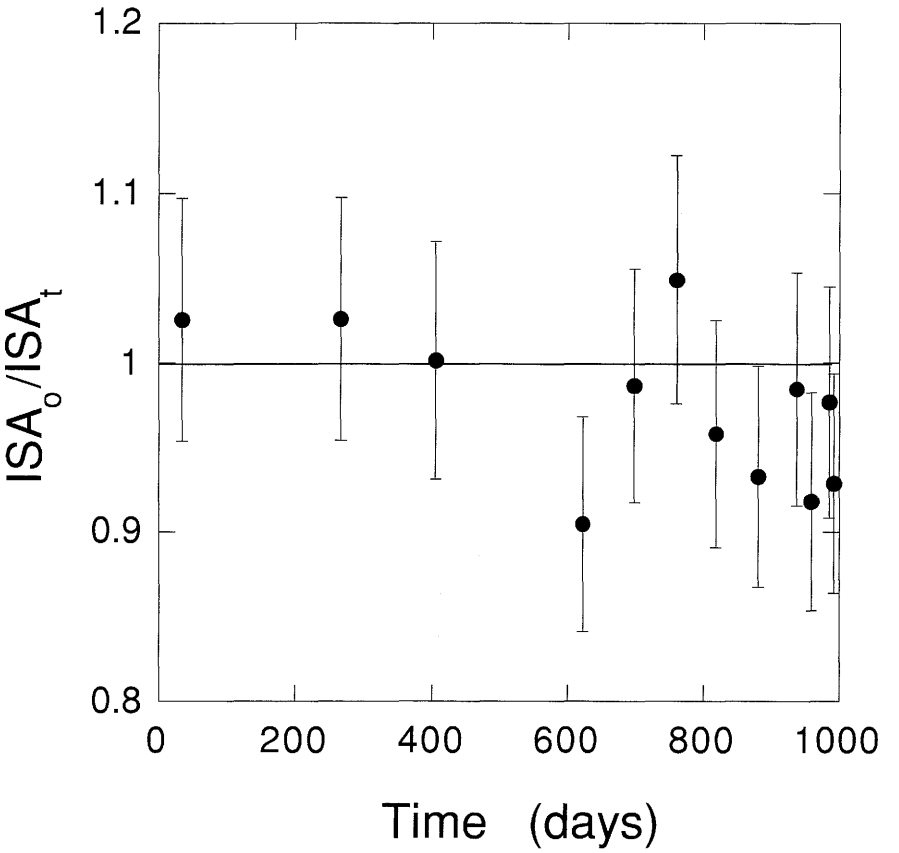

Figure 32: Stability of cellulose degradation products (α-ISA) at pH = 13.3 as a function of time. Time represents the time difference between the first and the second measurement.

Figure 32 shows the results of the ISA-stability tests carried out. The concentrations of α-ISA in the degradation solutions were measured twice, i.e. immediately after sampling, and after a given time t after sampling. The time-axis in Figure 32 represents the time difference between the first and the

second measurement. The Y-axis represents the ratio of the first and the second measurement for a given sample. If both measurements give identical results, this ratio will be one (shown by the solid line). Within the uncertainty of the measurements, the concentration of α-ISA in the samples stays constant as a function of time, indicating that α-ISA (and probably also β-ISA) is stable under the alkaline conditions of a cementitious repository and for the given time window, i.e. three years.
Microbial degradation of ISA was shown to be possible under slightly alkaline conditions (GREENFIELD et al. 1995). In our studies, microbial activity seems to be very low (or even absent), so that no effect could be observed within the timescale of the experiments.

6 SOLUBILITY OF $CA(ISA)_2$

The formation of sparingly soluble salts, e.g. with Ca^{2+}, is a process that can limit the concentration of a ligand L in interstitial pore waters (cement pore water or rock pore water) and consequently can limit the effect of a ligand on radionuclide sorption. As an example, it was shown earlier (VAN LOON & HUMMEL 1995) that the concentration of oxalate in a fresh cement pore water could not be higher than 10^{-5} M due to the formation of sparingly soluble Ca-oxalate solids (whewellite and weddelite). With respect to safety of radioactive waste repositories, such a process is very desirable, especially for ligands with a strong affinity towards tri- and tetravalent radionuclides such as gluconic acid (SAWYER 1964) and isosaccharinic acid. It is known from the literature that α-ISA forms sparingly soluble Ca-salts (WHISTLER & BeMILLER 1963) and that β-ISA forms "*highly soluble*" Ca-salts (WHISTLER & BeMILLER 1961). In a cement pore water, the concentration of Ca^{2+} is buffered due to the dissolution of $Ca(OH)_2$ (portlandite). If the stoichiometric equivalent of $Ca(OH)_2$ largely exceeds the stoichiometric equivalent of the ISA present in the pore water, the formation of solid $Ca(\alpha/\beta\text{-ISA})_2$ – and consequently also the concentration of free α/β-ISA – will be governed by the dissolution equilibrium of portlandite. The solubility products of $Ca(\alpha\text{-ISA})_2$ and $Ca(\beta\text{-ISA})_2$, however, are not known and therefore it is not possible to calculate the maximum concentration of these ligands in solution. In this study, we measured the solubility product of $Ca(\alpha\text{-ISA})_2$ by bringing the Ca-salt in equilibrium with

water at different temperatures. $Ca(\beta\text{-ISA})_2$ was not studied here because the β-isomer is very difficult to isolate and was not yet available in large quantities for this study.
The solubility products are used to calculate maximum concentrations of α-ISA in a fresh and an altered cement pore water. The qualitative information on the solubility of $Ca(\beta\text{-ISA})_2$ can be used to make some semi-quantitative estimates of the concentration of β-ISA in solution: $[\beta\text{-ISA}]_{max} >> [\alpha\text{-ISA}]_{max}$.

6.1 Materials and methods

6.1.1 Synthesis of $Ca(\alpha\text{-ISA})_2$

$Ca(\alpha\text{-ISA})_2$ was prepared by treating lactose with saturated limewater (WHISTLER & BeMILLER 1963) as described in section 5.1.5.

6.1.2 Solubility of $Ca(\alpha\text{-ISA})_2$

6.1.2.1 Solubility of $Ca(\alpha\text{-ISA})_2$ at constant temperature

About 150 mg of $Ca(\alpha\text{-ISA})_2$, 10 g of water and varying amounts of Chelex-100 (Biorad), between 0.25 g and 3 g, were mixed in a centrifuge tube (poly-sulphonate, Nalgene) and shaken end-over-end for 24 hours at 20 ± 1 °C. By using a cation exchange resin (in the Na^+-form), the concentration of Na^+, Ca^{2+} and α-ISA could be changed simultaneously without adding extra chemicals. The main cations in solution were Na^+ and Ca^{2+}, the main anion in solution was α-ISA. At equilibrium, the solutions were still saturated with respect to $Ca(\alpha\text{-ISA})_2$ (solutions were still turbid). Over-saturated solutions w.r.t. α-ISA were excluded by this procedure. The resin and the remaining $Ca(\alpha\text{-ISA})_2$ were filtered off by a membrane filter (0.45 μm) and the solutions were analysed for Na and Ca by ICP-AES and for α-ISA by ion chromatography (Dionex 2010i, HPIC-AS4A column, $Na_2CO_3/NaHCO_3$ eluent at a flow rate of $1 ml \cdot min^{-1}$, suppressed conductivity detection mode).

6.1.2.2 Solubility of Ca(α-ISA)$_2$ at varying temperature

About 300 mg of Ca(α-ISA)$_2$ were mixed with 20 ml water in 50 ml centrifuge tubes (polysulphonate, Nalgene). The mixtures were equilibrated for 24 hours in a temperature controlled shaking equipment. This time was found to be sufficient long to reach dissolution equilibrium. The temperature was varied between 2 °C and 50 °C. After equilibrium, the samples were filtered through a membrane filter (0.45 μm, Acrodisc, Gelman). The filtrates were diluted 100 times and 10 times for ISA-analysis and Ca-analysis respectively. ISA was measured by HPLC (Dionex DX-500, 80 mM NaOH eluent at a flow rate of 1ml·min^{-1}, suppressed conductivity detection mode) and Ca by ICP-AES. The use of a different method for analysing ISA was due to a change in the analytical equipment in our laboratory (replacement of the Dionex 2010i system by a Dionex DX-500 system).

6.2 Results and discussion

6.2.1 Solubility at constant temperature

Table 11 gives an overview of the composition of the solution in equilibrium with Ca(α-ISA)$_2$ and the Chelex-100 resin. With an increasing amount of ion exchange resin, the amount of calcium in solution decreases and the concentration of sodium and α-ISA increases. Ca^{2+} in solution adsorbs on the resin and is replaced by Na^+. The decrease of Ca^{2+} in solution results in a dissolution of Ca(α-ISA)$_2$ till the solubility equilibrium has been re-established. The dissolution equilibrium of the sparingly soluble Ca(α-ISA)$_2$ solid can be written as:

$$Ca(\alpha\text{-}ISA)_2 \Leftrightarrow Ca^{2+} + 2\,\alpha\text{-}ISA^- \qquad (86)$$

The solubility product, K^o_{sp}, is defined as:

$$K^o_{sp} = a_{Ca^{2+}} \cdot \left(a_{\alpha-ISA^-}\right)^2 \qquad (87)$$

Table 11: Concentration of Na, Ca and α-ISA in aqueous solutions in equilibrium with solid $Ca(\alpha\text{-ISA})_2$ at 20 °C, and corresponding solubility products.

resin (g)	[Na] (mM)	[Ca] (mM)	[α-ISA] (mM)	K°_{sp}	$\log K^{\circ}_{sp}$
0.251	12.0±0.2	3.62±0.18	18.4±0.9	$(5.6\pm0.5)\cdot10^{-7}$	-6.25
0.509	23.1±0.5	1.97±0.09	27.5±1.4	$(5.5\pm0.5)\cdot10^{-7}$	-6.26
0.749	30.1±0.6	1.45±0.07	32.7±1.6	$(5.9\pm0.5)\cdot10^{-7}$	-6.23
1.041	38.3±0.7	1.09±0.05	40.1±2.0	$(6.0\pm0.5)\cdot10^{-7}$	-6.22
1.275	43.9±0.8	0.91±0.05	44.0±2.2	$(6.2\pm0.5)\cdot10^{-7}$	-6.21
1.596	49.6±0.9	0.79±0.04	50.3±2.5	$(6.5\pm0.6)\cdot10^{-7}$	-6.19
1.746	51.8±1.0	0.73±0.04	52.3±2.6	$(6.3\pm0.5)\cdot10^{-7}$	-6.20
2.011	55.7±1.1	0.68±0.03	58.0±2.9	$(6.6\pm0.6)\cdot10^{-7}$	-6.18
3.088	65.7±1.3	0.53±0.03	67.6±3.4	$(6.6\pm0.6)\cdot10^{-7}$	-6.18

The pH of the solutions was between 6.5 and 8

with:

$a_{Ca^{2+}}$ = the activity of Ca^{2+} in solution

$a_{I\alpha-SA^-}$ = the activity of $\alpha\text{-ISA}^-$ in solution

Assuming that this is the only relevant reaction, the activities of Ca^{2+} and α-ISA^- are calculated from the analytical concentration of Ca and α-ISA in solution and the activity coefficients γ_i. The activity coefficients are calculated using the "Davies" extension of the Debye-Hückel equation (ROBINSON & STOKES 1959) given by:

$$\log\gamma_i = - A\cdot z_i^2\cdot\left(\sqrt{I}/(1 + \sqrt{I}) - 0.3\cdot I\right) \qquad (88)$$

where I is the ionic strength of the solution, z_i the charge of the ion i and A a constant defined by:

$$A = \frac{1.82\cdot10^6}{(\varepsilon\cdot T)^{3/2}} \qquad (89)$$

where ε is the dielectric constant of water (depending on temperature) and T is the absolute temperature (°K). The average value for $\log K^{\circ}_{sp}$ is -6.22 ± 0.03.

These results are in good agreement with measurements performed by ALEN (1996), who measured a solubility of Ca(α-ISA)$_2$ of 2.4 g·l^{-1} at 21 °C, from which a solubility product of $\log K^{\circ}_{sp}$ = -6.40 could be calculated.

6.2.2 Solubility at varying temperature

Table 12 gives an overview of the composition of the solutions in equilibrium with solid Ca(α-ISA)$_2$ at different temperatures. The concentration of Ca and α-ISA increases with increasing temperature, indicating that the solubility of Ca(α-ISA)$_2$ increases with temperature (endothermic reaction).

Table 12: Dependence of the composition of aqueous solutions in equilibrium with solid Ca(α-ISA)$_2$ on temperature.

T (°C)	α-ISA (mM)	Ca (mM)	K°_{sp}	$\log K^{\circ}_{sp}$
2.6	6.3±0.6	3.5±0.1	(8.0±0.8)·10^{-8}	-7.10
7.8	8.8±0.3	4.4±0.1	(1.7±0.1)·10^{-7}	-6.77
10	10.9±0.1	5.4±0.1	(3.1±0.1)·10^{-7}	-6.51
12.7	10.8±0.1	5.3±0.1	(2.9±0.1)·10^{-7}	-6.54
15.7	12.3±0.1	6.6±0.1	(4.5±0.1)·10^{-7}	-6.35
20.3	13.8±0.2	7.6±0.1	(6.2±0.2)·10^{-7}	-6.21
25.8	14.5±0.9	8.2±0.3	(7.1±0.9)·10^{-7}	-6.15
30.4	17.4±0.1	9.0±0.1	(1.1±0.1)·10^{-6}	-5.96
36	19.4±0.2	9.9±0.1	(1.4±0.1)·10^{-6}	-5.85
42	21.3±0.2	10.9±0.1	(1.7±0.1)·10^{-6}	-5.77
50.4	23.8±0.1	12.3±0.1	(2.3±0.1)·10^{-6}	-5.64

A plot of the concentration of Ca against the concentration of α-ISA (Figure not shown) gives a straight line with a slope close to 2:

$$[\alpha - \mathrm{ISA}] = (1.92 \pm 0.02) \cdot [\mathrm{Ca}] \qquad (90)$$

The concentration of α-ISA is twice the concentration of Ca, which is in excellent agreement with reaction (86). The solubility product was calculated applying equation (87). The activity coefficients were calculated using equation (88).

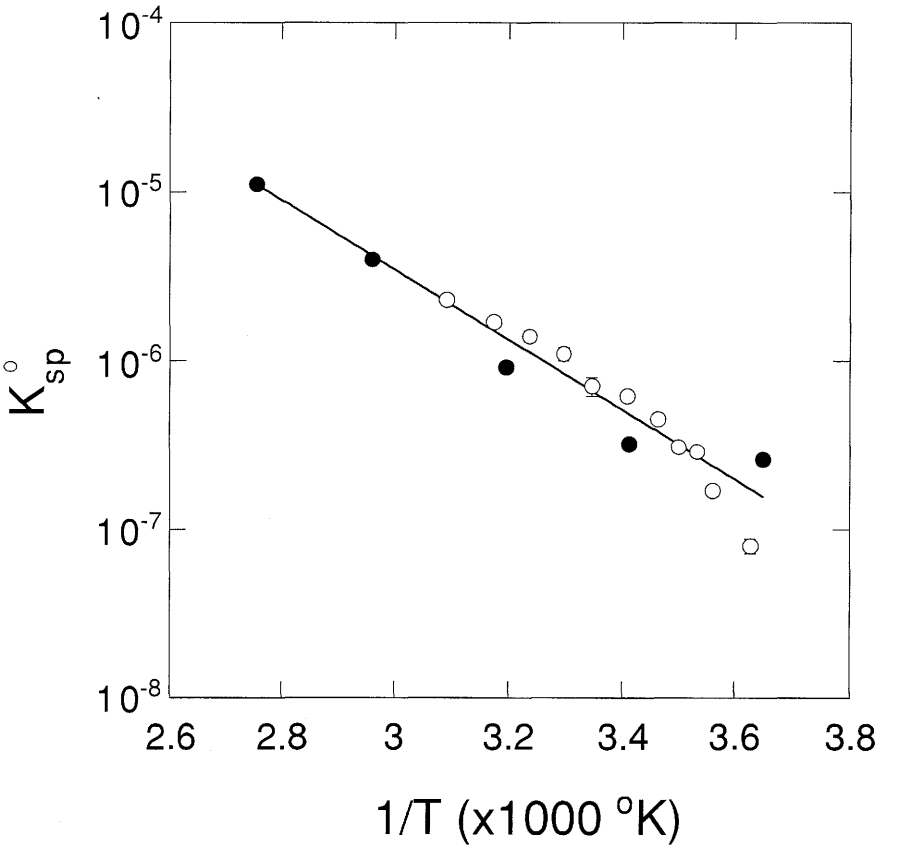

Figure 33: Plot of the solubility product of $Ca(\alpha\text{-ISA})_2$ against the reciprocal temperature. Filled symbols represent unpublished data of ALEN (1996). Open symbols are measurements from this study.

The standard reaction enthalpy (ΔH°) can be calculated from the temperature dependency of K°_{sp} at constant pressure by:

$$\frac{d \ln K^{\circ}_{sp}}{dT} = \frac{\Delta H^{\circ}}{R \cdot T^2} \qquad (91)$$

which is known as the van 't Hoff equation. Under the assumption that ΔH° is independent on temperature and that the heat capacity of the reaction, ΔC°_{p}, is

close to zero (STUMM & MORGAN 1996), equation (91) can be simply integrated to yield:

$$\ln K^{\circ}_{sp} = -\frac{\Delta H^{\circ}}{R \cdot T} + C \qquad (92)$$

where C is an integration constant. A plot of $\log K^{\circ}_{sp}$ against the reciprocal absolute temperature yields a straight line with slope $0.434 \cdot \Delta H^{\circ}/R$. The linear plot shown in Figure 33 indicates that these assumptions are justified for the solubility of Ca(α-ISA)$_2$ in the temperature range 280 °K < T < 363 °K. The standard reaction enthalpy for reaction (86) is 40±1 kJ·mol^{-1}. With the standard reaction enthalpy, the solubility product at a given temperature can be recalculated for another temperature by:

$$\ln \frac{K_{T_2}}{K_{T_1}} = \frac{\Delta H^{\circ}}{R} \cdot \left(\frac{1}{T_1} - \frac{1}{T_2} \right) \qquad (93)$$

6.3 Solubility of Ca(ISA)$_2$ in cement pore water.

The solubility product was used to estimate the maximum concentration of α-ISA that can be expected in a cement pore water. In the early degradation stage of the cement, dissolution of Na-K-OH determines the pH of the cement pore water (pH = 13.3). The Ca-concentration in such water is ~ 2 mM. In the second stage of cement degradation, dissolution of Ca(OH)$_2$ determines the water chemistry of the cement pore water (pH = 12.5). At this stage of cement degradation, the Ca-concentration in the pore water equals ~20 mM (BERNER 1990). The maximum concentration of α-ISA in the pore water was calculated with the PHREEQE geochemical code (PARKHURST et al. 1980) using the solubility equilibrium for Ca(α-ISA)$_2$:

$$Ca(ISA)_2 \Leftrightarrow Ca^{2+} + 2\ ISA^{-} \qquad (94)$$

with $\log K^{\circ}_{sp}$ = -6.2, and the complexation reaction:

$$Ca^{2+} + H_4ISA^{-} \Leftrightarrow CaH_3ISA^{\circ} + H^{+} \qquad (95)$$

with $\log K_{CaISA} = -10.5$. Table 13 shows the calculated maximum concentrations of α-ISA in equilibrium with Ca^{2+} for two stages of cement degradation. The measured values shown in Table 13 represent measurements reported in VERCAMMEN et al. (1997).

Table 13: Predicted and measured solubility of $Ca(\alpha\text{-ISA})_2$ at different pH values.

pH	Ca (M)	I (M)	$^{*}[ISA]_{max}$ (M)	$^{**}[ISA]_{measured}$ (M)
13.3	0.002	0.3	0.051	~0.050
12.5	0.020	0.05	0.021	~0.022

*calculated using equation (94) and (95); ** measured (VERCAMMEN et al. 1997)

The calculations show that the solubility limit of $Ca(\alpha\text{-ISA})_2$ results in a relatively high concentration of α-ISA in cement pore water. The solubility of $Ca(\alpha\text{-ISA})_2$ is too high to limit the maximum concentration of α-ISA in cement pore waters to levels where their effect on the sorption of radionuclides is negligible, i.e. $\leq 10^{-4}$ M (see chapter 8).
There is a good agreement between the calculated values and the values measured by VERCAMMEN et al. (1997).

7 SORPTION OF ISA ON CEMENT

The sorption of ISA on cement might be an important process that can reduce the ISA concentration in the cement pore water. No systematic studies on the sorption of ISA are known in the literature, consequently we started an investigation on the sorption of ISA on cement under repository conditions., i.e. a (Na,K)OH solution saturated with respect to $Ca(OH)_2$ (Portlandite) and having a pH value of 13.3.
In this study, we focus on measuring sorption isotherms for ISA at 25 °C and on determining the sorption capacity and the ISA-cement interaction constant. Some preliminary experiments on the sorption of ISA on CSH and CASH-phases are also presented and discussed. CSH and CASH phases are the

main components of a hydrated cement. It are gel-like phases composed of mainly Ca and Si (CSH) or Ca, Si and Al (CASH).

7.1 Materials and methods

7.1.1 Hardened Cement Paste

The sorbent used in the sorption experiments with cement was a hardened cement paste (CPA 55 HTS cement, Lafarge, France). An overview of the chemical and mineral composition of the HTS cement is given in Table 14. After complete hydration (6 years) the hardened cement paste was crushed and sieved. The particle fraction between 100 µm and 400 µm was used in the sorption experiments.

Table 14: Chemical and mineralogical composition of the CPA 55 HTS cement used in the sorption experiments.

oxide	wt %	oxide	wt %
CaO	66.4	K_2O	0.26
SiO_2	23.8	Na_2O	0.09
Al_2O_3	2.7	MgO	0.88
Fe_2O_3	2.8	TiO_2	0.12
SO_3	1.8		
	***Clinker composition**		
C_3S (Alite)	64.1	C_3A (Aluminate)	0.5
C_2S (Belite)	24.1	C_4AF (Ferrite)	7.6

*C: CaO; S:SiO_2; A: Al_2O_3;F: Fe_2O_3, e.g. C_3S: = $3CaO{\cdot}SiO_2$

7.1.2 CSH and CASH phases

The CSH- and CASH-phases were synthesised by the group of Prof. Glasser at the University of Aberdeen (UK) and were shipped to PSI as suspensions. The composition of the C(A)SH-phases are given in Table 15.

The gel suspensions were partially dried under a N_2-atmosphere in a glove box until the water content was about 50 %.

Table 15: Chemical composition of CSH and CASH phases used in the sorption experiment (ratios are based on oxides*).

	CSH	CASH
C/S	1.09	0.91
S/A	-	12.2
C/(S+A)	-	0.84

*C: CaO; S:SiO_2; A: Al_2O_3

7.1.3 Artificial cement pore water (ACW-I)

The composition of the artificial cement pore water (denoted hereafter as ACW-I) was taken from (BERNER 1990) and had a composition as discussed in 5.1.2. One liter of demineralised water was flushed with Argon for half an hour. 4.56 g NaOH (Merck, 100 %), 11.61 g KOH (Merck, 87 %) and 10 g of $Ca(OH)_2$ (Merck, 100 %) were added. All chemicals used were of analytical grade quality. The mixture was left standing for 24 hours after which the liquid was filtered off through a 0.45 µm membrane filter (cellulose nitrate, Schleicher & Schuell ME 25, Germany). All manipulations were carried out in a glove-box under a controlled N_2 atmosphere (CO_2, O_2 < 5 ppm). After preparation, the composition of ACW-I was checked by ICP-AES analysis and showed the following composition: 110.5 mM of Na, 176 mM of K, 1.75 mM of Ca. The measured pH of the solution was 13.30±0.05.

7.1.4 Sorption of ISA

7.1.4.1 Sorption of α-ISA on cement

The sorption of α-ISA on cement was studied by a batch technique. To cover a broad equilibrium concentration range of ISA, the sorption of ISA was carried

out with different solid to liquid (S:L) ratios ranging from 1:2 (10 g of cement : 20 ml of ACW-I) to 1:40 (1 g cement : 40 ml of ACW-I). The cement was placed in 50 ml polysulphonate centrifuge tubes (ISA was found not to sorb on these tubes) and the artificial cement pore water, containing ISA between 10^{-5} M and $3 \cdot 10^{-1}$ M, was added. The mixtures were shaken end-over-end for one day, one week and a few systems for one month, three months and nine months. All manipulations were performed in a glove-box under a controlled N_2-atmosphere. The suspensions were centrifuged at 27,000 x g for 15 minutes (Beckman L7-35 Ultracentrifuge). Since a thin film of cementitious material remained on the top of the supernatant, solutions were additionally filtered through a 0.45µm membrane filter (Acrodisc, Gelman, U.S) before analysis. The ISA in the equilibrium solution was measured by HPLC (Dionex DX 500) using a Carbopac PA-100 analytical column and an electrochemical detector (ED 40) in the suppressed conductivity detection mode. The eluent used contained 0.08 M NaOH. Standards were made up from pure $Ca(ISA)_2$ in demineralised water, or in ACW-I pre-equilibrated with cement. The average relative standard uncertainty on the HPLC measurements was 5 % for ISA concentrations $>10^{-4}$ M. For ISA concentrations $<10^{-4}$ M, the uncertainty on the measurement was at most 10%. The amount of ISA sorbed on the cement ($[ISA]_{sorbed}$, $mol \cdot kg^{-1}$) was calculated from the difference in concentration before and after sorption using the following equation:

$$[ISA]_{sorbed} = \frac{\left((ISA)_{in} - (ISA)_{eq}\right) \cdot V}{m} \qquad (mol \cdot kg^{-1}) \qquad (96)$$

where $(ISA)_{in}$ is the initial concentration of ISA (M), $(ISA)_{eq}$ is the equilibrium concentration of ISA (M), V is the volume of the liquid phase (l) and m is the amount of cement used (kg). The maximum relative error on the measured sorption values was ~ 20%.

7.1.4.2 Sorption of β-ISA on cement

The sorption of β-ISA on cement was determined in experimental systems containing volumes of 2 ml (GLAUS et al. 1997b). A stock solution of β-ISA was prepared from the pools collected by preparative HPLC (section 5.1.6).

The fractions collected by preparative HPLC containing β-ISA in pure form were pooled and brought to pH 11 by addition of a Chelex-100 ion exchange resin (protonated form). Afterwards, the ion exchange resin was filtered off and washed thoroughly with water. The filtrate and the washing water were pooled and brought to a volume of 10 ml by evaporation under reduced pressure (10 mbar) at 40°C. The concentration of β-ISA in this stock solution was determined by HPLC to be 0.11 M. The weighting of cement and the preparation of cement suspensions were performed in a glove box in a nitrogen atmosphere (CO_2, O_2 < 5ppm). Solutions of β-ISA were prepared under lab atmosphere. In a 6 ml ponyvial, cement and aliquots of β-ISA solutions, "ACW-I concentrate" (0.91g NaOH (100%) + 2.38g KOH (85%) filled up to a volume of 20 ml with water), water and 0.4 M $Ca(NO_3)_2$ were added according to Table 16. The suspensions were shaken from time to time for one week. After that, they were filtered through a 0.45 µm membrane filter (Acrodisc, Gelman, USA). The concentration of β-ISA in the filtrates as well as in the stock solutions was measured by HPLC as described in 5.1.4.5.

Table 16: Composition of the suspensions used to measure the sorption of β-ISA on cement.

[β-ISA] (M)	cement	β-ISA stock	"ACW-I conc"	Q-H_2O	$Ca(NO_3)_2$ 0.4 M	n
10^{-1}	0.4 g	1790 µl	200 µl	----	10 µl	2
10^{-2}	0.2 g	179 µl	200 µl	1610 µl	10 µl	3
10^{-3}	0.05 g	179 µl[2]	200 µl	1610 µl	10 µl	3
10^{-4}	0.05 g	179 µl[3]	200 µl	1610 µl	10 µl	3

[1]cement: 100 - 400 µm

[2]β-ISA stock solution diluted 1:10 in Q-H_2O

[3]β-ISA stock solution diluted 1:100 in Q-H_2O

"ACW-I conc" : ACW-I concentrate n: number of replicates

7.1.4.3 Sorption of α-ISA on CSH and CASH phases

The sorption of ISA on C(A)SH-phases was also studied by the batch sorption technique. A stock solution of both phases in ACW-I was prepared. The stock solutions were homogenised with a high speed mixer (Ultra-Turrax T-15, Janke & Kunkel, IKA). From these stock solutions, an aliquot was taken and placed in a 50 ml centrifuge tube. The solid to liquid ratio (S:L) ranged between $1 g \cdot l^{-1}$ and $20 g \cdot l^{-1}$ for the CASH phase and was $100 g \cdot l^{-1}$ in case of the CSH phase. ACW-I, containing ISA between 10^{-4} M and 10^{-1} M, was added. The mixtures were shaken end-over-end for two days. All manipulations were performed in a glove-box under a controlled N_2-atmosphere. The suspensions were centrifuged at 27,000 x g for 15 minutes (Beckman L7-35 Ultracentrifuge). The ISA in the equilibrium solution was measured by HPLC as described in 7.1.4.1. The amount of ISA sorbed was calculated in a similar way as described for the cement systems in 7.1.4.1 using equation (96).

7.1.5 Sorption of cellulose degradation products on cement

140 ml of degradation products were equilibrated with 40 g of cement (see 7.1.1) under a N_2 atmosphere in a glove-box. After equilibrating for one week, the suspensions were centrifuged at 27,000 x g for 30 minutes and the supernatant was analysed for DOC (see 5.1.4.2) and ISA (ion exchange chromatography, see 5.1.4.5).

7.2 Results and discussion

7.2.1 Sorption of α-ISA on cement

In a preliminary sorption experiment (data not shown) it was found that the equilibrium concentration of ISA was smaller than its initial concentration. This can be interpreted either by a sorption process or by a chemical transformation reaction. To discriminate between these two possibilities, a comparison between ΔISA and ΔDOC was made. This comparison is shown in Figure 34. The decrease of ISA-carbon ($6 \cdot \Delta$(ISA) = six times the difference between initial

and equilibrium concentration of ISA) is plotted against the decrease of DOC (Δ(DOC) = difference between the initial and equilibrium concentration of total dissolved organic carbon). The ratio between the decrease in ISA-carbon and the decrease in DOC ($6 \cdot \Delta(ISA)/\Delta(DOC)$ is close to unity (slope of the regression line is 1.03±0.02), indicating that the decrease of the ISA-concentration is caused by a sorption process. Degradation of ISA would result in values of this ratio being much smaller than one. A separate study on the stability of ISA in ACW-I in absence of cement showed that ISA is stable for months under such conditions (see section 5.2.6, Figure 32) and supports the exclusion of transformation of ISA in our sorption studies.

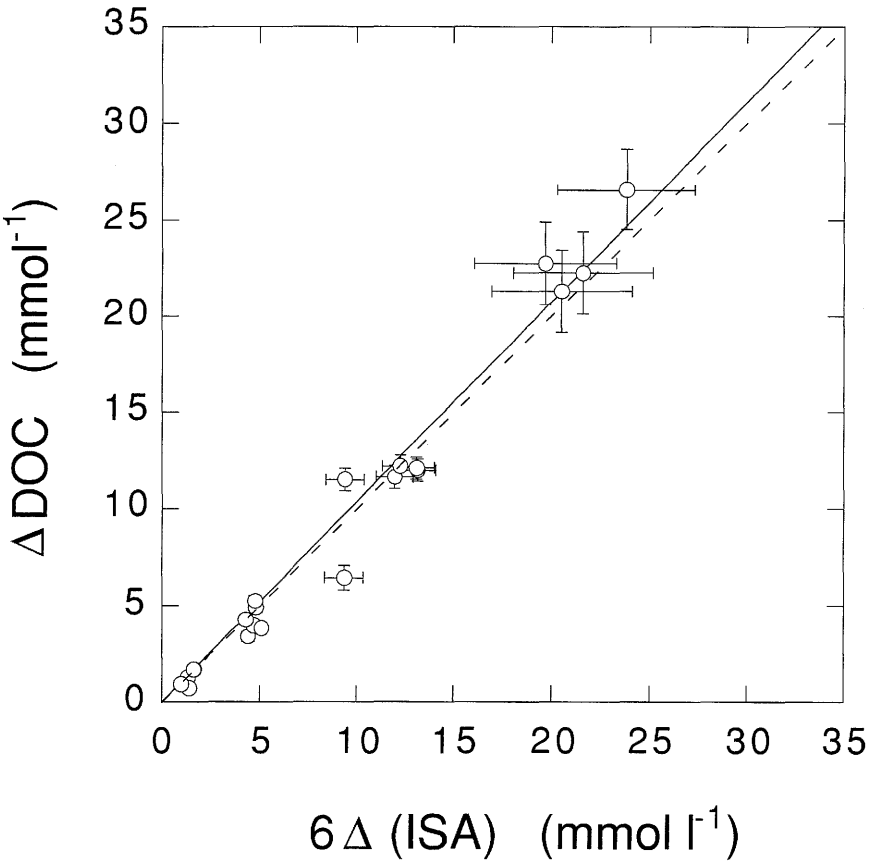

Figure 34: Relationship between the decrease of ISA-carbon in solution and the decrease of the total dissolved organic carbon (DOC). The symbols represent the experimental data. The solid line is a least squares fit with a slope of 1.03 ± 0.02 and a correlation coefficient of 0.98. The dashed line represents a straight line with a slope of unity.

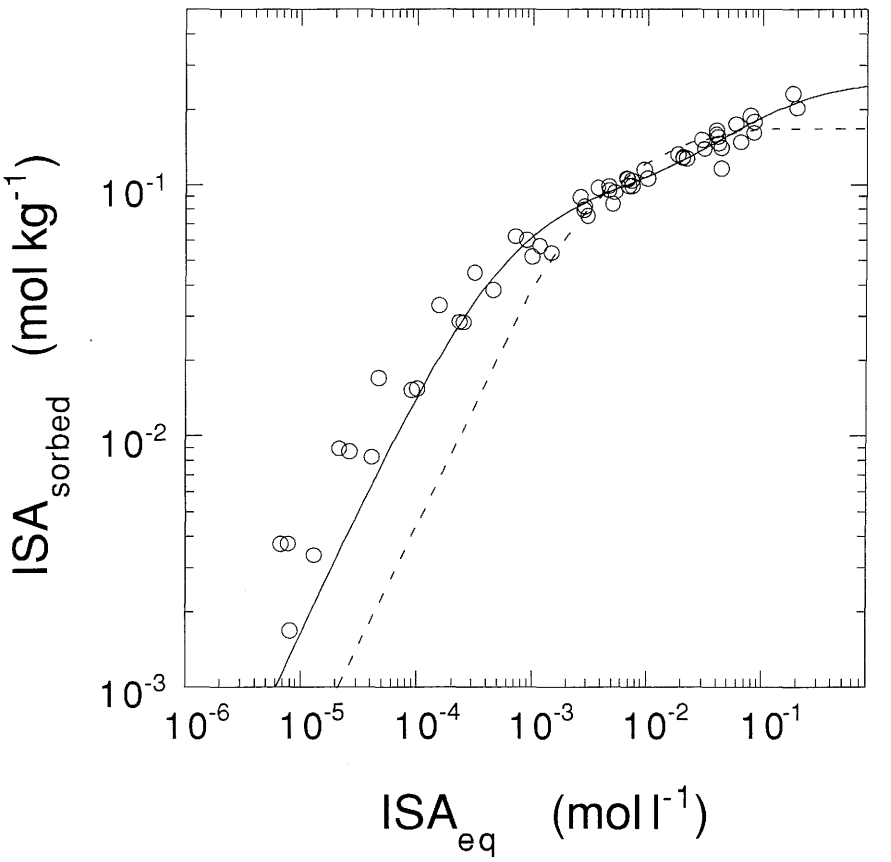

Figure 35: Sorption isotherm of α-ISA on Portland cement at pH = 13.3. The symbols are the experimental data for equilibrium times between 1 and 10 days. The dashed line represents the best fit by a Langmuir isotherm with one adsorption site (q = 0.17±0.01 mol·kg^{-1}; K = 286±41 l·mol^{-1}). The solid line represents the best fit using a two site model with Langmuir adsorption behaviour (q_1 = 0.1±0.01 mol·kg^{-1}; K_1 = 1730±385 l·mol^{-1}; q_2 = 0.17±0.02 mol·kg^{-1}; K_2 = 12±4 l·mol^{-1}) (see also VAN LOON & GLAUS 1997a).

Adsorption of ISA on the cement is not consistent with electrostatic concepts because of the repulsion between the negatively charged cement surface and the negatively charged ISA-molecules (at pH = 13.3 the carboxylic group of isosaccharinic acid is completely deprotonated). Strong specific interactions between ISA and the surface sites, however, can overcome this repulsion and can lead to sorption. Examples of the adsorption of anions by ligand exchange (= specific interaction) on Fe- and Al-oxides beyond the zero point of charge

(at high pH) are known in the literature (DZOMBAK & MOREL 1990, STUMM & MORGAN 1996, SIGG 1979).

The ISA adsorption data are summarised in Figure 35. The relative standard uncertainty on the amount of ISA sorbed (ISA_{sorbed}) is ~6% as long as the equilibrium concentration of ISA (ISA_{eq}) is $<10^{-2}$ M. For ISA_{eq} $>10^{-2}$ M, the relative standard uncertainty becomes 10-20 %. The plot shows data for equilibrium times ranging from one day to 10 days. The consistency of the data indicates that the sorption of ISA on cement is a fast process, almost reaching equilibrium after one day. The simplest assumption that can be made in adsorption phenomena is that only one adsorption site is involved and that this site becomes reversibly saturated with increasing concentration of adsorbate in the equilibrium solution. In such a case, the adsorption isotherm can be described by a Langmuir isotherm. For the ISA/cement system considered in this work, one can write:

$$[ISA]_{sorbed} = \frac{K \cdot q \cdot (ISA)_{eq}}{1 + K \cdot (ISA)_{eq}} \qquad (97)$$

where:

q	=	adsorption capacity of cement for ISA ($mol \cdot kg^{-1}$)
K	=	adsorption-affinity constant ($l \cdot mol^{-1}$)
$(ISA)_{eq}$	=	equilibrium concentration of ISA (M)
$[ISA]_{sorbed}$	=	amount of ISA sorbed ($mol \cdot kg^{-1}$)

Close inspection of the data in Figure 35, however, showed that the experimental results cannot be described by a Langmuir type of isotherm with only one adsorption site. The introduction of a second site with a Langmuir adsorption behaviour gives a much better fit of the experimental results as is shown in Figure 35:

$$[ISA]_{sorbed} = \frac{K_1 \cdot q_1 \cdot (ISA)_{eq}}{1 + K_1 \cdot (ISA)_{eq}} + \frac{K_2 \cdot q_2 \cdot (ISA)_{eq}}{1 + K_2 \cdot (ISA)_{eq}} \qquad (98)$$

where q_1 and q_2 represent the sorption capacities and K_1 and K_2 are the adsorption affinity constants for the two sites.

The introduction of additional sorption sites would undoubtedly give even a better fit to the experimental data. However, without more information on the solid phases responsible for the sorption and the underlying adsorption mechanism(s), we see no benefit from such an exercise. The total sorption capacity of the cement for ISA (q_1+q_2) is ~0.3 mol·kg^{-1}. This value is in good agreement with the value of 0.32 mol·kg^{-1} proposed by BRADBURY & SAROTT (1995). Attempts to fit the complete dataset with a Freundlich type of isotherm failed.

It is well known that many organic products such as lignosulphonate, naphtalenesulphonate etc. sorb on cement (BLANK et al. 1963, ROSSINGTON & RUNK 1968, COSTA & MASSAZZA 1984, ANDERSEN & ROY 1987, UCHIKAWA et al. 1992, SINGH et al. 1992, SPANKA & THIELEN 1995). This phenomenon found an application in the cement industry because the adsorption of organics changes the surface characteristics of the cement and consequently also its workability. It was shown that the sorption of lignosulphonate and naphtalenesulphonate on cement made the cement surface more negatively charged (COSTA & MASSAZZA 1984), resulting in modified rheological properties (fluidification). The adsorption mechanism of such organic molecules is still poorly understood. However, it was observed that especially the C_3A and C_4AF (see Table 14) phases and its hydration products showed a strong affinity for organic molecules (FUKAYA & KATO 1986). The adsorption was also found to be highly irreversible.

7.2.2 Sorption of β-ISA on cement

Figure 36 shows the sorption of β-ISA on cement together with the results of α-ISA presented in previous section. α- and β-ISA seems to behave similarly w.r.t. sorption on cement. This is not unexpected since both molecules have a similar structure (Figure 1). Sorption parameters were not determined for β-ISA because only a few measurements could be performed. However, from the similarity between α- and β-ISA, the same sorption parameters as for α-ISA can be taken (section 7.2.1).

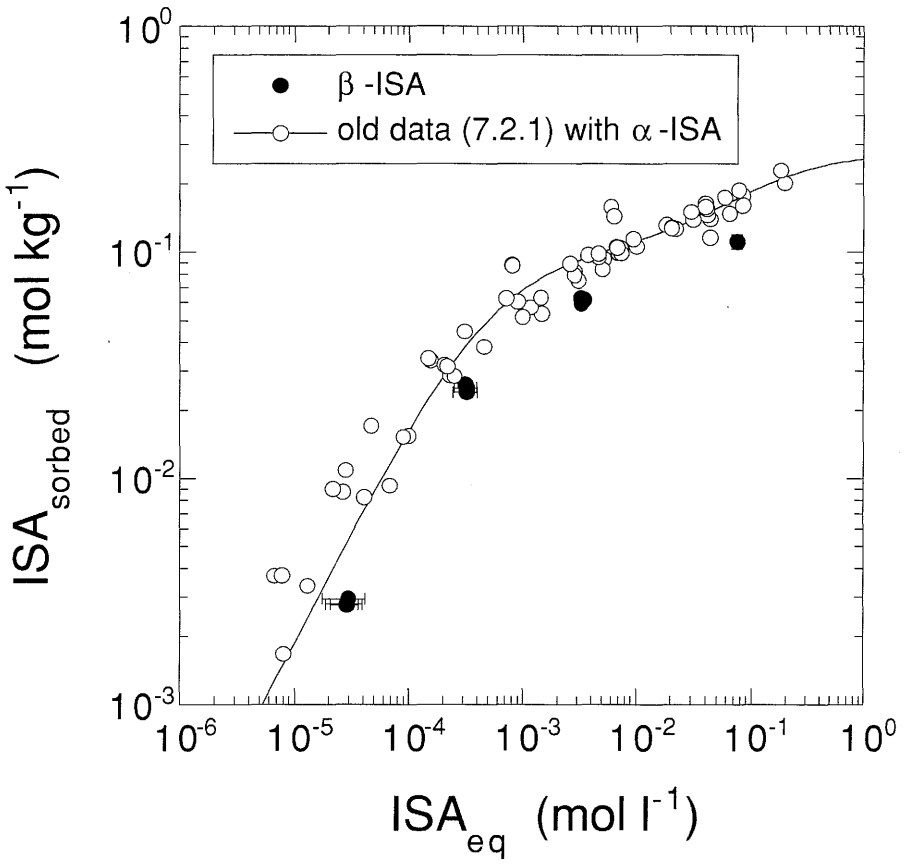

Figure 36: Sorption isotherm of β-ISA on cement at pH = 13.3. The results of the sorption of α-ISA (see also Fig. 34) are also shown for comparison.

7.2.3 Sorption of α-ISA on CSH- and CASH-phases

Figure 37 shows the results of the sorption of α-ISA on CASH and CSH-phases. α-ISA sorbs much stronger on the CASH-phase as it does on the CSH-phase. Since the only difference between the CASH- and CSH-phase is the aluminum content, this led us conclude that aluminum plays an important rôle in the sorption behaviour of ISA. It is known from the literature that similar compounds such as e.g. gluconic acid form strong complexes with aluminum in solution under alkaline conditions (SAWYER 1964, MOTEKAITIS & MARTELL 1984). Strong surface complexes between aluminum and ISA might explain the strong sorption on the CASH-phase and perhaps also on the cement. The interaction between calcium and α-ISA under alkaline conditions is much weaker (VERCAMMEN et al. 1997) and the weak interaction of ISA

with the pure CSH-phase and the weak sorption site on cement might be explained by a weak surface complex between calcium and ISA. This would be in agreement with the postulated correlation between the tendency to form solute complexes and the tendency to form surface complexes (STUMM & MORGAN 1996).

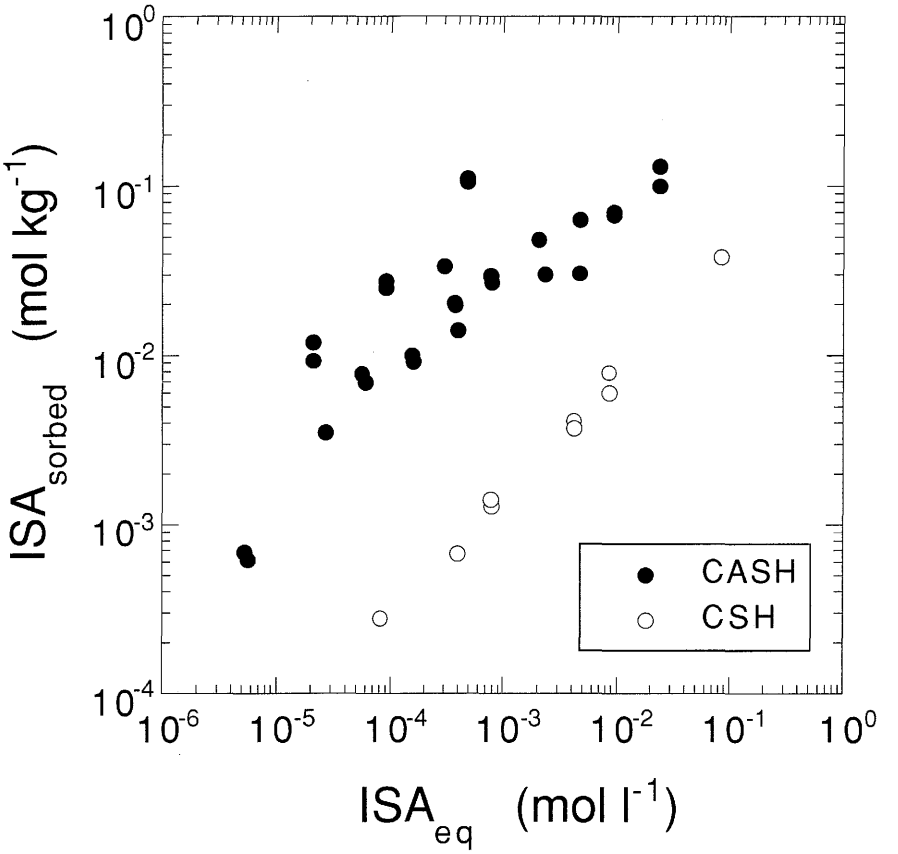

Figure 37: Sorption isotherm of α-ISA on CASH- and CSH-phases at pH = 13.3.

It can be concluded that the observed sorption behaviour of ISA on cement is very important for radwaste disposal since this sorption process drastically reduces the concentration of ISA in the pore water and consequently the adverse effect of ISA on radionuclide sorption. The adsorption behaviour of ISA on cement could be satisfactorily described by a Langmuir isotherm considering two sorption sites. However, the underlying mechanism(s) is (are) still unknown and further investigations in this field are necessary. From the many possible adsorption mechanisms, specific interaction (chemical

interaction) with the surface is the most likely one. Combination of surface analytical techniques such as reflection-absorption infrared spectroscopy (TEJEDOR-TEJEDOR & ANDERSON 1986, HUG & SULZBERGER 1994) and calorimetric measurements might give some valuable information on the mechanisms involved.

7.2.4 Sorption of degradation products on cement

Table 17 summarises the results of the sorption of cellulose degradation products on cement. Three samples were tested: degradation products of 2 weeks incubation time (A2), degradation products of 4 months degradation time (A5) and degradation products of 1 year degradation time (A9). Two parameters were measured to check the sorption: α-ISA and DOC. The α-ISA concentration in the A2 sample decreases from 12.7 mM to 2.33 mM. For the A5 sample, α-ISA decreases from 47.3 mM to 27.1 mM. The DOC in the A2 sample decreases from 181 to 62.3 mM and in the A5 sample from 685 to 444 mM. From these observations it is clear that the degradation products sorb on the cement. The decrease in DOC for the A2 sample is 119 mM. This corresponds to a decrease in total ISA of 19.8 mM. The decrease in α-ISA is 10.4 mM. The decrease in β-ISA thus has to be 9.4 mM. The decrease in both isomers is thus more or less the same. This means that the interaction of α-ISA and β-ISA with the cement phase is identical. This is confirmed by the chromatogram of the degradation products of A2 after being in contact with the cement (not shown here): the ratio in peak height before (α/β=1.2) and after sorption (α/β=0.95) is roughly the same, indicating that the two isomers sorb to the same extent. This is also in good agreement with the observations made earlier (7.2.1 and 7.2.2). The same observation was also made for the A5 sample. The decrease in DOC is about 242 mM, corresponding to a decrease in ISA of 40.2 mM. The decrease in α-ISA measured is 20.2 mM. The decrease in β-ISA is about 20 mM and of the same order of magnitude as α-ISA.

For A9, the decrease in DOC (236 mM). This corresponds with a decrease in ISA of 40 mM. This value is lower than the observed decrease in α-ISA (30 mM) and β-ISA (30 mM).

Table 17: Effect of contacting a solution of degradation products with cement on the concentration of α-ISA and DOC.

Sample	DOC (mM)	α-ISA (mM)	[1]α-ISA (mM)
A2 before	181	12.8	
A2 after	62.3	2.35	1.03
A5 before	685	47.5	
A5 after	443	27.2	24.5
A9 before	996	78.5	
A9 after	760	48.2	59.0

before : before contacting the solutions with cement
after : after contacting the solutions with cement
[1] calculated with equation (98)

The concentration of α-ISA in the equilibrium solution was also calculated using equation (98) with the sorption parameters as given in Figure 35. This could be done since both isomers sorb to the same extent on cement and since they are present in roughly the same amount in the degradation solutions. The total concentration of ISA after sorption was calculated. The concentration of α-ISA was estimated by dividing this total concentration of ISA by a factor of 2. This value is tabulated in Table 17. As can be seen, the calculated and the measured values are in good agreement with each other.

7.2.5 Effect of ISA on the Ca-concentration in ISA/Cement systems

Both ISA and Ca were measured in the solutions in equilibrium with cement. Figure 38 shows the Ca concentration as a function of the equilibrium concentration of α-ISA in the solutions. The concentration of Ca increases with increasing ISA concentration. Figure 38 also shows the Ca data from the cellulose degradation experiments (see Fig. 28 in section 5.2.5.1). Both data sets give a consistent picture. As already discussed in section 5.2.5.1, the increase in Ca can be explained by a complexation reaction between Ca and ISA according to equation (83). The solid line shown in Figure 38 is calculated

with PHREEQE using reaction (83) with $\log K_o = -10.5$ (at I = 0) and the portlandite equilibrium.

The complexation of Ca by ISA might have important consequences for the complexation of tri- and tetravalent metals, since Ca can affect the complexation reaction between such metals and ISA. A more detailed study on the complexation of Ca by ISA as a function of pH is given in VERCAMMEN et al. (1997).

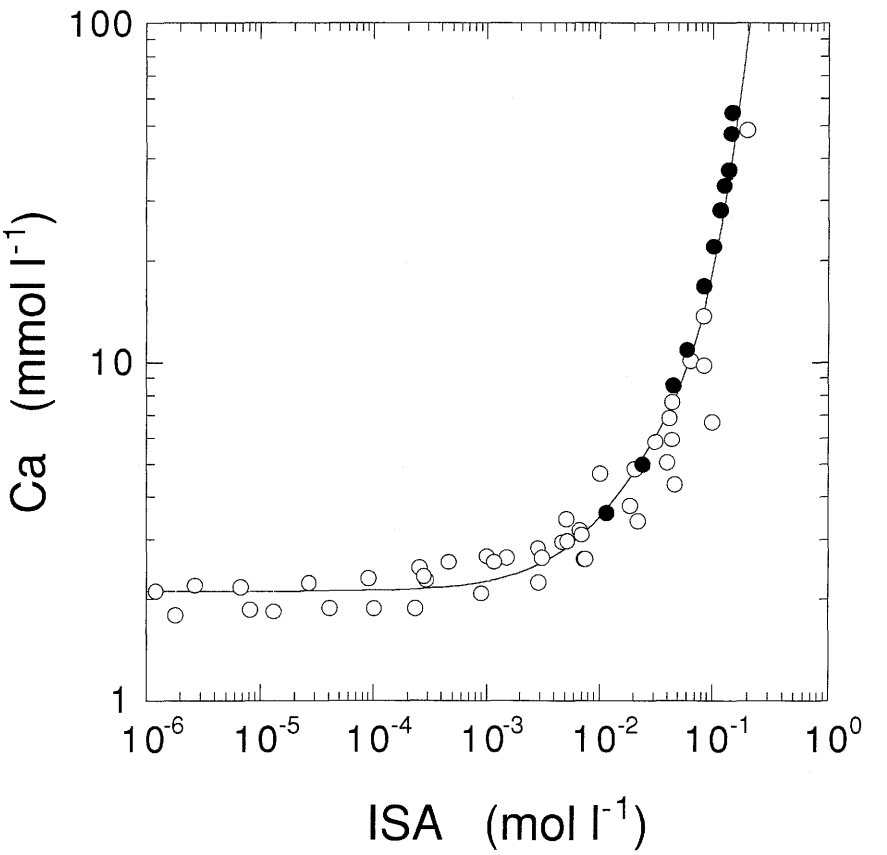

Figure 38: Dependence of the Ca concentration on the concentration of ISA in solution for ISA/cement systems and ISA/cellulose/portlandite systems at pH = ~13.3. Open symbols represent data from the ISA-sorption studies. Closed symbols are data from the long term cellulose degradation experiment. The solid line was calculated using reaction (83).

8 EFFECT OF CELLULOSE DEGRADATION PRODUCTS ON THE SORPTION OF NICKEL, EUROPIUM AND THORIUM

This chapter describes experiments on the effect of cellulose degradation products on the sorption of metals on a solid phase. The main goal of the experiments was to find out whether the organics in the cellulose degradation mixtures had complexing properties. A further aim of the sorption experiments was to test the formalism for sorption reduction discussed in the introduction of this report. For these purposes, a solid phase had to be used on which only metals sorb. The ligands and the complexes formed, however, should not sorb on the solid phase. Feldspar was found to fulfill these conditions.
The results of the sorption studies cannot be used as such for a cement system because, in a cement system, other processes such as sorption of complexes and/or irreversible sorption can occur. As already discussed in the introduction, if only the metal sorbs reversibly, the effect of a given ligand will have its maximum value. With respect to this, the results of the sorption experiments on feldspar can be regarded as being conservative.

8.1 Materials and methods

8.1.1 Solutions of degradation products, α-ISA and β-ISA

The degradation products were used undiluted and diluted in the sorption experiments. The dilutions were made by putting 100 ml, 10 ml or 1 ml respectively of the degradation products in a 100 ml flask. The volume was made up to 100 ml by adding ACW-I. The ACW-I was made as described in 7.1.3 Standard solutions of Na(α-ISA) were prepared in ACW-I in a concentration range between 10^{-6} and 10^{-1} M.
A stock solution of β-ISA was prepared from the pools collected by preparative HPLC (section 5.1.6). The fractions collected by preparative HPLC containing β-ISA in a pure form were pooled and brought to pH 11 by addition of a Chelex-100 ion exchange resin (protonated form). Afterwards, the ion exchange resin was filtered off and washed thoroughly with water. The filtrate and the washing water were pooled and brought to a volume of 10 ml by

evaporation under reduced pressure (10 mbar) at 40°C. The concentration of β-ISA in this stock solution was determined by HPLC to be 0.11 M.

8.1.2 Sorption of Eu(III)

20 mg of feldspar (orthoclase, Fronland, Norway, 63 μm) were incubated 2 hrs with 2 ml of ACW-I containing ^{152}Eu (4.44 kBq·ml^{-1}). After 2 hrs equilibration time, 28 ml of either ACW-I, Na(α-ISA) or degradation solutions were added. The final concentration of Eu in the ACW-I was approximately $6.7 \cdot 10^{-10}$ M. The suspensions were further equilibrated for 24 hrs. A 1 ml sample of the homogenised suspensions was taken without prior filtering or centrifuging and analysed for ^{152}Eu by γ-counting (Minaxi-γ, autogamma® 5000 series, Packard). The rest of the suspension was centrifuged for 15 minutes at 27,000 x g (L7-35 ultracentrifuge, Beckmann), the supernatant sampled (2 ml) and analysed for ^{152}Eu. Hereafter, the centrifuge tubes were emptied, rinsed with demineralised water and refilled with 10 ml of 0.1 M HCl. After shaking the tubes for 2 hrs, 2 ml of the HCl solution were sampled and analysed for ^{152}Eu. The measurements without prior filtering or centrifuging give information on the sum of ^{152}Eu on the solid phase (sorbed Eu) and the liquid phase. Measurements of the supernatant give information on the ^{152}Eu in the equilibrium solution only. The HCl extraction gives the amount of ^{152}Eu sorbed on the walls of the centrifuge tubes. The adsorption coefficient (K_d, ml·g^{-1}) was calculated by the difference in radioactivity before and after centrifugation:

$$K_d = \frac{(A_{bc} - A_{ac})}{A_{ac}} \cdot \frac{V}{m} \qquad (99)$$

where:

A_{bc} = the radioactivity of ^{152}Eu in the suspension (cpm·ml^{-1})
A_{ac} = the radioactivity of ^{152}Eu in the supernatant (cpm·ml^{-1})
V = volume of the suspension (ml)
m = mass of the solid phase (g)

The amount of Eu-152 on the vessel walls was measured to calculate the mass balance of ^{152}Eu:

$$A_{total} = A_{sorbed} + A_{solution} + A_{walls} \quad (100)$$

where:

A_{total} = total activity in the system (cpm)
A_{sorbed} = activity sorbed on the solid phase (cpm)
$A_{solution}$ = activity in the equilibrium solution (cpm)
A_{walls} = activity sorbed on the vessel walls (cpm)

and to compare this with the amount of ^{152}Eu added to the system. In the ideal case, the total amount of ^{152}Eu recovered (A_{total}) equals the total amount ^{152}Eu added to the system (A_{input}):

$$A_{total} = A_{input} \quad (101)$$

In general a recovery of 100 ± 5 % was found for ^{152}Eu.

Due to the restricted amount of β-ISA available in pure form, the sorption experiments had to be conducted in a reduced volume. Preliminary tests with α-ISA showed that it is possible to conduct sorption experiments in a volume of 2 ml by applying the following modifications (GLAUS et al. 1997b):

- equilibration of the suspensions is performed in 6 ml ponyvials normally used for γ-scintillation counting. Instead of end-over-end shaking, the vessels are only gently shaken from time to time by hand.
- phase separation is performed by 0.45 μm filtration instead of a centrifugation step.
- the ACW-I components Na^+, K^+ and Ca^{2+} are added as concentrated stock solutions.

The sorption experiments were conducted under laboratory atmosphere. 100 μl of a feldspar suspension (660 mg feldspar, Orthoclase <63 μm, + 20 ml ACW-I) were pre-equilibrated with 100 μl of ^{152}Eu spike solution (20 ml ACW-I + 80 μl ^{152}Eu stock solution (Amersham)) for one hour. Aliquots of the β-ISA stock solution, "ACW-I concentrate" (0.91g NaOH (100%) + 2.38g KOH (85%)

filled up to a volume of 20 ml with water), water and 0.4 M $Ca(NO_3)_2$ were added according to Table 18.

Table 18: Amounts of stock solutions added to the Eu^{3+} / feldspar system used for measuring the Eu^{3+} sorption in the presence of β-ISA.

[β-ISA] (M)	β-ISA stock	"ACW-I conc"	Q-H_2O	$Ca(NO_3)_2$ 0.4M	n
0.09	1590µl	200µl	—	10µl	2
0.009	200µl	200µl	1390µl	10µl	3
0.0009	200µl[1)]	200µl	1390µl	10µl	3
0.00009	200µl[2)]	200µl	1390µl	10µl	3
—	—	200µl	1590µl	10µl	3

[1)]β-ISA stock solution diluted 1:10 in Q-H_2O

[2)]β-ISA stock solution diluted 1:100 in Q-H_2O

"ACW-I conc" : ACW-I concentrate n: number of replicates

8.1.3 Sorption of Ni(II)

500 mg of feldspar (orthoclase, Fronland, Norway, 63 µm) were incubated with 30 ml of either ACW-I, Na(α-ISA) or degradation products and 1 ml ^{63}Ni (222 $Bq \cdot ml^{-1}$ in 0.001 M HCl). The total concentration of Ni in the ACW-I was approximately $3 \cdot 10^{-10}$ M. The suspensions were equilibrated for 24 hrs and centrifuged afterwards at 27,000 x g for 15 minutes (L7-35 ultracentrifuge, Beckmann). 8 ml of the supernatant were sampled and put in a 20 ml counting vial. The degradation solutions were coloured, causing quenching in the activity measurements. The coloured substances in the samples were oxidised by adding 100 µl of 30% H_2O_2 to the solutions. The solutions were left standing overnight, heated at 80 °C for one hour and finally 2 ml of 6 M HCl were added. After this treatment the solutions were (nearly) colourless. The activity of ^{63}Ni was measured by liquid scintillation counting (Tricarb® 2250 CA, Packard), using 10 ml Instagel® (Packard) as scintillation cocktail.

The centrifuge tubes were emptied, rinsed with demineralised water and refilled with 10 ml of 0.1 M HCl to remove the Ni sorbed on the vessel walls. After shaking the tubes for 2 hrs, 10 ml of the HCl solution were sampled, 10 ml Instagel added and analysed for ^{63}Ni by liquid scintillation counting.
The sorption coefficient (K_d) of Ni was calculated from the mass balance[2] as follows:

$$K_d = \frac{(A_{input} - A_{walls} - A_{solution})}{A_{solution}} \cdot \frac{V}{m} \qquad (102)$$

where:

A_{input} = activity of ^{63}Ni added to the system (cpm)
A_{walls} = activity of ^{63}Ni sorbed on the vessel wall (cpm)
$A_{solution}$ = activity of ^{63}Ni in the equilibrium solution (cpm)
V = volume of the suspension (ml)
m = mass of the solid phase (g)

8.1.4 Sorption of Th(IV)

20 mg of feldspar (orthoclase, Fronland, Norway, 63 µm) were incubated 2 hrs with 2 ml of ACW-I containing $^{234}Th/^{232}Th$. The carrier-free ^{234}Th was prepared from ^{238}U as described in DYRSSEN (1950). ^{232}Th was added as carrier. After 2 hrs equilibration time, 28 ml of either ACW-I, Na(α-ISA) or degradation solutions were added. The final concentration of Th (^{232}Th) in the ACW-I was approximately $6.7 \cdot 10^{-9}$ M. The suspensions were further equilibrated for 24 hrs and centrifuged afterwards at 27,000 x g for 15 minutes (L7-35 ultracentrifuge, Beckmann). 10 ml of the supernatant were sampled and put in a 20 ml counting vial. The coloured substances of the samples, causing quenching, were oxidised by adding 100 µl of 30% H_2O_2 to the solutions. The solutions were left standing overnight and finally heated at 80 °C for one hour. The activity of ^{234}Th was measured by liquid scintillation counting (Tricarb® 2250

[2] A similar procedure as used for Eu was not possible because of light scattering caused by the suspended particles. As a consequence, 100 % mass balance is an assumption used to calculate the distribution coefficient. The mass balance, however, cannot be checked.

CA, Packard) using the Cerenkov irradiation caused mainly by the daughter radioisotope ^{234}Pa.
The centrifuge tubes were emptied, rinsed with demineralised water and refilled with 10 ml of 0.1 M HCl. After shaking the tubes for 2 hrs, 10 ml of the HCl solution were sampled and analysed for ^{234}Th by liquid scintillation counting.
The sorption coefficient (K_d) of ^{234}Th was calculated from the mass balance[3] as follows:

$$K_d = \frac{(A_{input} - A_{walls} - A_{solution})}{A_{solution}} \cdot \frac{V}{m} \qquad (103)$$

where:

A_{input} = activity of ^{234}Th added to the system (cpm)
A_{walls} = activity of ^{234}Th sorbed on the vessel wall (cpm)
$A_{solution}$ = activity of ^{234}Th in the equilibrium solution (cpm)
V = volume of the suspension (ml)
m = mass of the solid phase (g)

8.2 Results and discussion

8.2.1 Effect of cellulose degradation products, α-ISA and β-ISA on the sorption of Eu(III) on feldspar

Figure 39 shows the effect of α-ISA and degradation products of the Aldrich cellulose on the sorption of Eu(III) on feldspar in ACW-I. The effect of the cellulose degradation products is plotted as a function of the α-ISA concentration in the degradation mixtures. The average uncertainty on the measured distribution coefficients was ± 0.5 log-units.
The good agreement between the reduction caused by pure α-ISA and by the degradation products of Aldrich cellulose is an indication that α-ISA in the

[3] A similar procedure as used for Eu was not possible because of light scattering caused by the suspended particles. As a consequence, 100 % mass balance is an assumption used to calculate the distribution coefficient. The mass balance, however, cannot be checked.

mixture of these cellulose degradation products is mainly responsible for the observed effect.

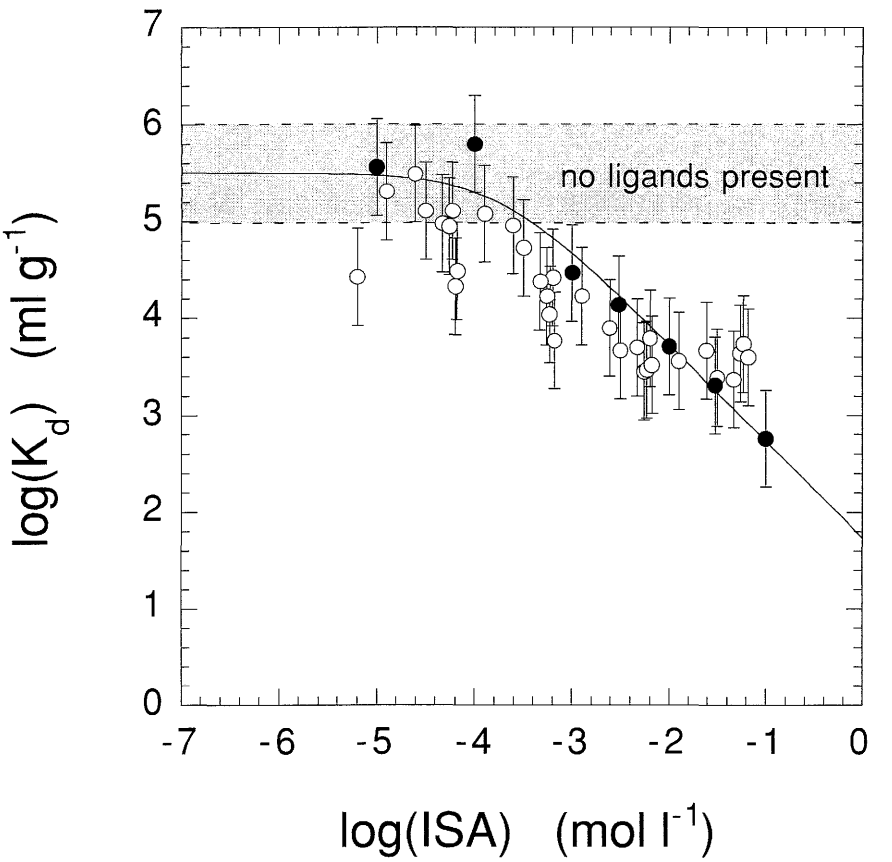

Figure 39: Dependence of the sorption of Eu on feldspar at pH = 13.3 on the concentration of α-ISA in pure α-ISA solutions (closed symbols) and in solutions containing Aldrich cellulose degradation products (open symbols). The solid line represents the case for a 1:1 complex between Eu and ISA.

The effect was - by analogy with gluconic acid - interpreted to be caused by a strong complexation between europium and ISA. A possible reaction, according to a generalised reaction scheme (VAN DUIN 1989), can be written as:

$$Eu^{3+} + H_4ISA^- + mH_2O \Leftrightarrow Eu(OH)_mH_{4-n}ISA^{2-(m+n)} + (m+n)H^+ \qquad (104)$$

H_4ISA^- used here corresponds to the ISA used throughout the text. "H_4" represents the protons of the 4 hydroxy-groups in ISA. The stability constant is defined by:

$$K_{EuHISA} = \frac{(Eu(OH)_mH_{4-n}ISA^{2-(m+n)}) \cdot (H^+)^{m+n}}{(H_4ISA^-) \cdot (Eu^{3+})} \quad (105)$$

where the terms in parenthesis represent activities of the species. In a first approach, we analysed our data assuming that reaction (104) takes place with – although this might not be a realistic case – m=0 and n=3. Equation (10) was rewritten as follows:

$$K_d = \frac{K_d^o}{1+\left(\frac{K_{EuHISA} \cdot [H_4ISA^-]}{[H^+]^3 \cdot A}\right)} \quad (106)$$

where:

$$A = 1+\sum_{i=1}^{n} \beta_i^{OH} \cdot [OH]^i \quad (107)$$

with:

K_d	=	distribution coefficient in presence of ISA
K_d^o	=	distribution coefficient in absence of ISA
K_{EuHISA}	=	the stability constant of the $EuHISA^-$ complex
$[H_4ISA^-]$	=	the concentration of ISA
β_i^{OH}	=	the overall hydrolysis constants of Eu(III)

The only inorganic complexes of relevance for the chemical conditions used in our experiments are Eu-hydroxo complexes. For Eu-hydroxo complexes, stability constants are only available as estimated constants from the hydrolysis behaviour of other lanthanides. The estimates of LEE & BYRNE (1992) are based on a rather extensive set of experimental data, as their analysis utilised data for more than hundred ligands. Their estimated values for Eu hydrolysis constants, as summarised in Table 19, compare well with the estimates of BAES & MESMER (1986). No attempt was made by LEE & BYRNE (1992) to estimate β_4^{OH} values by linear free energy relationships due

to the scarcity of experimental β_4 data. GLAUS et al. (1997c) assumed a linear decrease of the logarithms of stepwise stability constants and estimated a β_4^{OH} value as given in Table 19. All thermodynamic constants summarised in Table 19 were used for calculating side reactions. Since we worked at a constant pH of 13.3 and an ionic strength of I = 0.3 M, $[H^+]$ and the A-term in equation (106) are constant. The data in Figure 39 could be fitted well by using a value of $\log K_{EuHISA}$ = -19.1± 0.1 at I=0.3 M for the EuHISA-complex and logA = 17. This value can be extrapolated to zero ionic strength by the Davies equation resulting in a value of -18.3 ± 0.1. A more detailed study on the complexation of Eu by α-ISA is currently under investigation.

Table 19: Overview of the thermodynamic constants used to calculate the stability constants of the $EuHISA^-$ from Eu sorption experiments on feldspar at pH = 13.3 and I= 0.3 M.

Species	[1)]logK	Reference	Reaction
$Eu(OH)^{2+}$	6.1	LEE & BYRNE (1992)	$Eu^{3+} + OH^- \Leftrightarrow EuOH^{2+}$
$Eu(OH)_2^+$	11.6	LEE & BYRNE (1992)	$Eu^{3+} + 2OH^- \Leftrightarrow EuOH_2^+$
$Eu(OH)_3^o$	16.6	LEE & BYRNE (1992)	$Eu^{3+} + 3OH^- \Leftrightarrow EuOH_3^o$
$Eu(OH)_4^-$	21	GLAUS et al. (1997c)	$Eu^{3+} + 4OH^- \Leftrightarrow EuOH_4^-$

[1)] I = 0

WIELAND et al. (1998) studied the effect of α-ISA on the sorption of Eu on cement. They found a negligible effect of ISA on the sorption of Eu in the concentration range 10^{-5} M < [α-ISA] < 10^{-2} M. Only for [α-ISA] > 10^{-2} M, a significant effect could be observed. The difference between the effects observed by WIELAND et al. (1998) and those described in this study cannot be explained yet. A possible explanation might be the sorption of Eu-ISA complexes on the cement.

Figure 40 shows the effect of pure α-ISA and β-ISA on the sorption of Eu(III) on feldspar. The effect of β-ISA on the sorption of Eu(III) seems to be lower than the one of α-ISA. This might be explained by a difference in complexation behaviour. Why α- and β-ISA – although they have similar structures – have different complexing properties w.r.t. complexation with Eu is not clear yet and

is under investigation. The solid lines in Figure 40 are calculated assuming that a 1:1 complex between Eu(III) and ISA is formed according to equation (104) with m=0 and n=3. For α-ISA, the fitting procedure resulted in $\log K_{EuHISA}$ = -18.6±0.2 at I=0.3 M. In case of β-ISA, $\log K_{EuHISA}$ = -20.7±0.3 at I=0.3 M. The stability of the Eu-β-ISA complex seems to be roughly two orders of magnitude lower than the one of the Eu-α-ISA complex. Since both isomers are present in equal amounts, the speciation of Eu(III) in a cellulose degradation mixture will be dominated by α-ISA. This explains why the effect of cellulose degradation products and the effect of pure α-ISA on the sorption of Eu(III) is the same.

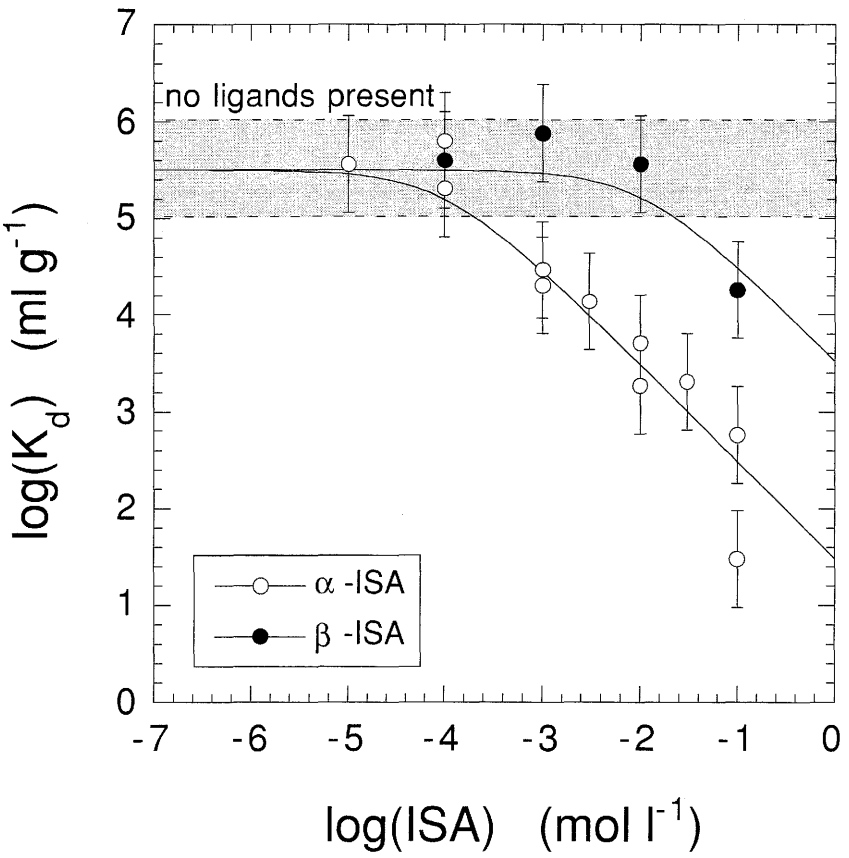

Figure 40: Effect of pure α-ISA and β-ISA on the sorption of Eu(III) on feldspar at pH =13.3.

For the other cellulosic materials (Tela tissues, cotton and recycling paper), the agreement is not so good (Figure 41). A larger effect on the sorption of Eu(III) on feldspar can be observed than for the pure α-ISA. Whether this effect is

caused by the presence of other ligands than ISA is not clear yet. As already discussed in 3.1.2, HPLC analysis showed the presence of other compounds, especially in the degradation mixture of cotton. Further investigations are planned to clarify these effects.

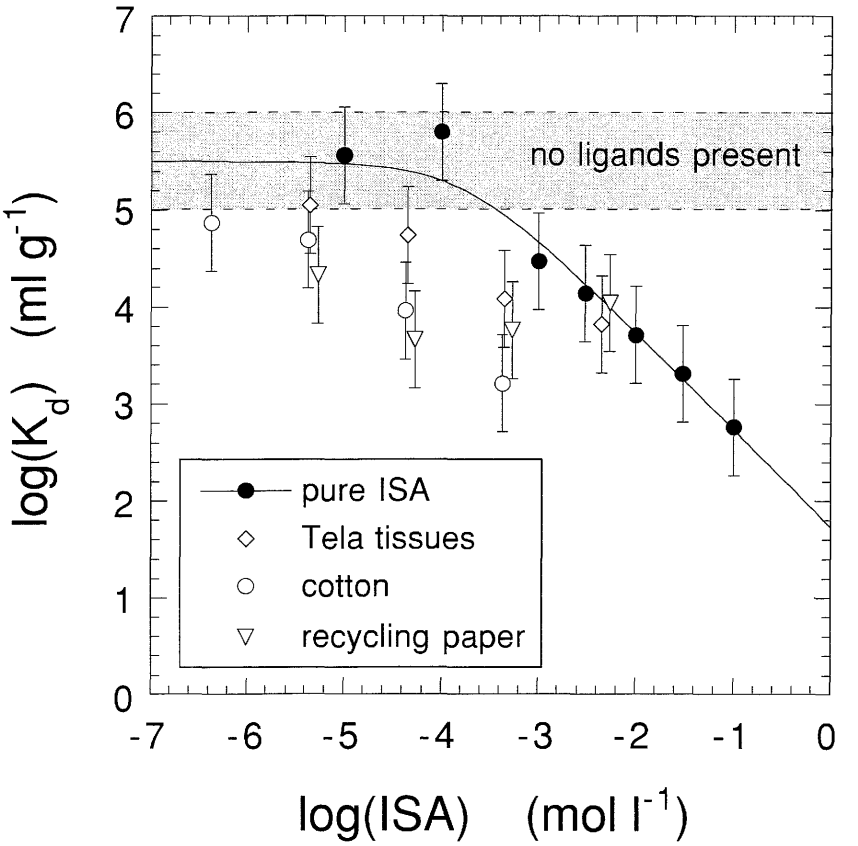

Figure 41: Dependence of the sorption of Eu on feldspar at pH = 13.3 on the concentration of α-ISA in pure α-ISA solutions and solutions containing degradation products of Tela tissues, cotton and paper.

8.2.2 Effect of cellulose degradation products and α-ISA on the sorption of Th(IV) on feldspar

Figure 42 and Figure 43 shows the effect of pure α-ISA and cellulose degradation products respectively on the sorption of thorium on feldspar. The average uncertainty on the measured distribution coefficients was ± 0.5 log-units. As can be clearly seen, α-ISA and cellulose degradation products have

an adverse effect on the sorption of thorium. If the data of the degradation products are normalised with respect to the α-ISA concentration, the agreement between pure α-ISA and the cellulose degradation products is good. Consequently, the effect of the cellulose degradation products on the sorption of Th can be explained very well by the presence of α-ISA.

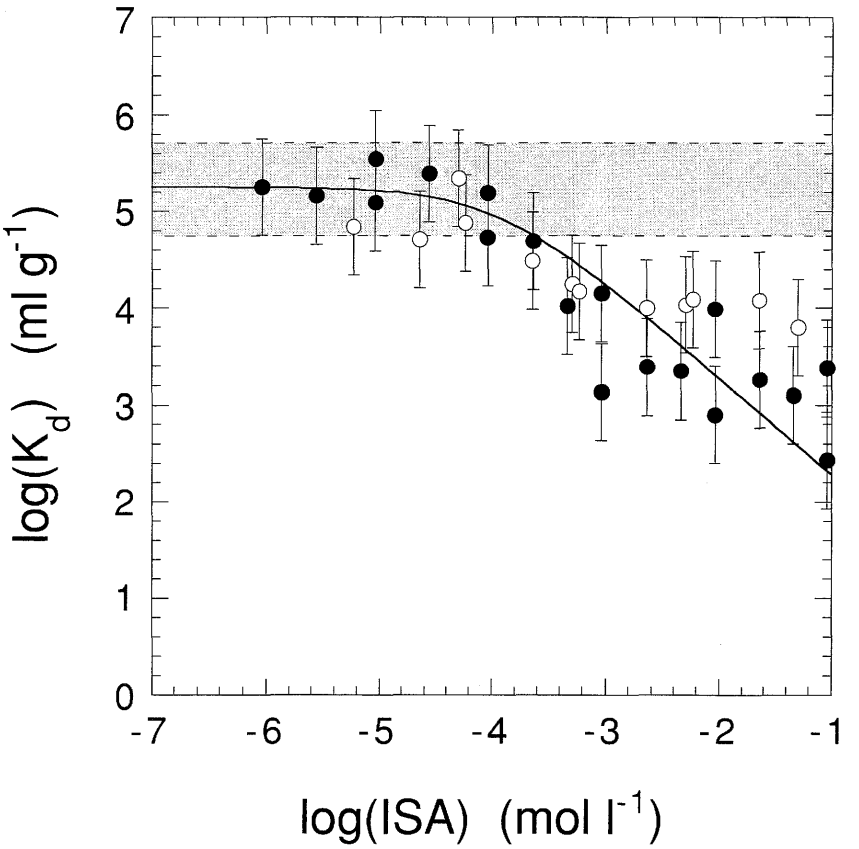

Figure 42: Effect of cellulose degradation products (open symbols: Aldrich, degradation time 1 year) and α-ISA (closed symbols) on the sorption of Th on feldspar at pH = 13.3. The curve represents the case for the formation of a 1:1 complex between Th and ISA.

WIELAND et al. (1998) studied the sorption of Th(IV) on cement under similar conditions. They found a significant effect of α-ISA on the sorption of Th in the concentration range 10^{-5} M < [α-ISA] < 10^{-2} M. The effect observed by WIELAND et al. (1998), however, was much higher than the effects described in this study. WIELAND et al. (1998) also found indications for the formation of a 1:2 Th-ISA complex according to:

$$Th + 2\ ISA \Leftrightarrow Th(ISA)_2 \qquad (108)$$

whereas in this study experiments could be satisfactorily explained by the formation of a 1:1 Th-ISA complex:

$$Th + ISA \Leftrightarrow ThISA \qquad (109)$$

Further investigations on the complexation of tri- and tetravalent metals with ISA to explain the observed differences are ongoing (see also VERCAMMEN et al. 1997).

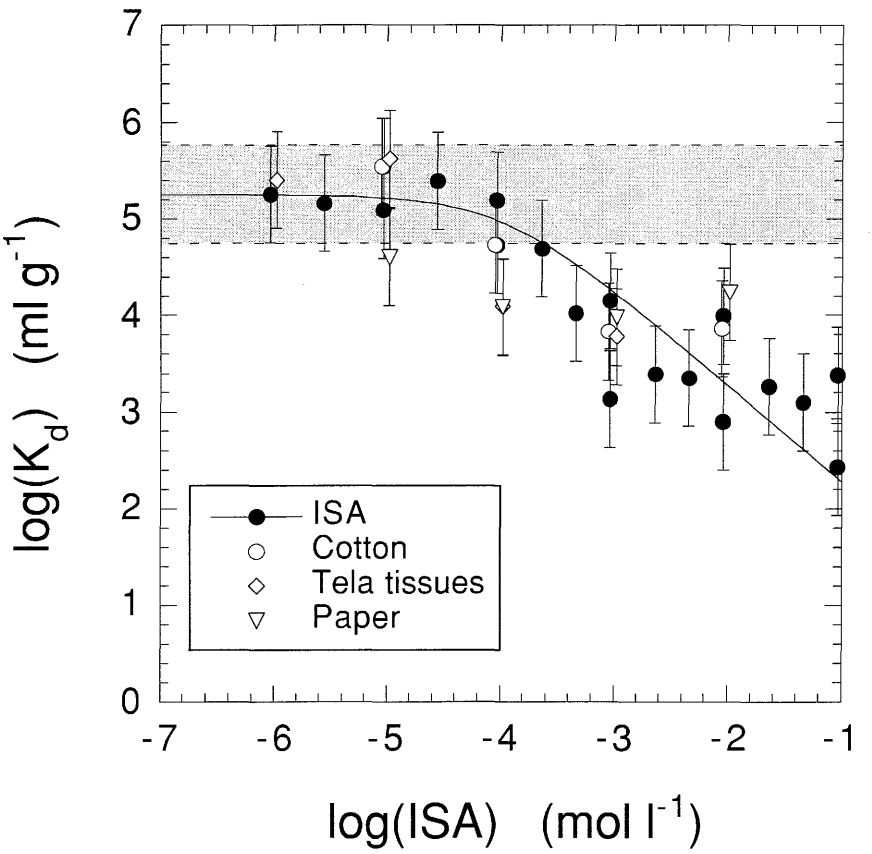

Figure 43: Effect of cellulose degradation products (open symbols: Tela, cotton, paper: degradation time 1 year) and α-ISA (closed symbols) on the sorption of Th on feldspar at pH = 13.3. The curve represents the case where a 1:1 complex is formed between Th and ISA.

8.2.3 Effect of cellulose degradation products and α-ISA on the sorption of Ni(II) on feldspar

Figure 44 and Figure 45 show the effect of α-ISA and cellulose degradation products on the sorption of Ni on feldspar.

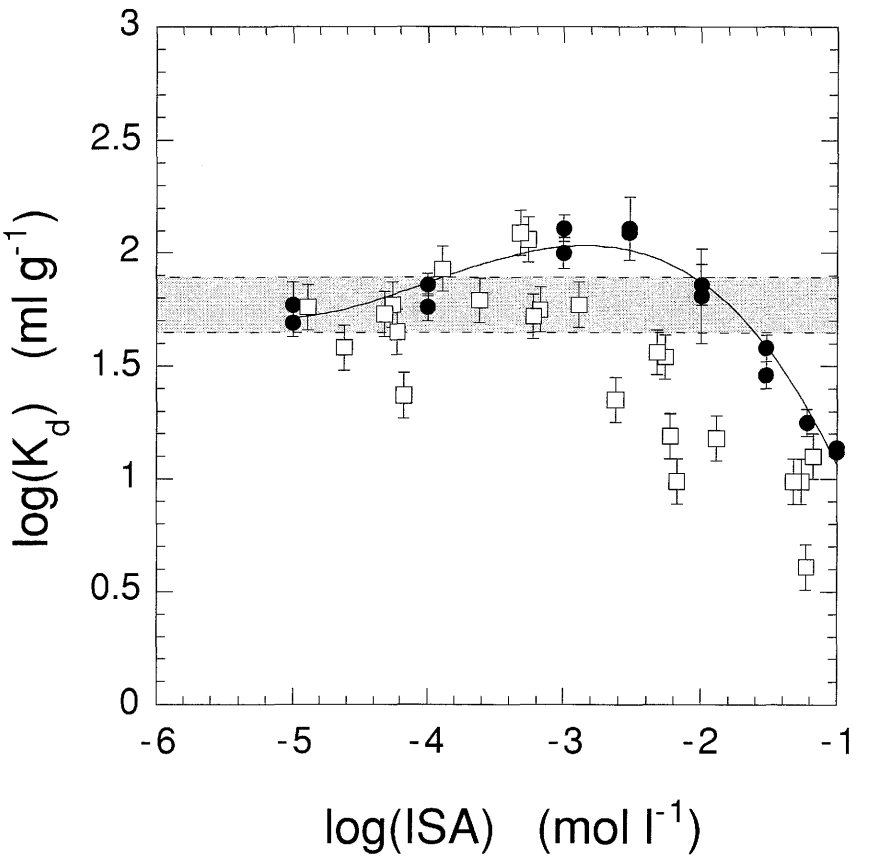

Figure 44: Dependence of the sorption of Ni on feldspar at pH = 13.3 on the concentration of α-ISA for pure ISA solutions (closed symbols) and solutions containing degradation products of Aldrich cellulose (open symbols). The line is used to guide the eye.

Also in the case of Ni, ISA and cellulose degradation products have an adverse effect on the sorption, indicating that a complex between ISA or cellulose degradation products and Ni is formed. The data for the degradation products are normalised with respect to α-ISA. The agreement between pure α-ISA and the Aldrich cellulose degradation products is reasonably good, although the degradation products tend to have a larger effect (Figure 44). In

case of Ni, the concentration of α-ISA in solution has to be larger than 10^{-2} M for significantly reducing the sorption, indicating that the Ni-ISA complex is much less stable than Th-ISA and Eu-ISA complexes.

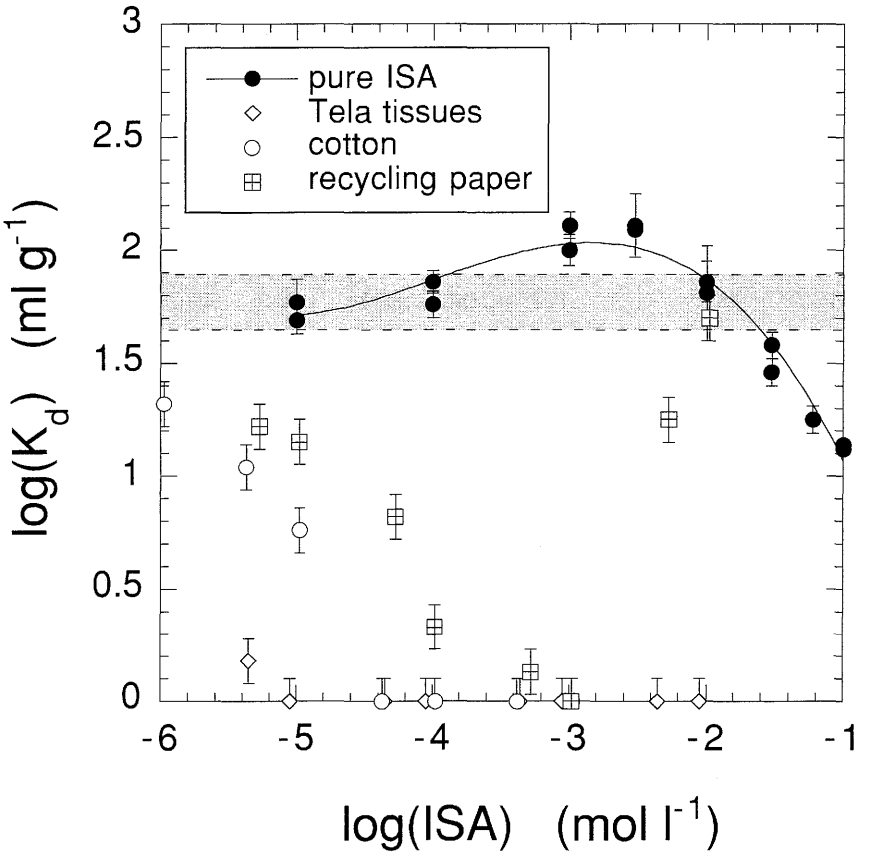

Figure 45: Dependence of the sorption of Ni on feldspar at pH = 13.3 on the concentration of α-ISA for pure ISA solutions (closed symbols) and solutions containing degradation products of cotton, Tela tissues and recycling paper (open symbols). The line is to guide the eye.

The degradation products of the other cellulosic materials seem to have a much stronger effect on the sorption of Ni on feldspar (Figure 45). This effect might be explained by the presence of other degradation products which form stronger complexes with Ni than the α-ISA isomer. Further studies are required here to obtain a complete picture. Some preliminary results on the effect of alkali soluble organics on the sorption of Ni and Eu on feldspar will be shown in section 8.2.4.

8.2.4 Effect of alkali-soluble compounds on the sorption of metals

In the previous section, it was shown that the degradation solutions of the cellulosic materials other than pure cellulose have a larger effect on the sorption of metals than could be explained by the presence of ISA. This indicates that other compounds must be present in the degradation solutions. These "other compounds" can be other (not yet identified) degradation products of cellulose or could be alkali soluble compounds present in the cellulosic materials. It is well known that, beside cellulose, wood contains other polysaccharides, i.e. hemicelluloses (see section 3.2). These hemicelluloses are alkali soluble and might also have an adverse effect on the sorption of radionuclides.

8.2.4.1 Preparation of extracts

The extracts were prepared as described in section 5.1.9.1

8.2.4.2 Sorption of Ni and Eu in presence of cellulose extracts

50 mg of feldspar (orthoclase, Fronland, Norway, 63 μm) were incubated 1 hr with 1 ml of ACW-I containing ^{152}Eu (4.44 kBq·ml^{-1}). After 1 hr equilibration time, 30 ml of either the extracts or ACW-I were added. The final concentration of Eu in the ACW-I was approximately $6.7 \cdot 10^{-10}$ M. The suspensions were further equilibrated for 24 hrs. A 1 ml sample of the homogenised suspensions was taken without prior filtering or centrifuging and analysed for ^{152}Eu by γ-counting (Minaxi-γ, autogamma® 5000 series, Packard). The rest of the suspension was centrifuged for 15 minutes at 27,000 x g (L7-35 ultra-centrifuge, Beckmann), the supernatant sampled (2 ml) and analysed for ^{152}Eu. Hereafter, the centrifuge tubes were emptied, rinsed with demineralised water and refilled with 10 ml of 0.1 M HCl. After shaking the tubes for 2 hrs, 2 ml of the HCl solution were sampled and analysed for ^{152}Eu. The adsorption coefficient (K_d, ml·g^{-1}) was calculated by the difference in radioactivity before and after centrifugation using equation (99).

500 mg of feldspar (orthoclase, Fronland, Norway, 63 μm) were incubated with 30 ml of either ACW-I or alkaline extracts and 1 ml ^{63}Ni (222 $Bq \cdot ml^{-1}$ in 0.001 M HCl). The total concentration of Ni in the ACW-I was approximately $3.2 \cdot 10^{-10}$ M. The suspensions were equilibrated for 24 hrs and centrifuged afterwards at 27,000 x g for 15 minutes. 8 ml of the supernatant were sampled and put in a 20 ml counting vial. The alkaline extracts were coloured, causing quenching in the activity measurements. The coloured substances of the samples were oxidised by adding 250 μl of 30% H_2O_2 to the solutions. The solutions were left standing overnight, heated at 80 °C for one hour and finally 0.5 ml of 6 M HCl were added. The activity of ^{63}Ni was measured by liquid scintillation counting (Tricarb® 2250 CA, Packard), using 10 ml Instagel® (Packard) as scintillation cocktail.

The centrifuge tubes were emptied, rinsed with demineralised water and refilled with 10 ml of 0.1 M HCl to remove the Ni sorbed on the vessel walls. After shaking the tubes for 2 hrs, 10 ml of the HCl solution were sampled, 10 ml Instagel added and analysed for ^{63}Ni by liquid scintillation counting. Sorption coefficients were calculated using equation (102).

8.2.4.3 Results and discussion

Table 20 gives the amount of extractable carbon for the four cellulosic materials used, together with their effect on the sorption of europium and nickel on feldspar. The effect of the extractable compounds on the sorption of Eu is relatively small. The largest effect can be noticed for the paper. In case of Ni, however, the effect of the extracts on the sorption is clear for all four cellulosic materials used. The largest effect can be observed for the Tela and cotton cellulose.

These results enables one to interpret better earlier data on the effect of alkaline degradation products of cellulosic materials on the sorption of Ni (section 8.2.3). The slightly larger effect observed for the degradation products of Aldrich cellulose compared to the effect of α-ISA (see Figure 44), and the much larger effect of the alkaline degradation products of cotton, Tela and paper (see Figure 45) seems to be caused by alkali soluble organics present in these cellulosic materials. The nature of these organics, however, is still unknown and further investigations are necessary.

Table 20: Alkali-extractable organic matter for different cellulosic materials and their effect on the sorption of europium and nickel on feldspar at pH = 13.3.

Sample	DOC (mM)	$\log K_d^{Ni}$ ($ml \cdot g^{-1}$)	$\log K_d^{Eu}$ ($ml \cdot g^{-1}$)
ACW-I	0.8	1.86±0.07	4.37±0.43
Aldrich cellulose	16.6	1.26±0.03	3.90±0.06
Tela	70	0.21±0.08	3.91±0.01
Cotton	4	0.67±0.04	4.01±0.03
Paper	240	1.11±0.08	3.66±0.06

9 ASSESSMENT OF THE EFFECT OF CELLULOSE DEGRADATION ON REPOSITORY SAFETY

9.1 Degradation kinetics and extent of degradation of cellulose under repository conditions

The alkaline degradation of cellulose is governed by the two processes discussed in section 4, i.e. peeling off and alkaline hydrolysis. The overall degradation of cellulose can be expressed by combining equation (28) and (60), resulting in:

$$(\text{celdeg}) = 1 - \left(\frac{1 - \frac{k_1}{k_t} \cdot (G_r)_o \cdot (1 - e^{-k_1 \cdot t}}{e^{k_{obs} \cdot x_n \cdot t}} \right) \qquad (110)$$

were (celdeg) represents the fraction of cellulose degraded after time t. Figure 46 shows the fraction of degraded cellulose as a function of time for a repository temperature of 25 °C. The values of the kinetic parameters k_1/k_t, k_t, $k_{obs} \cdot x_n$ and the amount of reducing end groups $(G_r)_o$ used, are given in Table 21. The ratio k_1/k_t as well as the value for k_t at 25 °C and OH = 0.3 M, were taken from measurements performed on different types of cellulosic materials as described in 5.2.4. Values for $k_{obs} \cdot x_n$ at 25 °C could not be determined experimentally. Therefore, a value was extrapolated from data measured at higher temperatures, using the Arrhenius equation (see 4.2.2.3). The uncertainty on this extrapolated value was assumed to be large and was taken to be ± one order of magnitude. Cellulose was assumed to be present mainly as tissues and paper. A good average value for the degree of polymerisation for this kind of cellulose is 1500±500 (GASCHE 1996, VUORINEN 1996). The mole fraction of reducing end groups for this cellulose, $(G_r)_o$, was estimated using 1/DP. It was assumed that the pH of the cement pore water stays 13.3 for 10^6 years. This is most probably not the case because the water flow through the repository will wash out Na- and KOH resulting in a decrease of the pH to 12.5. Further, during the peeling off reaction, ~1.2 equivalents of protons will be formed per molecule of glucose split off from the cellulose chain. Therefore the assumption of a constant high pH 13.3 reflects a worst case scenario since

under this condition, the degradation rate will be overestimated. The calculated amount of ISA produced will therefore reflect an upper limit.
The curve in Figure 46 represents the reference case. For this case, the average values of the parameters in Table 21 were used. In the initial stage (10^4-10^5 years), the degradation is dominated by the fast peeling off process. At this stage, about 3 % of the cellulose will degrade. The rest of the cellulose will degrade by a combination of a slow alkaline hydrolysis and peeling off reaction. A complete degradation of cellulose is expected to occur for $t > 10^5$ years. The shaded area represents the uncertainty range of the parameters in Table 21. The uncertainty on the ratio k_1/k_t, $(G_r)_o$ and the kinetic constant k_t has only a small effect on the calculated amount of degraded cellulose in the first stage of cellulose degradation. The lower limit of degraded cellulose is ~1 % and the upper limit ~4%. The uncertainty on the kinetic constant of the alkaline hydrolysis, $k_{obs} \cdot x_n$, has a larger effect. Increasing the rate constant by a factor of 10 ($k_{obs} \cdot x_n = 8.6 \cdot 10^{-10} h^{-1}$) results in a shortening of the first stage, where peeling off dominates, by a factor of 10. After 10^5 years, about 60 % of the cellulose will be degraded mainly by alkaline hydrolysis. Decreasing the rate constant by a factor of 10 ($k_{obs} \cdot x_n = 8.6 \cdot 10^{-12} h^{-1}$) results in a prolongation of the first stage.

Table 21: Parameters used to calculate the overall degradation of cellulose under the alkaline conditions of a cementitious repository (Figure 46).

parameter	value
k_1/k_t	25±13
k_t	$(2.6 \pm 0.9) \cdot 10^{-4}$ h^{-1}
$k_{obs} \cdot x_n$	$8.6 \cdot 10^{-10}$-$8.6 \cdot 10^{-12} h^{-1}$
DP	1500±500
$(G_r)_o$	$(7.5 \pm 2.5).10^{-4}$

From the assessment point of view, the first stage of cellulose degradation is the most important one, since in this stage the rate of ingrowth of isosaccharinic acid in the pore water is larger than the pore water exchange rate. In the second stage of cellulose degradation, the degradation rate of

cellulose is smaller than the pore water exchange rate resulting in only a slow ingrowth of isosaccharinic acid.

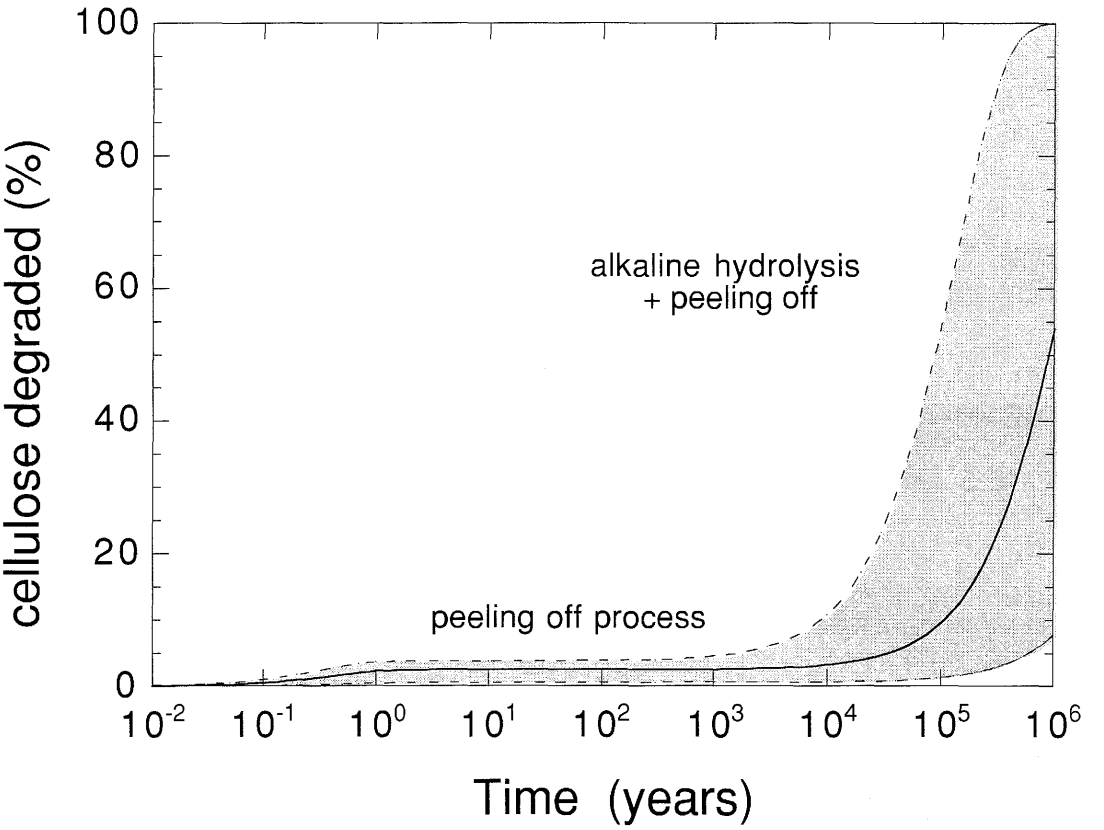

Figure 46: Overall degradation of cellulose at 25 °C and 0.3 M OH^- as a function of time. The solid line represent the reference case calculated using equation (110) with the parameters listed in Table 21. The shaded area reflects the uncertainty on the parameters in Table 21.

9.2 Concentration of ISA in cement pore water

As already discussed earlier (see 1.2), the concentration of degradation products (ISA) in the pore water of a repository is one of the key factors for assessing the effect of cellulose degradation on the release of radionuclides from a repository. The concentration of ISA depends on the cellulose loading in the waste, the extent of degradation of cellulose, the porosity of cement, the sorption behaviour of ISA on cement, the chemical stability of ISA under the

existing alkaline repository conditions and the water flow through the repository. In this chapter it is shown how all these processes can be combined for estimating the concentration of ISA in a cement pore water. Figure 47 shows a flow diagram for doing such estimations.

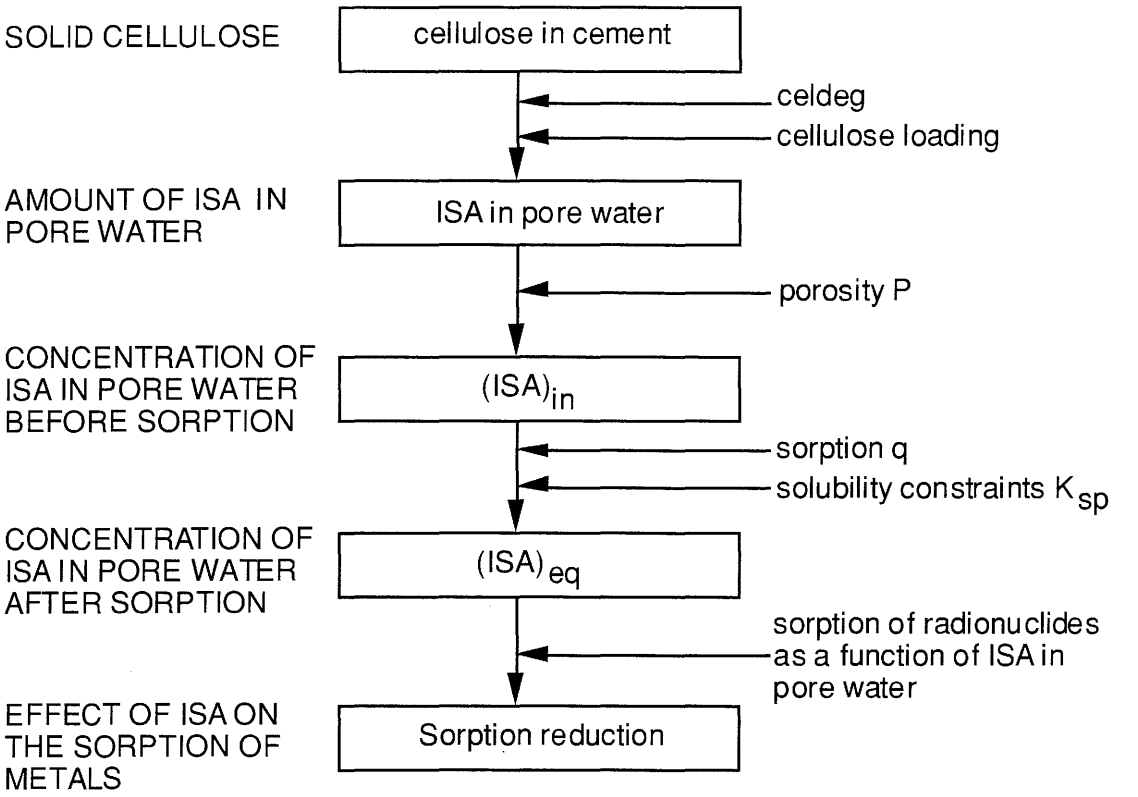

Figure 47: Flow diagram for calculating the concentration of ISA in a cement pore water of a repository with a given cellulose loading.

Figure 48 shows the calculated ISA concentration in the pore water of a repository as a function of the cellulose loading. The parameters used are listed in Table 22. The effect of ISA-sorption on the concentration is clearly illustrated in this plot. One can see that this sorption process reduces the concentration of ISA in the pore water by almost three orders of magnitude.

The average organic matter loading in that part of the repository containing cellulose (SMA-4) is ~ 60 $kg \cdot m^{-3}$ (SUTER 1996). Under the assumption that all the organic matter is cellulose and that the average density of the waste is 1000 - 2000 $kg \cdot m^{-3}$, the average cellulose loading (on a weight basis) in a repository is 3 - 6 %.

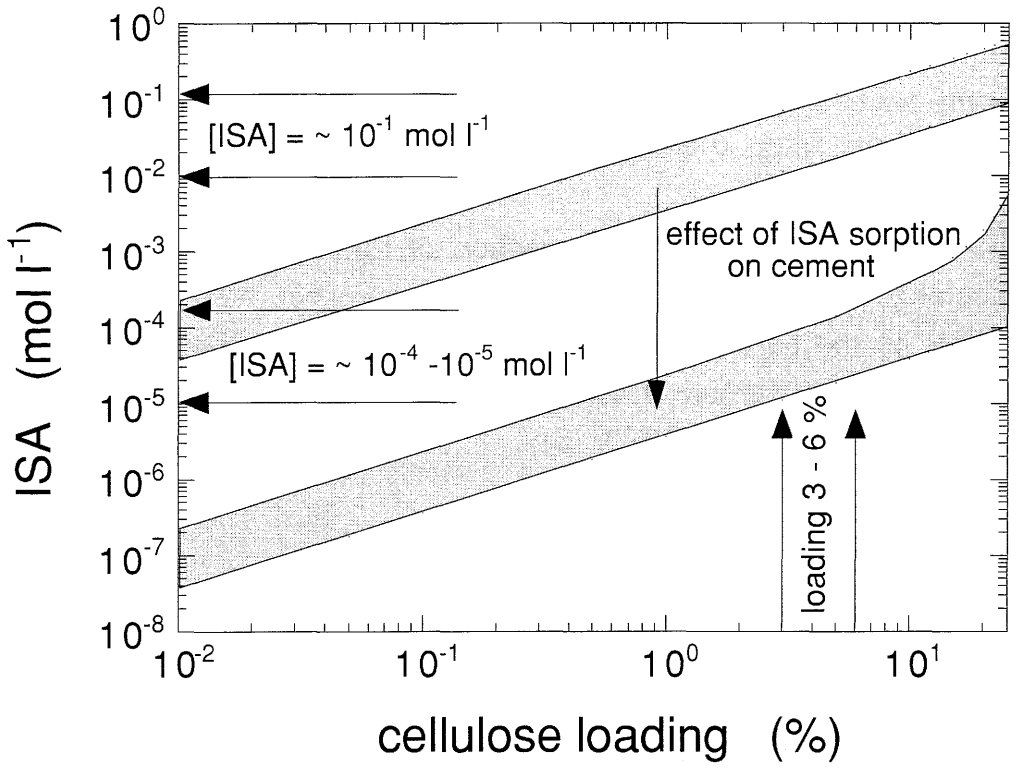

Figure 48: Estimated concentration of ISA in the pore water of a cementitious repository for varying cellulose loading. The shaded areas reflect the uncertainty in the parameters used (Table 22). The lower area shows the effect of the sorption of ISA on cement.

Table 22: Parameters used to estimate the concentration of ISA in the pore water of a cementitious repository (Figure 48).

Parameter	Value
porosity	0.1
cement content	580 kg·m^{-3}
DP	1500±500
k_1/ k_t	25±13
k_t	(2.6±0.9)·10^{-4} h^{-1}
K_1	1730 l·mol^{-1}
q_1	0.1 mol·kg^{-1}
K_2	12 l·mol^{-1}
q_2	0.17 mol·kg^{-1}

For a cellulose loading of 3-6 %, the concentration of ISA is reduced by sorption from 0.1 - 0.01 M to about 10^{-4} - 10^{-5} M. From Figures 39 and 42 it is clear that the effect of 10^{-4} - 10^{-5} M ISA on the sorption of Eu(III) and Th(IV) is negligibly small. For Ni(II), no effect on the sorption is expected at this low ISA concentration.

WIELAND et al. (1998) studied the sorption of Eu(III) and Th(IV) on HTS Portland cement. They came to the same conclusion that, below 10^{-4} M, ISA had no effect on the sorption of these metals on cement. Above 10^{-4} M the sorption of Th was adversely affected. The sorption of Eu, however, was affected at a concentration of $>10^{-2}$ M ISA.

10 GENERAL CONCLUSIONS

Under the physico-chemical conditions of the planned WLB cementitious repository, i.e. pH = 13.3 and T = 25 °C, cellulose will degrade by a peeling off reaction, by which reducing end groups are successively split off from the cellulose chain. The presence of Ca in the pore water (saturation with respect to portlandite) catalyses the formation of water-soluble isosaccharinic acid (ISA) by this peeling off reaction. Two diastereoisomers – i.e. α- and β-ISA – are formed in roughly equal amounts. A simultaneous stopping reaction, by which reducing end groups of the cellulose are transformed in non-reducing end groups or end groups no longer available, competes with the peeling off reaction. The overall effect of both processes is a partial degradation only of the cellulose. Long term experiments, carried out under relevant conditions with different types of cellulosic materials, have shown that the extent of degradation depends mainly on the mole fraction of reducing end groups of the cellulose in a repository, and on its degree of crystallinity (accessibility). The results from the long term degradation studies are in agreement with those of several reported studies, performed under different, more extreme physico-chemical conditions (i.e. high temperature and alkali concentration).
Based on this study and literature data, calculations have shown that during the first 10^4 - 10^5 years, about 5 % of the cellulose present in a cementitious repository, will degrade by the peeling off reaction. The rest of the cellulose will be degraded by a combined alkaline hydrolysis/peeling off reaction.

The isosaccharinic acid formed sorbs strongly on the cement phases. This process controls the concentration of ISA in the pore water of a repository. For an average cellulose loading of 3-6 %, the equilibrium concentration of isosaccharinic acid in the pore water will be of the order of $2 \cdot 10^{-4}$ - 10^{-5} M.

Isosaccharinic acid is a polyhydroxy type of ligand and forms – by analogy with gluconic acid – strong water-soluble complexes with many radionuclides, especially under alkaline conditions. Because of this strong complexation, ISA has an adverse effect on the sorption of radionuclides on cement phases. Especially the sorption of tri- and tetravalent radionuclides will be affected mostly because such metals form the strongest complexes with ISA. Sorption reduction depends mainly on the concentration of ISA in the pore water. For tri- and tetravalent metals such as Eu(III) and Th(IV), a significant sorption reducing effect can be observed when the concentration in solution is larger

than 10^{-4} M -10^{-3} M. For bivalent metals such as Ni(II), the concentration must be larger than 10^{-2} M before a significant sorption reduction can be observed. Since the expected concentration of ISA in the pore water is ~10^{-4} - 10^{-5} M, no significant effect of the degradation products of cellulose on radionuclide sorption should be expected.

Cellulosic materials contain, beside cellulose, also alkali soluble organics. Non-cellulosic polysaccharides (hemicellulose) form one class of these organics. The amount of these hemicelluloses is variable and depends on the type of cellulosic materials and their manufacturing processes used. They can contribute to a large extent to dissolved organic matter in the pore solution. Alkaline extracts of different cellulosic materials show a strong effect on the sorption of especially Ni. Whether this effect is due to the hemicelluloses or other organics is still unclear and is currently under investigation.

The presence of micro-organisms in a repository can't be ignored and – up till now – it is still unclear to what extent they will have an effect on repository performance. So far, it can't be ruled out that micro-organisms might also play a (significant) rôle in cellulose degradation. However, although micro-organisms are present in a repository, it is likely that their activity will be very low because of the extreme physico-chemical conditions in a cementitious repository. Nevertheless, the potential rôle of micro-organisms should be carefully evaluated. A progress in this field, however, can only be achieved by innovative procedures, rather than by classical microbial techniques applied so far (MADSEN 1998).

11 REFERENCES

ALÉN, R. (1996), Unpublished results, personal communication.

ANDERSEN, P.J., ROY, D.M. & GAIDIS, J.M. (1987): The Effect of Adsorption of Superplasticizers on the Surface of Cement. Cement and Concrete Research, 17, 805-813.

BERNER, U. (1990): A Thermodynamic Description of the Evolution of Pore Water Chemistry and Uranium Speciation during the Degradation of Cement. PSI-Bericht 62, Paul Scherrer Institute, Villigen, Switzerland. Also published as Nagra Technical Report NTB 90-12, Nagra, Wettingen, Switzerland.

BLANK, B., ROSSINGTON, D.R. & WEINLAND, L.A. (1963): Adsorption of Admixtures on Portland Cement. Journal of the American Ceramic Society, 46, 395-399.

BLEARS, M.J., MACHELL, G. & RICHARDS, G.N. (1957): Alkaline Degradation of 4-O-Substituted Glucose Derivatives. Chem. and Ind. August 24, 1150-1151.

BOURBON X. (1994): Etude de la mobilisation, par des complexants organiques, des radionucléides contenus dans les déchets radioactifs de faible et moyenne activité. PhD. Thesis, Université Pierre et Marie Curie, Paris, France.

BOURBON, X. & TOULHOAT, P. (1996): Influence of Organic Degradation Products on the Solubilisation of Radionuclides in Intermediate and Low Level Radioactive Wastes. Radiochimica Acta 74, 315-319.

BRADBURY, M.H. & BAEYENS, B. (1995): A Quantitative Mechanistic Description of Ni, Zn and Ca sorption on Na-Montmorillonite. Part III: Modelling. PSI-Bericht 95-12, Paul Scherrer Institute, Villigen, Switzerland. Also published as Nagra Technical Report NTB 95-06, Nagra, Wettingen, Switzerland.

BRADBURY, M.H. & SAROTT, F.A. (1995): Sorption Databases for the Cementitious Near-field of a L/ILW Repository for Performance Assessment. PSI-Bericht 95-06, Paul Scherrer Institute, Villigen, Switzerland. Also published as Nagra Technical Report NTB 93-08, Nagra, Wettingen, Switzerland.

BRADBURY, M.H. & VAN LOON, L.R. (1997): Cementitious Near-Field Sorption Data Bases for Performance Assessment of a L/ILW Repository in a Palfris Marl Host Rock, CEM-94: UPDATE I, June 1997. PSI-Bericht Nr. 98-01, Paul Scherrer Institute, Villigen, Switzerland. Also published as Nagra Technical Report NTB 96-04, Nagra, Wettingen, Switzerland.

BRYCE, J.R.G. (1980): Alkaline Pulping. In: CASEY, J.P. (ed.): Pulp and Paper, Chemistry and Chemical Technology, third edition, Volume 1, John Wiley & Sons, New York, pp. 429-436.

BROUWER, E., BAEYENS, B., MAES, A. & CREMERS, A. (1983): Cesium and Rubidium Ion Equilibria in Illite Clay. J. Phys. Chem. 87, 1213-1219.

BUCHER-JOHNSSON, K., GASCHE, U. & SIEBER, F. (1970): Zur Bestimmung der Carbonylgruppen in Zellstoff. Mitteilungen der Fachausschüsse des Vereins der Zellstoff- und Papier-Chemiker und -Ingenieure 18, 16-17.

CHIANG, V.L. & SARKANEN, K.V. (1984): Kinetic Study of End Group Stabilization in Hydrocellulose by Hydrogen Sulfide. Journal of Wood Chemistry and Technology 4, 1-18.

COLBRAN, R.L. & DAVIDSON, G.F. (1961): The Degradative Action of Hot Dilute Alkalis on Hydrocelluloses. J. Textile Inst. 52, T73-T87.

COSTA, U. & MASSAZZA, F. (1984): Adsorption of Superplasticizers on β-C_2S – Changes in Zeta Potential of Particles and the Rheology of Pastes. Il Cemento 3, 127-140.

DIN 54 356 (1977): Bestimmung der Alkalilöslichkeit von Zellstoff. Deutsches Institut für Normung e.V.: Normenausschuss Papier und Pappe.

DYRSSEN, D. (1950): The Preparation of Carrier-free Thorium^{234} (UX_1) by Ion Exchange. Svensk Kemisk Tidskrift 62, 153-164.

DZOMBAK, D.A. & MOREL, F.M.M. (1990): Surface Complexation Modelling, Hydrous Ferric Oxide. John Wiley & Sons, Inc., New York.

FISCHER, K., CHODURA, A., KOTALIK, J., VOLLNER, L. & BIENIEK, D. (1996): Aliphatische Carbonsäuren und Zuckersäuren - Reaktionsprodukte der alkalischen Hydrolyse von Cellulose und Cellulosederivaten. Nagra Unpublished Internal Report, Nagra, Wettingen, Switzerland.

FISCHER, K. (1997): Ergebnisse vergleichender strukturanalytischer und chromatographischer Untersuchungen an Isosaccharinsäurelactonen und α-Isosaccharinsäure. Nagra Unpublished Internal Report, Nagra, Wettingen, Switzerland.

FRANZON, O. & SAMUELSON, O. (1957): Degradation of Cellulose by Alkali Cooking. Svensk Papperstidning 23, 872-877.

FUKAYA, Y & KATO, K. (1986): Adsorption of Superplasticizers on CSH(I) and Ettringite. 8th Int. Congr. Chem. Cem., Rio de Janeiro 3, 142-147.

GASCHE, U. (1996): personal communication. Cellulose Attisholz AG, Luterbach Switzerland.

GLAUS, M.A., HASELBECK, S. & VAN LOON, L.R. (1997a): Determination of the Number of Reducing End Groups in Cellulose. Technical Report TM-44-97-02, Paul Scherrer Institute, Villigen, Switzerland.

GLAUS, M.A., STALLONE, S. & VAN LOON, L.R. (1997b): Durchführung von Sorptionsexperimenten in einem miniaturisierten Ansatz. Technical Report TM-44-97-12, Paul Scherrer Institute, Villigen, Switzerland.

GLAUS, M.A., HUMMEL, W. & VAN LOON, L.R. (1997c): Experimental Determination and Modelling of Trace-Humate Interactions: A Pragmatic Approach for Applications in Groundwater. PSI-Bericht 97-13, Paul

Scherrer Institute, Villigen, Switzerland. Also published as Nagra Technical Report NTB 97-03, Nagra, Wettingen, Switzerland.

GREENFIELD, B.F., HARRISON, W.N., ROBERTSON, G.P., SOMERS, P.J. & SPINDLER, M.W. (1993): Mechanistic Studies on the Alkaline Degradation of Cellulose in Cement. NSS/R272, AEA-D&R-0219, AEA Technology, Harwell, UK.

GREENFIELD, B.F., HOLTOM, G.F., HURDUS, M.H., O'KELLY, N., PILKINGTON, N.J., ROSEVAER, A., SPINDLER, M.W. & WILLIAMS, S.J. (1995): The Identification and Degradation of Isosaccharinic Acid, a Cellulose Degradation Product. Mat. Res. Soc. Symp. Proc. 353, 1151-1158.

HAAS, D.W., HRUTFIORD, B.F & SARKANEN, K.V. (1967): Kinetic Study on the Alkaline Degradation of Cotton Hydrocellulose. J. Appl. Polym. Sci. 11, 587-600.

HUG, S. & SULZBERGER, B. (1994): In Situ Fourier Transform Infrared Spectroscopic Evidence for the Formation of Several Different Surface Complexes of Oxalate on TiO_2 in the Aqueous Phase. Langmuir 10, 3587-3597.

JEFFRIES, R., JONES, D.M., ROBERTS, J.G., SELBY, K., SIMMENS, S.C. & WARWICKER, J.O. (1969): Current Ideas on the Structure of Cotton. Cell. Chem. Technol. 3, 255-274.

KRAGTEN, J. (1978): Atlas of Metal-Ligand Equilibria In Aqueous Solution. Ellis Horwood Ltd., p. 272.

KRÄSSIG, H. (1985): Structure of Cellulose and its Relation to Properties of Cellulose Fibers. In: KENNEDY, J.F., PHILLIPS, G.O, WEDLOCK, D.J. & WILLIAMS, P.A. (eds.): Cellulose and its Derivatives – Chemistry Biochemistry and Applications. Marcel Dekker Inc., New York, Chichester, Brisbane, pp. 3-25.

LAI, Y.Z. & SARKANEN, K.V. (1967): Kinetics of Alkaline Hydrolysis of Glycosidic Bonds in Cotton Cellulose. Cellulose Chem. Technol. 1, 517-527.

LAI, Y.Z. & SARKANEN, K.V. (1969): Kinetic Study on the Alkaline Degradation of Amylose. J. Polymer Sci., Part C, 28, 15-26.

LAI, Y.Z. (1972): Kinetic Evidence of Anionic Intermediates in the Base-Catalyzed Cleavage of Glycosidic Bonds in the Methyl D-Glucopyranosides. Carbohydrate Research 24, 57-65.

LAI, Y.Z. & ONTTO, D.E. (1979): Effects of Alkalinity on Endwise Depolymerization of Hydrocellulose. J. Appl. Polym. Sci. 23, 3219-3225.

LAI, Y.Z. (1981): Kinetics of Base-Catalyzed Cleavage of Glycosidic Linkages. The Eckman Days, vol. 2, International Symposium on Wood and Pulping Chemistry, Stockholm, June 9-12, 26-33.

LAI, Y.Z. (1991): Chemical Degradation. In: HON, D.N.-S. & SHIRAISHI, N. (eds.): Wood and Cellulosic Chemistry. Marcel Dekker Inc., New York and Basel, pp. 455-523.

LEE, J.H. & BYRNE, R.H. (1992): Examination of Comparative Rare Earth Element Complexation Behavior Using Linear Free-Energy Relationships. Geochim. Cosmochim. Acta 56, 1127-1137.

LEWIN, M. (1985): New Chemical Approaches to the Structure of Cellulose. In: KENNEDY, J.F., PHILLIPS, G.O, WEDLOCK, D.J. & WILLIAMS, P.A. (eds.): Cellulose and its Derivatives – Chemistry Biochemistry and Applications. Marcel Dekker Inc., New York, Chichester, Brisbane, pp. 27-35.

MACHELL, G. & RICHARDS, G.N. (1958): Stabilization of Cellulose Towards Alkaline Degradation. TAPPI 41, 12-16.

MACHELL, G. & RICHARDS, G.N. (1960): Mechanisms of Saccharinic Acid Formation. Part II. The αβ-Dicarbonyl Intermediate in Formation of D-Glucoisosaccharinic Acid. J. Chem. Soc., Part A, 2, 1932-1939.

MADSEN, E.L. (1998): Epistemology of Environmental Microbiology. Environ. Sci. Technol. 32, 429-439.

McGINNIS, G.D. & SHAFIZADEH, F. (1980): Cellulose and Hemicellulose. In: CASEY, J.P. (ed.): Pulp and Paper, Chemistry and Chemical Technology, third edition, Volume 1, John Wiley & Sons, New York, pp. 429-436.

MORETON, A.D. (1993): Thermodynamic Modelling of the Effect of Hydroxycarboxylic Acids on the Solubility of Plutonium at High pH. Mat. Res. Soc. Symp. Proc. 294, 753-758.

MOTEKAITIS, R.J. & MARTELL, A.E. (1984): Complexes of Aluminium(III) with Hydroxy Carboxylic Acids. Inorg. Chem. 23, 18-23.

NAGRA (1992): Nukleare Entsorgung Schweiz - Konzept und Realisierungsplan. Nagra Technical Report NTB 92-02, Nagra, Wettingen, Switzerland.

NAGRA (1994): Endlager für schwach- und mittelaktive Abfälle (Endlager SMA). Bericht zur Langzeitsicherheit des Endlagers SMA am Standort Wellenberg (Gemeinde Wolfenschiessen, NW). Nagra Technical Report NTB 94-06, Nagra, Wettingen, Switzerland.

NEALL, F. (1994): Modelling of the Near-Field Chemistry of the SMA Repository at the Wellenberg Site, PSI-Bericht 94-18, Paul Scherrer Institute, Villigen, Switzerland. Also published as Nagra Technical Report NTB 94-04, Nagra, Wettingen, Switzerland.

OKAMURA, K. (1991): Structure of Cellulose. In: HON, D.N.-S. & SHIRAISHI, N. (eds.): Wood and Cellulosic Chemistry. Marcel Dekker Inc., New York and Basel, pp. 89-112.

PAZUR, J.H. (1994): Neutral Polysaccharides. In: KENNEDY, J.F. & CHAPLIN, M.F. (eds.): Carbohydrate Analysis, a Practical Approach. Oxford University Press, Oxford, New York, Tokyo, pp. 73-124.

PROCTER, A.R. & WIEKENKAMP, R.H. (1969): The Direct Preparation of 1-thio-D-Glucitol and Its Disulfide from D-Glucose. Carbohydrate Research 10, 459-462.

PROCTER, A.R. & APELT, H.M (1969): Reactions of Wood Components with Hydrogen Sulfide – III. The Efficiency of Hydrogen Sulfide Pretreatment Compared to Other Methods for Stabilizing Cellulose to Alkaline Degradation. TAPPI 52, 1518-1522.

REHDER, W., PHILIPP, B. & LANG, H. (1965): Ein Beitrag zur Analytik der Carbonylgruppen in Oxycellulosen und technischen Zellstoffen. Das Papier 19, 503-509.

RICHTZENHAIN, H., LINDGREN, B.O., ABRAHAMSSON, B. & HOLMBERG, K. (1954): Ueber den alkalischen Abbau von Polysacchariden –I. Mitteil.: Abbau von Baumwollhydrocellulose. Svensk Papperstidn. 57, 363-366.

ROBINSON, R.A. & STOKES, R.H. (1959): Electrolyte Solutions – The Measurement and Interpretation of Conductance, Chemical Potential and Diffusion in Solutions of Simple Electrolytes. 2nd Edition, Butterworths, London.

ROSSINGTON, D.R. & RUNK, E.J. (1968): Adsorption of Admixtures on Portland Cement Hydration Products. Journal of the American Ceramic Society 51, 46-50.

SAARNIO, J., WATHÉN, K. & GUSTAFSSON, C. (1954): Structure of an Acidic Xylan Isolated from Birch Wood Holocellulose. Acta Chemica Scandinavica 8, 825-828.

SAWYER, D.T. (1964): Metal-Gluconate Complexes. Chem. Rev. 64, 633-643.

SCHINDLER, P. (1990): Co-adsorption of Metal Ions and Organic Ligands: Formation of Ternary Surface Complexes. In: HOCHELLA, M.F., Jr., & White, A.F. (eds.): Mineral-Water Interface Geochemistry. Reviews in Mineralogy, Vol. 23, Mineral Society of America, pp. 281-307.

SHIMIDZU, K. (1991): Chemistry of Hemicelluloses. In: HON, D.N.-S. & SHIRAISHI, N. (eds.): Wood and Cellulosic Chemistry. Marcel Dekker Inc., New York and Basel, pp. 177-214.

SIGG, L.M. (1979): Die Wechselwirkung von Anionen und schwachen Säuren mit α-FeOOH (Goethit) in wässriger Lösung. PhD. Dissertation, Swiss Federal Institute of Technology Zürich, Diss. ETHZ Nr. 6417, Zürich, Switzerland.

SIHTOLA, H., KURKLUND, B., LAAMANEN, L. & PALENIUS, I. (1963): Comparison and Conversion of Viscosity and DP-values Determined by Different Methods. Papper och Trä, Special number 4a, 225-232.

SINGH, N.B., SARVAHI, R. & SINGH, N.P. (1992): Effect of Superplasticizers on the Hydration of Cement. Cement and Concrete Research, 22, 725-735.

SJÖSTRÖM, E. (1977): The Behaviour of Wood Polysaccharides during Alkaline Pulping Processes. Tappi 60, 151-154.

SPANKA, G. & THIELEN, G. (1995): Untersuchungen zum Nachweis von verflüssigenden Betonzusatzmitteln und zu deren Sorptions- und Elutionsverhalten. Beton 5, 320-327.

SPECK, J.C., Jr. (1958): The Lobry de Bruyn-Alberda van Ekenstein Transformation. Advan. Carbohydr. Chem. 24, 63-103.

STUMM, W. & MORGAN, J.J. (1996): Aquatic Chemistry. John Wiley & Sons, Inc., New York, 1996.

SUTER, D. (1996). Memo Nr. 2371/04 Version 2, Colenco Power Consulting AG, 5400 Baden, Switzerland.

TEJEDOR-TEJEDOR, M.I. & ANDERSON, M.A. (1986): In-Situ Fourier Transform Infrared Studies of the Goethtite (α-FeOOH)-Aqueous Solution Interface. Langmuir 2, 203-210.

TÖPPEL, O. (1967): Diskussionsvorlage für den Fachausschuss für Faserstoffe. Deutscher Verein der Zellstoff- und Papier-Chemiker und -Ingenieure.

UCHIKAWA, H., HANEHARA, S., SHIRASAKA, T., SAWAKI, D. (1992): Effect of Admixture on Hydration of Cement, Adsorptive Behavior of Admixture and Fluidity and Setting of Fresh Cement Paste. Cement and Concrete Research 22, 1115-1129.

VAN DUIN, M., PETERS, J.A., KIEBOOM, A.P.G. & VAN BEKKUM, H. (1989): A General Coordination-Ionization Scheme for Polyhydroxy Carboxylic Acids in Water. Recl. Trav. Chim. Pays-Bas 108, 57-60.

VAN LOON, L.R. & HUMMEL, W. (1995): The Radiolytic and Chemical Degradation of Organic Ion Exchange Resins under Alkaline Conditions: Effect on Radionuclide Speciation. PSI-Bericht 95-13, Paul Scherrer Institute, Villigen, Switzerland. Also published as Nagra Technical Report NTB 95-08, Nagra, Wettingen, Switzerland.

VAN LOON, L.R. & GLAUS, M.A. (1997a): Sorption of Isosaccharinic Acid, a Cellulose Degradation Product, on Cement. Environ. Sci. Technol. 31, 1243-1245.

VAN LOON, L.R. & GLAUS, M.A. (1997b): Review of the Kinetics of Alkaline Degradation of Cellulose in View of its Relevance for Safety Assessment of Radioactive Waste Repositories. Journal of Environmental Polymer Degradation 5, 97-109.

VERCAMMEN, K., GLAUS, M.A. & VAN LOON, L.R. (1997): The Complexation of Ca with Isosaccharinic Acid under Alkaline Conditions. PSI Technical Report TM-44-97-08, Paul Scherrer Institute, Villigen, Switzerland.

VUORINEN, T. & SJÖSTRÖM, E. (1982): Kinetics of Alkali-Catalyzed Isomerization of D-Glucose and D-Fructose in Ethanol-Water Solutions. Carbohydrate Research 108, 23-29.

VUORINEN, T. (1996): personal communication.

VUORINEN, T (1988): Mechanisms and Kinetics of Isomerization, Degradation, and Oxidation of Reducing Carbohydrates; Reaction Paths in Alkaline Solutions Containing Oxygen and 2-Anthraquinonesulfonic Acid. Ph.D. Thesis, Helsinki University of Technology, Espoo, Finland, p.25.

WHISTLER, R.L. & BeMILLER, J.N. (1958): Alkaline Degradation of Polysaccharides. Advances in Carbohydrate Chemistry and Biochemistry 13, 289-329.

WHISTLER, R.L. & BeMILLER, J.N. (1961): Alkaline Degradation of Guaran and Characterization of β-D-Isosaccharinic Acid. Journal of Organic Chemistry 26, 2886-2892.

WHISTLER, R.L. & BeMILLER, J.N. (1963): "α"-D-Isosaccharino-1,4-lactone. In: WOLFROM, M.L. & BeMILLER, J.N. (eds.): Methods in Carbohydrate Chemistry; Vol. 2: Reactions of Carbohydrates, 477-479.

WIELAND, E., TITS, J., SPIELER, P. & DOBLER, J.P. (1998): Interaction of Eu(III) and Th(IV) with Sulphate-resisting Portland Cement. Mat. Res. Soc. Symp. Proc. 506, 573-578.

YOUNG, R.A., SARKANEN, K.V., JOHNSON, P.G. & ALLAN, G.G. (1972): Marine Plant Polymers. Part III: A Kinetic Analysis of the Alkaline Degradation of Polysaccharides with Specific Reference to (1-3)-β-D-Glucans. Carbohydrate Research 21, 111-122.

ZWAHLEN, K., GASCHE, U. & JONSSON, K. (1967): Zur Bestimmung der Carbonylgruppen in Zellstoffen. Mitteilungen der Fachausschüsse des Vereins der Zellstoff- und Papier-Chemiker und -Ingenieure 15, 15-21.

12 ACKNOWLEDGEMENTS

This work was partially financed by the National Cooperative for the Disposal of Radioactive Waste (NAGRA) under project management of Dr. I. Hagenlocher. The authors would like to thank S. Stallone, A. Laube and S. Haselbeck for their technical assistance. We also thank Dr. K. Fischer and coworkers (GSF Forschungszentrum München) for the analysis of degradation products and Dr. U. Gasche (Attisholz) for the determination of the degree of polymerisation of different cellulosic materials.
Prof. I Grenthe and Prof. I. Albertsson (RIT, Stockholm), and Drs. I. McKinley, P. Zuidema and I. Hagenlocher (NAGRA) are warmly thanked for carefully reviewing the report and giving useful suggestions to improve the manuscript.